수의학 박사 학위 논문

마우스 위암 모델을 이용한 위암의 발생 및 전이에서 E-cadherin, Smad4, 그리고 p53 의 역할

The Roles of E-cadherin, Smad4, and p53 in the Development and Metastasis of Gastric Cancer using Mouse Gastric Cancer Model

2014 년 2 월

서울대학교 대학원

수의학과 수의병리학 전공

박 준 원

ABSTRACT

The roles of E-cadherin, Smad4, and p53 in the Development and Metastasis of Gastric Adenocarcinoma

(Supervisor: Dae-Yong Kim, D.V.M., Ph.D.)

Jun-Won Park

Department of Veterinary Pathology, College of Veterinary Medicine,
Graduate School, Seoul National University

Loss of E-cadherin (*Cdh1*), Smad4 and p53 have all been shown to play important roles in gastric cancer formation. Compound conditional knockout mice for Smad4, p53, and E-cadherin were generated to further define and compare the roles of these genes in gastric, intestinal and breast cancer development by crossing them with *Pdx-1-Cre*, *Villin-Cre* and *MMTV-Cre* transgenic mice. We have determined that gastric adenocarcinoma was more frequent in *Pdx-1-Cre;Smad4*$^{F/F}$*;Trp53*$^{F/F}$*;Cdh1*$^{F/+}$ mice than in *Pdx-1-Cre;Smad4*$^{F/F}$*;Trp53*$^{F/F}$ mice [P<0.001]. *Pdx-1-*

Cre;Smad4$^{F/F}$*;Trp53*$^{F/F}$*;Cdh1*$^{F/+}$ mice developed gastric adenocarcinomas without E-cadherin expression. However, intestinal and mammary adenocarcinomas with the same genetic background retained the E-cadherin expression and were phenotypically similar to mice with both wild-type *Cdh1* alleles. *Pdx-1-Cre;Smad4*$^{F/F}$*;Trp53*$^{F/F}$*;Cdh1*$^{F/+}$ mice developed gastric adenocarcinomas more rapidly than *Pdx-1-Cre;*$^{F/F}$*;Trp53* $^{F/F}$*;Cdh1*$^{F/F}$ mice, demonstrating that *Cdh1* heterozygosity accelerates the development and progression of gastric cancer, in combination with loss of Smad4 and p53. Lung metastases were identified in 14.2% *Pdx-1-Cre;Smad4*$^{F/F}$*;Trp53*$^{F/F}$*;Cdh1*$^{F/+}$ mice, but not in the other genotypes. Nuclear β-catenin accumulation was identified at the invasive tumor front of gastric adenocarcinomas arising in *Pdx-1-Cre;Smad4*$^{F/F}$*;Trp53*$^{F/F}$*;Cdh1*$^{F/+}$ mice. This phenotype was less prominent in mice with intact E-cadherin or Smad4, indicating that the inhibition of β-catenin signaling by E-cadherin or Smad4 may down-regulate signaling pathways involved in metastases in *Pdx-1-Cre;Smad4*$^{F/F}$*;Trp53*$^{F/F}$*;Cdh1*$^{F/+}$ mice. Knockdown of β-catenin significantly inhibited migratory activity of *Pdx-1-Cre;Smad4*$^{F/F}$*;Trp53*$^{F/F}$*;Cdh1*$^{F/+}$ cell lines. Thus, loss of E-cadherin and Smad4 cooperate with p53 loss to promote the development and metastatic progression of gastric adenocarcinomas, with similarities to human diffuse-type gastric cancer.

Furthermore, a primary cell line, designated NCC-S1 was primarily cultured from a gastric cancer developed from a *Villin-*

Cre;Smad4$^{F/F}$*;Trp53*$^{F/F}$*;Cdh1*$^{F/+}$ mouse to establish a metastatic gastric cancer model. A cancer subpopulation of NCC-S1 cells was isolated from lung metastases that developed from heterotopic tumors transplanted into severe combined immunodeficiency mice. The metastasis derived cells, designated NCC-S1M, formed orthotopic tumors and exhibited a significant improvement in *in vivo* metastatic potential compared with the parental cell line, showing epithelial to mesenchymal transition (EMT) features. NCC-S1M cells demonstrated many features of cancer stem cells, including the ability to initiate tumor formation and chemoresistance. Importantly, Sca-1 was found to be over-expressed in NCC-S1M cells than NCC-S1 cells. Sca-1 positive cells demonstrated increased ability to initiate tumor formation and *in vivo* chemoresistance than Sca-1 negative cells, showing up-regulation of interleukin 1 signaling pathway. Over-expressed genes in Sca-1 positive NCC-S1 cells clustered in 123 metastatic gastric cancer patients according to overall survival following cisplatin/fluorouracil chemotherapy. Taken together, we have identified Sca-1 as a murine gastric cancer stem cell marker using this unique metastatic cell line models.

Keywords: E-cadherin, Smad4, p53, β-catenin, metastasis, Sca-1, cancer stem cell,

Student Number: 2011-31099

CONTENTS

ABBREVIATIONS

BCL-2: B-cell lymphoma 2

BMP: bone morphogenic protein

CDH1: Cadherin-1

CGH: comparative genomic hybridization

DAVID: database for annotation, visualization an integrated discovery

EMT: epithelial to mesenchymal transition

FACS: flow cytometry

GAPDH: glyceraldehydes 3-phosphate dehydrogenase

HDGC: human diffuse type gastric cancer

IL-1: interleukin 1

IL1R1: interleukin 1 receptor type 1

IL1RAP: interleukin 1 receptor accessory protein

IL1RL1: interleukin 1 receptor-like type 1

JNK: c-Jun N-terminal kinase

LEF: lymphoid enhancer factor

LOH: loss of heterozygosity

Ly6a: lymphocyte antigen 6 complex

MMP: matrix metalloproteinases

MMTV: mouse mammary tumor virus

Pdx1: pancreatic and duodenal homebox 1

Smad: Mothers against decapentaplegic homolog

TCF: T-cell factor

TFF2: trefoil factor 2

TGF: transforming growth factor

TNF: Tumor necrosis factor

TSA: Trichostatin A

5-Aza: 5-aza-2'-deoxycitidine

5-Fu: fluorouracil

LITERATURE REVIEW

Introduction

Gastric cancer is the second most common cause of cancer death worldwide (Alberts, Cervantes et al. 2003). According to Lauren's histological classification, gastric cancer can be subdivided into two main histological subtypes: diffuse and intestinal (Lauren 1965). Intestinal-type gastric cancer is the most common variant at high risk and is composed of gland-like structures that mimic the glandular architecture of the intestinal mucosa. Intestinal gastric cancer is recognized by a series of premalignant lesions such as atrophy, intestinal metaplasia, and dysplasia. Diffuse-type gastric cancer is relatively less frequent than intestinal-type and lacks the formation of glandular structure. Unlike intestinal-type gastric cancer, diffuse gastric cancer usually arises in the context of chronic inflammation without any identifiable histological precursor lesions (Correa and Shiao 1994). Environmental factors, such as diet and Helicobacter pylori (H. pylori) infection, strongly influence the development and progression of intestinal-type gastric cancer, whereas the role of genetic influences is more important than environmental factors in diffuse-type gastric cancer.

p53, Smad4, and E-cadherin are frequently inactivated in human gastric cancer. *TP53* mutations are reported in 0%-21% of diffuse-type and 36%-43% of intestinal-type gastric cancers,

respectively (Maesawa, Tamura et al. 1995). Smad4, a co-Smad involved in both branches of the TGF-β/BMP signaling system (Schmierer and Hill 2007), is inactivated in 40% of human gastric cancers by loss of heterozygosity (LOH), promoter hypermethylation, and somatic mutation (Wang, Kim et al. 2007). The *CDH1* gene, coding for E-cadherin, is frequently inactivated in familial and sporadic diffuse-type gastric cancers (Becker, Atkinson et al. 1994). Although the inactivation of these genes has been implicated in gastric carcinogenesis and the need for research in this field is undisputed, a murine gastric cancer model for the systemic evaluation of the effects of these genes in gastric development and progression is lacking.

To explore gastric carcinogenesis, genetically engineered mouse models, particularly in knockout mice, have been used because these models have considerablely contributed to understanding the pathways and mechanisms underlying gastric carcinogenesis. There are only a few murine gastric cancer cell lines available in the scientific community, but not of them are genetically defined since the tumors were carcinogen-induced. Several genetically engineered mouse models for gastric cancer have been reported, but they have been generated using K14 and Atb6 promoters. These models have been generated in the lineage of parietal cells (Wang, Dangler et al. 2000; Oshima, Matsunaga et al. 2006; Shimada, Mimata et al. 2012), from which no human gastric cancer

ever originate. Thus, in the scientific and pharmaceutical communities, there is a need for genetically defined, murine gastric cancer cell models that closely recapitulate human gastric cancer to facilitate a comprehensive understanding of the mechanisms underlying the function of *Cdh1*, Smad4, and p53 in the suppression of tumorigenesis.

E-cadherin in cancer

E-cadherin, encoded by the *CDH1* gene, is a tumor suppressor protein prominently associated with tumor development, tumor invasion, metastasis, and poor patient prognosis (Schipper, Frixen et al. 1991; Oka, Shiozaki et al. 1993; Umbas, Isaacs et al. 1994). E-cadherin is a single-span transmembrane that forms the core of the epithelial adherens junction by establishing a homophilic interaction with the adjacent E-cadherin of neighboring cells (Nagafuchi, Shirayoshi et al. 1987; Gumbiner 2005). It is well known that the loss E-cadherin-mediated cell-to-cell adhesion is a prerequisite for tumor development, invasion and metastasis (Birchmeier and Behrens 1994).

Other than its structural role in stabilizing cell-to-cell contact, E-cadherin/β-catenin complex in its intracellular region serves an important role in activating the Wnt signaling pathway (Tian, Liu et al. 2011). Disrupting this complex by loss of E-cadherin increases the amount of stabilized cytoplasmic β- catenin, which then translocates to the nucleus and functions as an activator for T-cell factor (TCF)/lymphoid enhancer factor (LEF) (Fig 1). The activated Wnt signaling pathway subsequently modulates the expression of TCF/LEF1 target genes, including the proto-oncogene c-Myc and cyclin D1.

The mechanisms of E-cadherin inactivation include gene mutation, promoter hypermethylation, chromatin remodeling, post-

translational modification and transcriptional repression (Guilford, Hopkins et al. 1998; Hirohashi 1998; Rashid, Sanda et al. 2001). E-cadherin is frequently inactivated in familial and sporadic diffuse-type gastric cancers (Becker, Atkinson et al. 1994). Germline *CDH1* mutations are associated with an 80% lifetime risk of diffuse-type gastric cancer, and somatic inactivating E-cadherin mutations have been reported in 33%-50% of sporadic diffuse-type gastric cancers (Becker, Atkinson et al. 1994). Promoter hypermethylation of *CDH1*, identified in up to 80% of patients with diffuse-type gastric cancers, is the most common second hit in the inactivation of the wild type *CDH1* allele, but mechanisms leading to the inactivation of the wild type *CDH1* allele remain largely unknown (Machado, Oliveira et al. 2001; Rosivatz, Becker et al. 2002). A better understanding of the stepwise inactivation of E-cadherin would provide an opportunity for therapeutic intervention in gastric cancer.

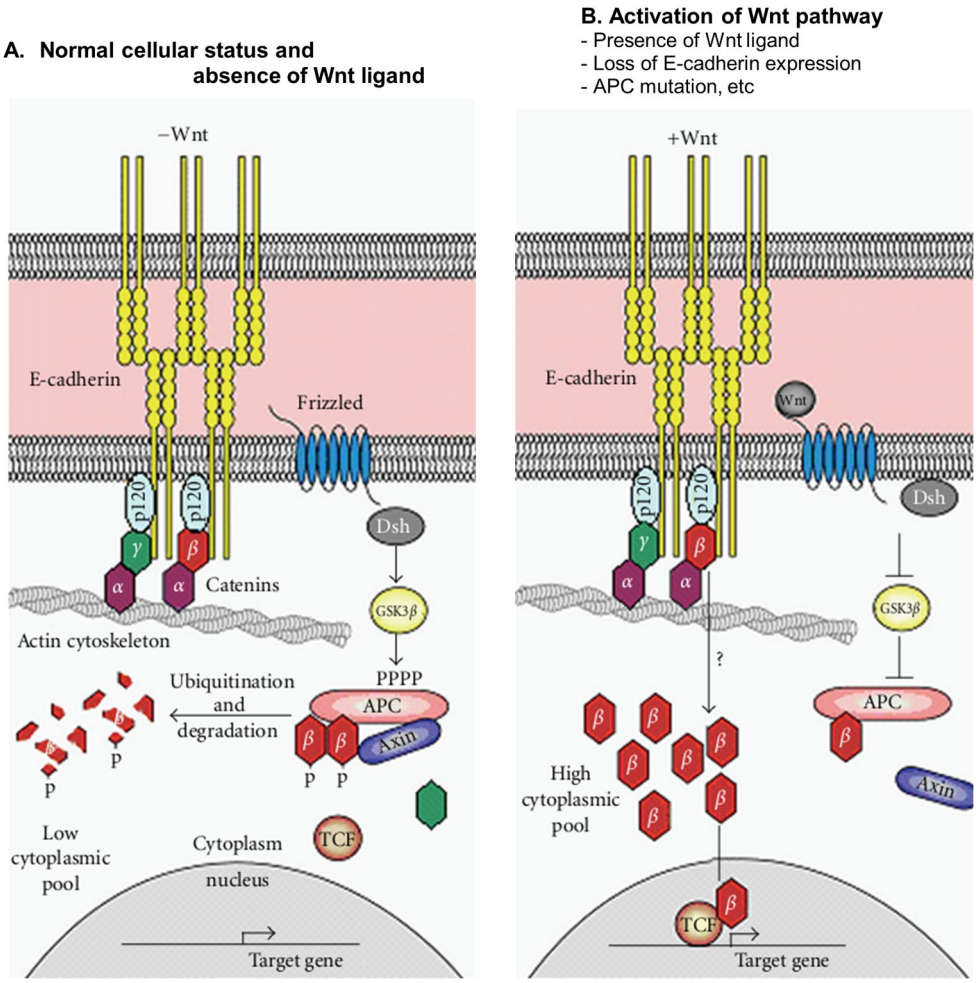

Fig 1. E−cadherin/β- catenin complex in epithelial cell−cell adhesion and Wnt signaling (modified from Tian, Liu et al. 2011).

Smad4 and p53 in gastric cancer

Smad proteins are the critical components of the transforming growth factor-β (TGF-β) signaling pathway that regulate many cellular functions including cell growth, adhesion, migration, cell-fate determination and differentiation, and apoptosis (Schmierer and Hill 2007). Smad4 is a co-Smad involved in both branches of the TGF-β/BMP signaling system (Fig 2). Complex formation of the phosphorylated receptor-regulated SMADs with SMAD4 translocated to the nucleus and the nuclear accumulation of active SMAD complexes directly regulate gene transcription in conjunction with transcription factors.

During initiation and early progression of the tumor, TGF-β/BMP signaling serves as a tumor suppressor by inhibiting proliferation and accelerating apoptosis, which is supported by various *in vitro* and *in vivo* studies via either cell-autonomous or non-cell autonomous mechanisms and loss or mutation of the members of the TGF-β/BMP signaling pathway in human cancer (Dhawan, Singh et al. 2005; Yang and Yang 2010). Alteration of Smad4 gene is frequently observed in gastrointestinal tumors such as familial juvenile polyposis, an autosomal dominant disease characterized by predisposition to gastrointestinal polyps and cancer (Miyaki and Kuroki 2003). Smad4 is inactivated in 40% of human gastric cancers by loss of heterozygosity (LOH), promoter hypermethylation, and somatic mutation (Wang, Kim et al. 2007).

Oncogenic roles in tumorigenesis have been investigated in human cancer. In the late stage of tumor progression, upregulated TGF-β/BMP signaling might promote tumor cell migration, invasion, and angiogenesis with being associated with poor prognosis for cancer patients (Elliott and Blobe 2005). However, the dual roles of TGF-β/BMP signaling in cancer is both cell-specific and context-dependent. Therefore, there is an urgent need to evaluate the roles of TGF-β/BMP signaling in gastric carcinogenesis and establish crosstalk communication with other pathways.

p53 plays a critical role in maintaining the genetic intergrity of proliferating cells, thereby making it renowned as the "Guardian of the Genome"(Lane 1992). In its wild-type form, p53 is a major tumor suppressor whose function is critical for protection against cancer. In addition, inactivation of the protein is a frequent event in tumorigenesis (Rivlin, Brosh et al. 2011). It is well established that p53 inactivation and mutant p53 expression can grant cells with additive growth and survival advantages, such as increased proliferation, evasion of apoptosis, and chemoresistance (Sigal and Rotter 2000; Brosh and Rotter 2009). *TP53* mutations are reported in 0%-21% of diffuse-type and 36%-43% of intestinal-type gastric cancers, respectively (Maesawa, Tamura et al. 1995).

Under normal conditions, both Sma4 and p53 act as gene-specific transcription factors to regulate various genes producing tumor suppressive effects. Due to the broad ranging nature of these

proteins, the convergence of p53 and Smad4 signaling pathways have been investigated in several studies. However, the convergence of these proteins has not been demonstrated in gastric carcinogenesis. A systemic evaluation of the effects of these proteins in gastric development and progression in gastric cancer is required to facilitate a comprehensive understanding of the mechanisms underlying the function of Smad4 signaling and p53 in the suppression of tumorigenesis.

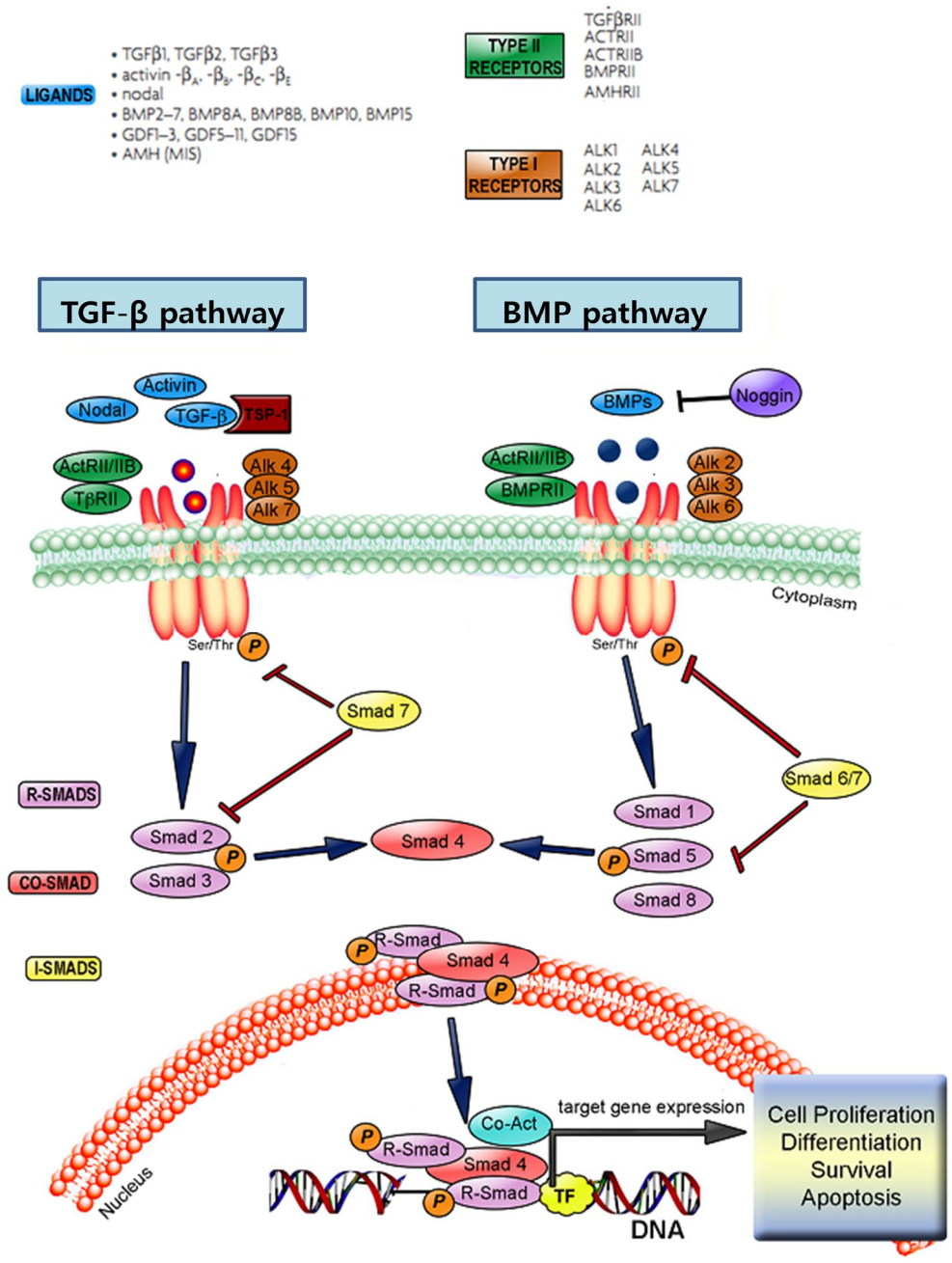

Fig 2. Core signaling in the mammalian TGF−β/BMP signaling − SMAD pathways (Schmierer and Hill 2007).

Gastric cancer stem cell

It is postulated that tumors are composed of heterogeneous cancer cells and that only a rare subpopulation of cells known as cancer stem cells (CSC) are responsible for sustaining tumorigenesis and establishing the heterogeneity inherent in tumors (Visvader and Lindeman 2012). Tumors may originate from the CSCs that are able to maintain tumor growth, tumor recurrence, apoptosis, and chemoresistance (Visvader and Lindeman 2012). Thus, CSCs promise the development of anticancer drugs. They exhibit characteristics that are similar to normal stem cells such as unlimited self-renewal and multi-lineage differentiation. Despite many uncertainties about the existence of CSCs, recent *in vivo* experiments suggest that tumors originate from CSCs (Driessens, Beck et al. 2012; Schepers, Snippert et al. 2012).

The first prospective identification of CSCs was made by Dick et al for acute myeloid leukemia(AML), subsequently demonstrating their existence in diver solid tumors (Visvader and Lindeman 2008). Putative CSCs are usually identified based on the expression of specific cell surface markers. Recently, gastric CSCs have been proposed in many gastric cancer cell lines and primary tumors using several candidate cell surface markers (Table 1). Lineage tracing studies have shown that Lgr5+ cells are multipotent stem cells responsible for the long-term renewal of the entire gastric epithelium. In addition, the inactivation of APC in Lgr5+ cells

rapidly formed tumors in the pylori epithelium in animal models (Barker and Clevers 2010). However, Lgr5 has been described as being expressed in both tumorigenic and non-tumorigenic cells (Takaishi, Okumura et al. 2009). Among the numerous surface markers currently under investigation, CD44 have proven to be the most useful for the identification of CSCs in gastric cancers (Takaishi, Okumura et al. 2009). Using the flow cytometry cell sorting method, Takaishi et al. isolated CD44+ cells from a panel of human gastric cancer cell lines, which formed spheroid colonies under non-adherent conditions in serum-free media and xenograft tumors in immunodeficient mice. CD44+ cells showed the properties of self-renewal and formed differentiated progeny of CD44- cells.

The rapidly evolving field of CSC research has generated great interest in its therapeutic application in gastric cancer. Over the last few years, using lineage tracing and molecular marker labeling, several gastric CSC populations have been defined and have shown that heterogeneity exists in gastric cancer, which suggests that we need to use a combination of these markers to target different populations of gastric CSCs. Therefore, further investigation is required to evaluate CSC phenotypes using different markers, different experimental approaches, and gene expression signatures to lead to a greater understanding of gastric CSC pathways and identify new candidate therapies that target CSCs.

Table 1. Summary of putative gastric stem/progenitor cells and cancer stem cell markers (Singh 2013)

Markers	Location and function	
	Normal stomach	*Gastric cancer*
Lgr5	Base of pyloric gland, give rise to all cell types (lineage tracing)	Luminal surface, tumor centre and invasion front (Immunostaining, 100 GC patients analyzed)
TFF2	Isthmus region of corpus, gland base (mRNA expression) in mice, give rise to neck, chief and parietal cells only (lineage tracing)	Expressed in SPEM following DMP−777 treatment, due to trans−differentiation of chief cells Progressive loss of expression in H. pylori−positive gastritis, IM and GC in human and mice
DCKL1/DCAMKL1	Isthmus region of corpus (immunostaining)	Expression expanded in murine models of acute gastritis, chronic ulcer and in Kras environment
Sox2	1 and 2 cells above the base of corpus and antrum in mice stomach, give rise to cells in both the corpus and pylorus (lineage tracing)	Expression associated with invasion and lymph node metastasis in GC (Immunostaining, 290 GC patients analyzed)
Sox9	Weak expression in neck/isthmus of corpus, moderate expression in neck/isthmus of pylorus (immunostaining)	Strong expression observed in GC (46 patients analyzed by immunostaining)
Bmi−1	Weak to moderate expression in pits and isthmus of corpus and neck region of antrum	Strong expression in GC (immunostaining)
Oct4	Isthmus region of pit gland, pyloric antrum of human stomach (immunostaining)	Increased expression in GC

CD44	Strong expression in lower glandular cells of the gastric antrum and rare expression in corpus	Strong expression GC (isolated cells from cancer cell lines and mouse and human gastric samples produce spheroid colonies, and show tumorigenicity)
CD71−cell	n/t	Show higher tumorigenicity and multipotency, highly invasive and to exist in the invasive fronts of cancer foci
CD133	Base of gastric glands, antrum	Strong expression in GC, expressed on the luminal surface membrane of gland−forming cells (patient samples)
EpCAM+/CD44+	n/t	Isolated cells produce spheroid colonies, and show tumorigenicity
CD44+CD24+	n/t	Isolated cells from gastric tissues of patients produce spheroid colonies, and show tumorigenicity
CD44+CD54+	n/t	Isolated cells from human gastric tumor tissues and peripheral blood of patients produce spheroid colonies, and show tumorigenicity
CD90	n/t	Isolated cells from gastric primary tumors produce spheroid colonies, and show tumorigenicity

*n/t: not tested

Objective

p53, Smad4, and E-cadherin are frequently inactivated in human gastric cancer. However, the functional roles of these genes in gastric cancer development and progression have not been fully evaluated using *in vivo* models. We generated compound conditional knockout mice for Smad4, p53, and E-cadherin to define and compare the roles of these genes in gastric, intestinal and breast cancer development by crossing them with *Pdx-1-Cre*, *Villin-Cre* and *MMTV-Cre* transgenic mice. Moreover, we established the murine gastric cancer cell line model which was useful for testing immunotherapeutics and, possibly, anti-metastasis agents. Using this novel mouse gastric cancer cell line model, we tried to identify candidate murine gastric cancer stem cell markers and demonstrate this biomarker-related pathway.

CHAPTER I.

LOSS OF E-CADHERIN AND SMAD4 COOPERATE TO PROMOTE THE DEVELOPMENT OF DIFFUSE-TYPE GASTRIC ADENOCARCINOMA

Abstract

Loss of E-cadherin (*Cdh1*), Smad4 and p53 have all been shown to play important roles in gastric, intestinal and breast cancer formation. Compound conditional knockout mice for Smad4, p53, and E-cadherin were generated to further define and compare the roles of these genes in gastric, intestinal and breast cancer development by crossing with *Pdx-1-Cre*, *Villin-Cre* and *MMTV-Cre* transgenic mice. We have determined that gastric adenocarcinoma was more frequent in *Pdx-1-Cre;Smad4*$^{F/F}$*;Trp53*$^{F/F}$*;Cdh1*$^{F/+}$ mice than in *Pdx-1-Cre;Smad4*$^{F/F}$*;Trp53*$^{F/F}$ mice [P<0.001]. *Pdx-1-Cre;Smad4*$^{F/F}$*;Trp53*$^{F/F}$*;Cdh1*$^{F/+}$ mice developed gastric adenocarcinomas without E-cadherin expression. However, intestinal and mammary adenocarcinomas with the same genetic background retained the E-cadherin expression and were phenotypically similar to mice with both wild-type *Cdh1* alleles. Early onset human gastric cancer with *CDH1* germline mutation demonstrated very low level of E-cadherin. Promoter hypermethylation of the *CDH1* gene was not identified in the gastric cancer as in our mutant mice. Thus, loss of E-cadherin and Smad4 cooperate with p53 loss to promote the development of gastric adenocarcinomas, with similarities to human diffuse-type gastric cancer.

Introduction

p53, Smad4, and E-cadherin are frequently inactivated in human gastric cancer. *TP53* mutations are reported in 0% to 21% of diffuse- and 36% to 43% of intestinal-type gastric cancers, respectively (Maesawa, Tamura et al. 1995). Smad4, a co-Smad involved in both branches of the TGF-β/BMP signaling system (Schmierer and Hill 2007), is inactivated in 40% of human gastric cancers by loss of heterozygosity (LOH), promoter hypermethylation, and somatic mutation (Wang, Kim et al. 2007). The *CDH1* gene, coding for E-cadherin, is frequently inactivated in familial and sporadic diffuse-type gastric cancers (Becker, Atkinson et al. 1994). Germline *CDH1* mutations are associated with an 80% lifetime risk of diffuse-type gastric cancer, and somatic inactivating E-cadherin mutations have been reported in 33-50% of sporadic diffuse-type gastric cancers (Becker, Atkinson et al. 1994). Promoter hypermethylation of *CDH1*, identified in up to 80% of patients with diffuse-type gastric cancers, is the most common second hit in the inactivation of wild type *CDH1* allele, but mechanisms leading to the inactivation of the wild type *CDH1* allele remain largely unknown (Machado, Oliveira et al. 2001; Rosivatz, Becker et al. 2002). A better understanding of the stepwise inactivation of E-cadherin would provide an opportunity for therapeutic intervention.

Valuable biological insights into these gastric tumor suppressors

have been obtained through studies of genetically engineered mouse models. Knockout of Smad4 in the germline of mice results in embryonic lethality (Sirard, de la Pompa et al. 1998), whereas mice heterozygous for mutant Smad4 in the germline develop *in situ* gastric carcinomas after 18 month of age (Xu, Brodie et al. 2000). It still remains to be elucidated how the loss of Smad4 in gastric epithelium, alone and in combination with other tumor suppressors, promotes the progression of gastric cancers.

While it was recently reported that *Atb4*-driven p53 and E-cadherin knockout mice develop diffuse-type gastric cancers (Shimada, Mimata et al. 2012), the impact of E-cadherin heterozygosity on the development and progression of gastric cancer has not been previously evaluated. Based on human mutation profiles and prior studies, we assessed the role of one allelic loss of E-cadherin, alone or in combination with the loss of Smad4 and p53, on the development of diffuse-type gastric adenocarcinomas in mice. Additionally, we compared this gastric cancer model with intestinal and mammary cancer models of the same genetic background.

Materials and Methods

Mice

Mouse studies were conducted with the approval of the Animal Care and Use Committees of National Cancer Center of Korea (NCC-12-050E) and the National Cancer Institute (Bethesda, MD). *Pdx-1-Cre* mice (B6.FVB-Tg(Ipf1-cre)1Tuv), originally generated by Dr. Lowy (Hingorani, Petricoin et al. 2003), were provided through the Mouse Models of Human Cancers Consortium (MMHCC) repository at the NCI Frederick Cancer Research Center. B6.Cg-Tg(Vil-Cre)20Sy, FVB/N-Tg(MMTV-Cre)7Mul, and FVB.129-*Trp53*^{tm1Brn} (Jonkers, Meuwissen et al. 2001) mice were also provided by the MMHCC. B6.129-*Cdh1*^{tm2Kem}/J mice, which have *loxP* sites flanking exons 6-10, were purchased from The Jackson Laboratory (Boussadia, Kutsch et al. 2002). Conditional Smad4 knockout mice (*Smad4*$^{F/F}$) on the Black Swiss, B6 and 129 backgrounds were previously described (Yang, Li et al. 2002). Compound conditional knockouts of Smad4, p53, and E-cadherin were bred with *Pdx-1-Cre* mice, *Villin-Cre* mice, and *MMTV-Cre* mice, to perform targeted deletion for these genes in gastric, intestinal, and mammary epithelium, respectively. *Pdx-1-Cre* mice express Cre in mucosal epithelial cells of the gastric antrum and duodenum as well as the pancreatic islet cells (Larsson, Madsen et al. 1996). *Villin-Cre* mice expressed Cre in progenitor cells of the

intestinal epithelial mucosa (el Marjou, Janssen et al. 2004) and of the antrum (Qiao, Ziel et al. 2007). *MMTV-Cre* mice expressed Cre in mammary epithelial cells and striated ductal cells of the salivary gland (Andrechek, Hardy et al. 2000). The strain background for crosses was controlled in order to avoid confounding variables of strain background in order to compare tumor-free survival across the genotypes. Offspring mice were genotyped using polymerase chain reaction (PCR) assays for tail DNA. PCR genotyping primers for *Cdh1* were F: 5'-CTTATACCGCTCGAGAGCCGGA-3' and R: 5'-GTGTCCCTCCAAATCCGATA-3'. Amplicons of 900 and 980 bp were expected for wild-type and floxed alleles, respectively. PCR genotyping primers for *Trp53* were F: 5'-TGGAGATATGGCTTGGAGTAG-3' and R: 5'-CAACTTACTTCGAGGCTTGTC-3'. PCR products of 420 and 500 bp were expected for wild-type and floxed alleles, respectively. PCR genotyping primers for *Smad4* were F: 5'-GGGCAGCGTAGCATATAAGA-3' and R: 5'-GACCCAAACGTCACCTTCAC-3'. PCR products of 390 and 480 bp were expected for wild-type and floxed alleles, respectively. Primers for *Pdx1-Cre* were F: 5'-CTGGACTACATCTTGAGTTGC-3' and R: 5'-CAGATTACGTATATCCTGGCAG-3'. Primers for *Villin-Cre* were F: 5'-TCCTCTAGGCTCGTCCCG-3' and R: 5'-

CAGATTACGTATATCCTGGCAG-3'. Primers for *MMTV-Cre* were F: 5'-GTCGATGCAACGAGTGATGAG-3' and R: 5'-TCATCAGCTACACCAGAGACG-3'.

Necropsy protocols

Mice positive for *Pdx-1-Cre* or *Villin-Cre* genes were monitored until they became moribund or showed signs of distress, at which time necropsies were performed. Scheduled sacrifice was also conducted for sentinel mutant mice without signs of distress, in order to evaluate the presence or absence of asymptomatic microscopic disease in stomach. *MMTV-Cre* positive female mice were euthanized when mammary tumors reached 2 cm in diameter. Carcinoma-free intervals were compared by log-rank test. When no carcinomatous lesions were identified in a given organ, it was censored for the development of carcinoma on the day of necropsy (Leung, Elashoff et al. 1997). Liver, spleen, and lung were harvested at necropsy to assess for metastases.

For necropsy of *Pdx-1-Cre*- and *Villin-Cre*-positive mice, the entire gastrointestinal tract was immediately removed, and the stomach was incised along the greater curvature. The intestine was dissected into two pieces and designated as colon and small intestine, which were cut into equal thirds (duodenum, jejunum, and ileum). Each piece of intestine was carefully opened longitudinally with a scissors, and spread onto a piece of filter paper. After

flushing with ice-cold saline, the intestine was rolled, luminal side up from its proximal to distal end, onto a wooden stick and the ends of each roll were fixed in place with a 26-gauge needle. After 1 day of fixation in neutral buffered 10% formalin, the stomach was cut into six strips and the rolls of intestine were cut in half with a razor blade along the duodenal to the ileal axis.

Quantitative real-time RT-PCR (QRT-PCR)

For mouse samples, total RNA was isolated from fresh frozen tissue using AllPrep DNA/RNA/Protein Mini Kit (Qiagen, Valencia, CA) according to the manufacturer's instructions. Stroma was trimmed out using an H&E-stained top slide, before RNA isolation. 0.3 μg of total RNA was reverse transcribed using random hexamers and *amfiRivertII* Reverse Transcriptase (GenDEPOT, Barker, TX) according to the manufacturer's standard protocols.

For human samples, total RNA was isolated from fresh frozen tissue using *mir*Vana^{TM} Isolation Kit (Ambion), according to the manufacturer's instructions. Stroma was trimmed out using a H&E-stained top slide, before RNA isolation. Isolated RNA was treated with DNase I (Sigma, St. Louis, MO) according to the manufacturer's protocol. Total RNA was reverse transcribed using random hexamers by using SuperScript III First-Strand Synthesis System (Invitrogen) according to the manufacturer's standard protocol. PCR reactions were performed on a Roche LC480 (Roche Diagnostics, Penzberg, Germany) using QuantiTect SYBR Green

PCR Master Mix (Qiagen). QRT-PCR primers for mouse gene were F: 5'-GCTGCAGGTCTCCTCATG-3' and R: 5'-CATCCTTCAAATCTCACTCTGC-3' for *Cdh1,* F: 5'-GGTCGGTGTGAACGGATTTG-3' and R: 5'-GTGAGTGGAGTCATACTGGAAC-3' for *Gapdh.* QRT-PCR primers for human gene were F: 5'-CGCATTGCCACATACACTCTC-3' and R: 5'-GGTTCCTGGAAGAGCACCTTC-3' for *CDH1*, and F: 5'-GAGTCAACGGATTTGGTCG-3' R: 5'-TGGAATCATATTGGAACATGTAAAC-3' for *GAPDH1*.

Genomic DNA quantitative real-time PCR (QPCR)

Genomic DNA was isolated from 5 fresh frozen tissue samples and 13 formalin-fixed paraffin-embedded blocks of gastric cancers formed in *Pdx-1-Cre;Smad4*$^{F/F}$*;Trp53*$^{F/F}$*;Cdh1*$^{F/+}$ mice, using AllPrep DNA/RNA/Protein Mini Kit (Qiagen) and QIAamp DNA FFPE Tissue Kit (Qiagen) and respectively according to the manufacturer's instructions. PCR reactions were performed in a total volume of 10 μl containing 5 μl of QuantiTect Probe PCR kit (Qiagen), 400 nM of each primer, 200 nM of TaqMan probe and 60 ng of genomic DNA using a Roche LC480 (Roche Diagnostics). PCR conditions were as follows: 15 min at 95 ºC, followed by 99 cycles each consisting of 20 s at 94 ºC, 20 s at 55 ºC, and 20 s at 72 ºC. Data were analyzed using the LC480 software (Roche Diagnostics).

TaqMan probe/primers were targeted to exons 6, 8, and 10 of the mouse *Cdh1* gene. The QPCR primers were as follows: *Cdh1*−Exon6−F/R, 5'−TCTATTCTCATGCCGTGTCATC−3'/5'−GCCTGTTGTCATTCTGATCTGTC−3'; *Cdh1*−Exon8−F/R, 5'−CCTACATACACTCTGGTGGTTC−3'/5'−CGTGCTTGGGTTGAAGACAG−3'; *Cdh1*−Exon10−F/R, 5'−AGCAGCAATACATCCTTCATG−3'/5'−GTCTACCACGTCCACAGTGAC−5', specifically for exon6, exon8 and exon10 (between LoxP luci) of *Cdh1* focusing on only non−functional *Cdh1* allele; Rnu6−F/R, 5'−GCTTCGGCAGCACATATACTA−3'/5'−TTGCGTGTCATCCTTGCGCAG−3'. The TaqMan probes were as follows: *Cdh1*−Exon6−Probe, 5'−FAM−AGGATCCCATGGAGATAGTGATCACAGT−BHQ−1−3'; *Cdh1*−Exon8−Probe, 5'−FAM−CTGACCTTCAAGGTGAAGGCTTGAGC−BHQ−1−3'; *Cdh1*−Exon10−Probe, 5'−FAM−TCTCTTGTCCCTTCCACAGCCACT−BHQ−1−3'; Rnu6−Probe, 5'−FAM−ATTGGAACGATACAGAGAAGATTAGCATGG−BHQ−1−3'. *Rnu6* gene was used as a loading control. Tumor data were normalized against data obtained for genomic DNA obtained from *Pdx−1−Cre*−negative mice, which was serially diluted as standards for quantitation. LOH was defined as the average $\log_2$ ratio of three probes of tumor to normal DNA < −1.5 (Gutierrez, Dahlberg et al. 2010), given the median tumor nuclei content of 60% in gastric

cancers that formed in *Pdx-1-Cre; Trp53*$^{F/F}$*;Cdh1*$^{F/+}$ mice.

Immunohistochemistry and immunofluorescence

The mouse tissues and clinical human samples were fixed in neutral buffered 10% formalin, processed by standard methods and embedded in paraffin. 5 μm cross paraffin sections were dewaxed, rehydrated and subjected to antigen retrieval for immunostaining by heating at 100℃ for 20 minutes in 0.01 M citrate buffer (pH 6.0). The ABC method (Vectastain Elite ABC kit and Vectastain M.O.M. kit, Vector Laboratories, Burlingame, CA) was used according to the manufacturer's protocol. The slides were subjected to colorimetric detection with ImmPact DAB substrate (SK-4105, Vector Laboratories). The slides were counterstained with Meyer's hematoxylin for 10 seconds. Negative controls were performed by omitting the primary antibody and substitution with diluent. The following antibodies were used in this study; rabbit polyclonal anti-E-cadherin antibody (1:200; Cell Signaling, #3195, Danvers, MA), rabbit polyclonal anti p53 antibody (1:50; Santa Cruz, sc-6243), mouse monoclonal anti spasmolytic polypeptide antibody (1:50; Abcam, ab49536), mouse monoclonal anti mucin 6 antibody (1:100; Novus Biologicals, NB120-11335), mouse monoclonal anti mucin 5ac antibody (1:100; Abcam, ab3649), and rabbit polyclonal anti somatostatin antibody (1:1000; Immunostar, 20067).

For immunofluorescence analyses, primary antibodies were incubated overnight at 4℃ and secondary antibodies (FITC goat anti-rabbit secondary antibody (1:250; Vector Laboratories FI-1000)) were incubated for 30 minutes at room temperature. Slides were mounted with Vectashield mounting media (Vector Laboratories, H-1200). Mouse monoclonal anti Smad4 antibody (1:50; Santa Cruz, sc-7966) and rabbit polyclonal anti Ki-67 antibody (1:200; Abcam, ab15580) were used as primary antibodies. At least three *200x* microscopic field was examined to assess the percentage of Ki-67 positive cells.

Western blot analysis

Primary cancer cells were collected and lysed with T-PER Tissue Protein Extraction Reagent (Thermo Fisher Scientific, Hudson, NH, U.S.A) supplemented with protease inhibitor. After removal of cellular debris, protein concentration was quantitated by using a BCA reagent kit (Thermo Fisher Scientific) according to manufacturer's instruction. Protein sample was prepared by making a 3 in 4 dilution with 4x Laemmli sample buffer (250 mM Tris-HCl (pH 6.8), 4% SDS, 40% glycerol, 0.05% bromphenol blue, 4% 2-mercaptoethanol) and boiling for 5 minute. Equal amounts of protein were separated on SDS-polyacrylamide gel and transferred onto nitrocellulose membrane by electrophoresis and blotting apparatus (Bio-Rad, Hercules, CA). The proteins were probed with the

relevant primary antibodies and horseradish peroxidase (HRP)-conjugated secondary antibodies at the recommended dilutions. Rabbit polyclonal anti E-cadherin antibody (1:1000; #3195, Cell Signaling, Danvers, MA), rabbit monoclonal anti acetyl H3K9 (1:1000; #9649, Cell Signaling Technology), and mouse monoclonal anti GAPDH (1:1000; sc-32233, Santa Cruz, CA) were applied. Immunodetection were performed by using an enhanced chemiluminescence (ECL) detection kit (Thermo Fisher Scientific).

Expression array analyses

Total RNA was isolated from tumor-rich area of fresh frozen gastric adenocarcinomas formed in 4 *Pdx-1-Cre; Trp53*$^{F/F}$*;Cdh1*$^{F/+}$ mice and from normal gastric mucosa samples obtained from 4 *Cre*-negative mice. 1 μg of total RNA was subjected to GeneChip Mouse Gene 1.0 ST Arrays (Affymetrix, Santa Clara, CA) and summarized with robust multichip average (RMA) using R (version 2.15.2). Student *t*-test was used to identify differentially expressed genes. Pathway analysis was performed using Gene Set Enrichment Analysis (GSEA) (http://www.broadinstitute.org/gsea). Genes differentially expressed between tumor and normal samples at $P<0.001$ were subject to the GSEA of canonical pathways and transcription factor targets.

Affymetrix's GeneChip miRNA 2.0 Array was used for microRNA analysis. Microarray data were normalized using R and Student t-

test was used to identify microRNAs differentially expressed between *Pdx-1-Cre;Trp53*$^{F/F}$*;Cdh1*$^{F/+}$ gastric adenocarcinomas (n=2) and normal tissue (n=2). A P value less than 0.001 was used as the cutoff to identify differentially expressed microRNAs.

Bisulfite sequencing

Genomic DNA was bisulfite-modified and PCR-amplified with *Cdh1*-BGS-F (5'-GTGGAATAGGAAGTTGGGAAGTT-3') and *Cdh1*-MSP-Un-R primers, as in Methylation Specific PCR. After PCR products were purified using gel extraction kit (Macrogen, Seoul, Korea), the purified PCR products were cloned into the TOPO-TA vector (Invitrogen) and transformed of *E-coli* according to the manufacturer's instructions. After isolation of plasmid DNA from 8-10 clones per each sample using plasmid Mini-Prep kit (Macrogen), each plasmid sample was sequenced with M13-F (-20) primer (5'-GTAAAACGACGGCCAG-3').

Methylation Specific PCR

For mouse samples, genomic DNA was isolated from gastric adenocarcinomas that formed in *Pdx-1-Cre;Smad4*$^{F/F}$*;Trp53*$^{F/F}$*;Cdh1*$^{F/+}$ mice using AllPrep DNA/RNA/Protein Mini Kit (Qiagen) according to the manufacturer's instructions. Using macrodissection, stromal tissue was trimmed out as much as possible. Each 0.3 μg of genomic

DNA was bisulfite-converted by using EZ DNA Methylation™ kit (Zymo Research, Irvine, CA) according to the manufacturer's protocol. Methylation-specific PCR was performed in a reaction volume of 10 μl consisting of 0.05 μl of HotStarTaq (Qiagen), 0.8 μl of 2.5 mM dNTP, 1 μl of 10× PCR buffer, 2 μl of 5× Q-Solution, 400 nM of each primer and 1.5 μl of bisulfite-modified (20 μl-eluted) genomic DNA sample. The following primers were used- F: 5'-TGTTTATTGGTGTGGGAGTTGTG-3' and R: 5'-CAAAACCCTCCACATACCTACAAC-3' to detect unmethylated CpG sites, and F: 5'-GTTTATTGGTGTGGGAGTCGC-3' and R: 5'-CAAAACCCTCCACATACCTACAAC-3' for methylated CpG sites.

For human samples, genomic DNA samples were isolated from fresh frozen gastric tissue of 3 E-cadherin-negative patients, using DNeasy Blood & Tissue Kit (Qiagen) according to the manufacturer's protocol. Methylation-specific PCR for human *CDH1* was performed as described above. Primers were designed as reported previously (Graff, Herman et al. 1997). The following primers were targeted to the CpG island 1; F: 5'-TAATTTTAGCTTAGAGGGTTATTGT-3' and R: 5'-CACAACCAATCAACAACACA-3' for unmethylated CpG sites, and F: 5'-TTAGGTTAGAGGGTTATCGCGT-3' and R: 5'-TAACTAAAAATTCACCTACCGAC-3' for methylated CpG sites. The following primers were targeted to the CpG island 2; F: 5'-

GGTGGGTGGGTTGTTAGTTTTGT-3' and R: 5'-AACTCACAAATCTTTACAATTCCAACA-3' for unmethylated CpG sites, and F: 5'-GTGGGCGGGTCGTTAGTTTC-3' and R: 5'-CTCACAAATACTTTACAATTCCGACG-3' for methylated CpG sites. The following primers were targeted to the CpG island 3; F: 5'-GGTAGGTGAATTTTTAGTTAATTAGTGGTA-3' and R: 5'-ACCCATAACTAACCAAAAACACCA-3' for unmethylated CpG sites, and F: 5'-GGTGAATTTTTAGTTAATTAGCGGTAC-3' and R: 5'-CATAACTAACCGAAAACGCCG-3' for methylated CpG sites. The following primers were targeted to the CpG island 4; F: 5'-GGGGTGTTTGGTTGTGGAGTTT-3' and R: 5'-TTCCCTCAAAAATCATCCCCAC-3' for unmethylated CpG sites, and F: 5'-GCGTTTGGTCGCGGAGTTC-3' and R: 5'-TTCCCTCAAAAATCGTCCCCAC-3' for methylated CpG sites.

In vivo 5-aza-2'-deoxycitidine (5-Aza) challenge

5-aza-2'-deoxycytidine (5-Aza) was purchased from Sigma-Aldrich (St. Louis, MO). 5-Aza was dissolved in DMSO to a concentration of 10 mM. Two *Pdx-1-Cre;Smad4*$^{F/F}$*;Trp53*$^{F/F}$*;Cdh1*$^{F/+}$ mice were given 2.5 mg/kg of 5-Aza by intraperitoneal injection in a volume of 1.1 μl DMSO per gram body weight (Day 1). The same dose was repeated on Day 3. Three days after the first 5-Aza dose, mice were sacrificed and

fresh frozen gastric cancer tissue was subjected to RNA isolation and real-time RT-PCR as described above.

In vivo Trichostatin A treatment

Trichostatin A (TSA) was purchased from Sigma-Aldrich. Gastric cancer of a *Pdx-1-Cre;Smad4*$^{F/F}$*;Trp53*$^{F/F}$*;Cdh1*$^{F/+}$ mouse was harvested at the necropsy, and immediately minced into small tissue fragments using scissors and blades in RPMI-1640 media supplemented with 10% FBS. Tissue fragments were incubated in the media containing TSA for 24 hours. Then, tissue fragments were collected and total proteins extraction was performed using T-PER Tissue Protein Extraction Reagent (Thermo Fisher Scientific).

Exome sequencing of human samples

Frozen gastric cancer tissue samples and adjacent normal tissue samples were obtained, with the IRB approval and signed informed consents, from 13 gastric cancer patients who underwent gastrectomy at Keimyung University Dongsan Hospital in Taegu, Korea, and at Asan Medical Center in Seoul, Korea. Tissue samples were cryosectioned and H&E-stained. Guided by the H&E-stained top slide, macrodissection was performed for each sample. Median tumor nuclei content in all tumor samples was 75%. 20 mg of each of macrodissected normal and cancerous tissues were pulverized

using metal mortar and pestle. Tissue powder was subjected to total RNA and genomic DNA isolation, using *mir*Vana™ Kit (Ambion, TX) and DNeasy Blood & Tissue Kit (Qiagen), respectively. Total RNA was treated with DNase I (Sigma) using the following reagents: 1/10 volume of DNase I buffer, 1/10 volume of DNase I, 1/20 volume of dithiothreotol (DTT, Qiagen) and 1/40 volume of RNass inhibitor (RNasin, Promega, WI). Then, the total RNA was purified by using Trizol (Ambion), following manufacturer's instruction. In-solution RNase A (100mg/ml, Qiagen) treatment was performed for isolated genomic DNA. Exome sequencing was performed using HiSeq 2000 instrument (Illumina, Hayward, CA), after capturing using SureSelect Human All Exon V4+UTR kit (Agilent Technologies, Santa Clara, CA). Fastq files were aligned and duplicates were removed using BWA and PICARD, respectively. Somatic single nucleotide variations were identified and annotated using VarScan and Annovar, respectively.

PCR test for Helicobacter pylori (H. pylori)

Genomic DNA was isolated from fresh frozen tissue sample obtained from adjacent normal tissue of 13 young gastric cancer patients analyzed in this study. Primers to detect the 16S rDNA gene of H. pylori were designed as described in a study of H. pylori murine vaccine model (Roussel, Harris et al. 2007). PCR reaction mixture contained 0.15 μl of *i*-StarTaq (Intron), 1.5 μl of 2.5 mM

dNTP, 1.5 μl of 10× PCR buffer, 500 nM of each primer (F:5'-TTTGTTAGAGAAGATAATGACGGTATCTAAC-3' and R:5'-CATAGGATTTCACACCTGACTGACTATC-3'), 3 μl of 5× Q-solution (Qiagen) and 30 ng of genomic DNA in a final volume of 15 μl. Cycling conditions were as follows: 2 min at 95℃, followed by 60 cycles each consisting of 35 s at 94℃, 30 s at 57℃ and 30 s at 72℃, and 3 min at 72℃. Distilled water and H. pylori DNA (1 mM and 0.1 mM, mixed with SNU-16 cells), was used as negative and positive controls, respectively.

Results

Gastric tumors formed in Pdx-1-Cre;Smad4$^{F/F}$;Trp53$^{F/F}$;Cdh1$^{F/+}$ mice recapitulate human diffuse-type gastric adenocarcinomas

Twenty one of 25 *Pdx-1-Cre;Smad4$^{F/F}$;Trp53$^{F/F}$;Cdh1$^{F/+}$* mice (84%) developed spontaneous tumors in the glandular stomach (Table 1). The most common cause of death in *Pdx-1-Cre;Smad4$^{F/F}$;Trp53$^{F/F}$;Cdh1$^{F/+}$* mice was duodenal obstruction, followed by gastric outlet obstruction. Grossly, these mutant mice developed ulceroinfiltrative gastric tumors mainly at pyloric antrum and gastroduodenal junction (Fig 1Aii). Histologically, tumors arising in the glandular stomach of *Pdx-1-Cre;Smad4$^{F/F}$;Trp53$^{F/F}$;Cdh1$^{F/+}$* mice resemble human diffuse-type gastric adenocarcinomas based on the H&E findings, and were invasive into muscle layers and regional lymph nodes (Fig 1B).

Duodenal adenocarcinomas and forestomach squamous cell carcinomas were also identified in 36% and 24% of these mice, respectively (Table 1). In addition, 2 mice were noted to have adenocarcinomas in the pancreas (8%), which were interpreted as invasion of primary duodenal or gastric adenocarcinomas. This pattern of tumor distribution is consistent with the known tissue-specificity of the *Pdx-1* promoter (Larsson, Madsen et al. 1996).

Since gastric adenocarcinoma was the most common type of carcinoma in *Pdx-1-Cre;Smad4$^{F/F}$;Trp53$^{F/F}$;Cdh1$^{F/+}$* mice, we

focused our analysis on adenocarcinomas arising in the glandular stomach. DNA microarray and immunohistochemistry analyses of gastric cancers arising from *Pdx−1−Cre;Trp53*$^{F/F}$*;Cdh1*$^{F/+}$ mice compared to normal stomach epithelium revealed that these tumors were positive for mucin 6 and TFF2, and negative for mucin 5a, pepsinogen C, somatostatin, and gastric intrinsic factors, suggesting the deep antral gland origin of these tumors (Ho, Takamura et al. 2004) (Fig 2).

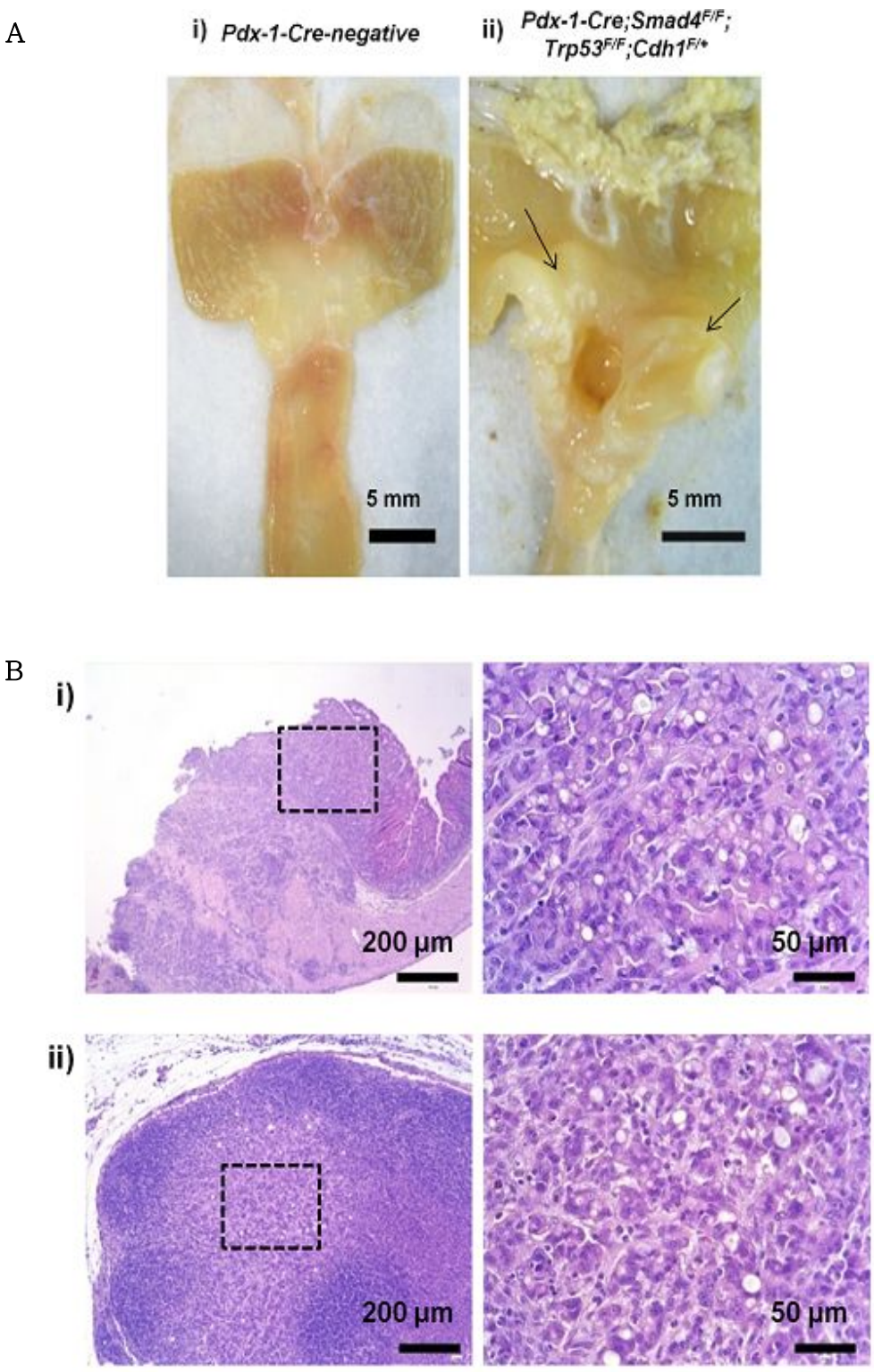
A
i) Pdx-1-Cre-negative
ii) Pdx-1-Cre;Smad4F/F;
Trp53F/F;Cdh1F/+
5 mm
5 mm
B
i)
200 µm
50 µm
ii)
200 µm
50 µm

Fig 1. (A) Representative gross feature of a gastric cancer (*arrows*), an ulceroinfiltrative mass in the antral mucosa, arising in *Pdx-1-Cre;Smad4*$^{F/F}$*;Trp53*$^{F/F}$*;Cdh1*$^{F/+}$ mice *(Aii).* Gastric lumen of a *Pdx-1-Cre*-negative mouse of the same age is shown for comparison (*Ai).* (B) Representative histologic findings of the gastric cancer (*Bi*) and lymph node metastasis (*Bii*). Boxed regions of left panels are shown at higher magnification in the right panels.

Table 1. Incidence of adenocarcinomas in each organ according to the genotype

Genotype	Median gastric adenocarcinoma −free survival	Stomach	Duodenum	Pancreas	Distant Metastasis
Pdx1−Cre; Smad4$^{F/F}$;Trp53$^{F/F}$; Cdh1$^{F/+}$	8.0 months	21/25 (84%)	9/25 (36%)	2/25 (8%)	3/25 (12%)
Pdx1−Cre; Smad4$^{F/F}$;Trp53$^{F/F}$	Not reached	1/28 (3.5%)	13/28 (46.4%)	1/28 (3.5%)	0/28 (0%)
Pdx1−Cre; Trp53$^{F/F}$;Cdh1$^{F/F}$	9.4 months	6/15 (40%)	0/15 (0%)	1/15 (6.7%)	0/15 (0%)
Pdx1−Cre; Trp53$^{F/F}$;Cdh1$^{F/+}$	Not reached	0/7 (0%)	0/7 (0%)	0/7 (0%)	0/7 (0%)

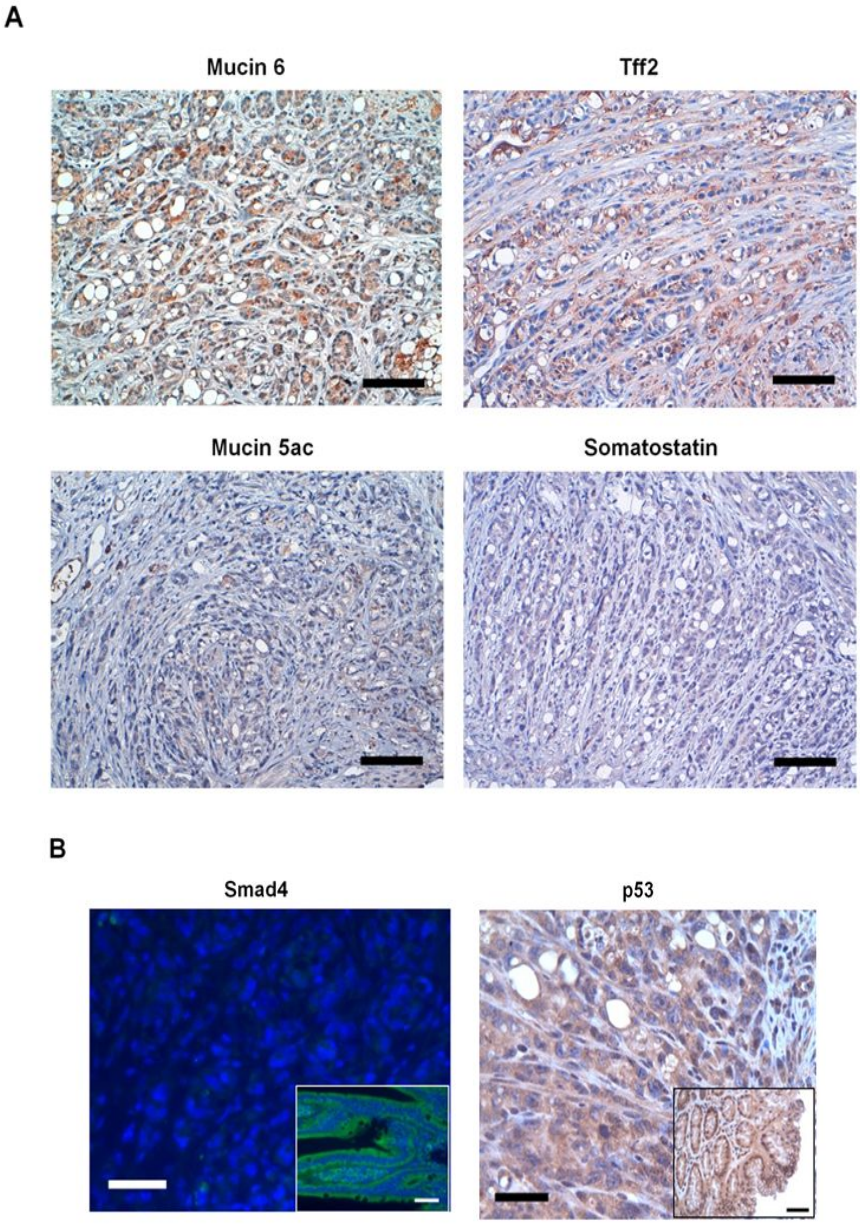

Fig 2. (A) Immunohistochemistry for the tissue origin of the gastric adenocarcinomas arising in *Pdx-1-Cre;Smad4*$^{F/F}$*;Trp53*$^{F/F}$*;Cdh1*$^{F/+}$ mice. Bar=100 μm.(B) Immunofluorescence and immunohistochemistry for the confirmation of loss of Smad4 and p53 in *Pdx-1-Cre;Smad4*$^{F/F}$*;Trp53*$^{F/F}$*;Cdh1*$^{F/+}$ tumors. Bar=50 μm.

E-cadherin loss is required for the development of diffuse-type gastric adenocarcinoma

Scheduled sacrifices performed at 4 and 5 months revealed no gastric premalignant lesions, such as atrophic gastritis, metaplasia, or dysplasia, in *Pdx-1-Cre;Smad4*$^{F/F}$*;Trp53*$^{F/F}$*;Cdh1*$^{F/+}$ mice. In 2 of 4 *Pdx-1-Cre;Smad4*$^{F/F}$*;Trp53*$^{F/F}$*;Cdh1*$^{F/+}$ mice screened at 6 months of age, intramucosal adenocarcinomas were observed (Fig 3Ai). Interestingly, E-cadherin immunostaining was lost in adenocarcinoma cells by 6 months of age, suggesting that E-cadherin loss is an early event required for the diffuse-type gastric carcinogenesis in mice.

To further evaluate the role of E-cadherin in constraining diffuse-type gastric carcinogenesis, a cohort (n=25) of *Pdx-1-Cre;Smad4*$^{F/F}$*;Trp53*$^{F/F}$*;Cdh1*$^{F/+}$ mice was compared with a cohort (n=28) of *Pdx-1-Cre;Smad4*$^{F/F}$*;Trp53*$^{F/F}$ mice. The median gastric adenocarcinoma-free survival of *Pdx-1-Cre;Smad4*$^{F/F}$*;Trp53*$^{F/F}$*;Cdh1*$^{F/+}$ was 8.0 months, while only one gastric adenocarcinoma was identified by a scheduled sacrifice at 9 month of age, in the *Pdx-1-Cre;Smad4*$^{F/F}$*;Trp53*$^{F/F}$ mouse cohort [Log-rank $P<0.001$] (Fig 3B). Whereas E-cadherin was retained in a gastric adenocarcinoma arising in *Pdx-1-Cre;Smad4*$^{F/F}$*;Trp53*$^{F/F}$ (Fig 3Aii).

E-cadherin loss in the stomach epithelium was also identified in a gastric adenocarcinoma arising in our *Villin-Cre*-positive mice (Fig 3C), and is therefore not limited to the *Pdx-1* developmental context.

A

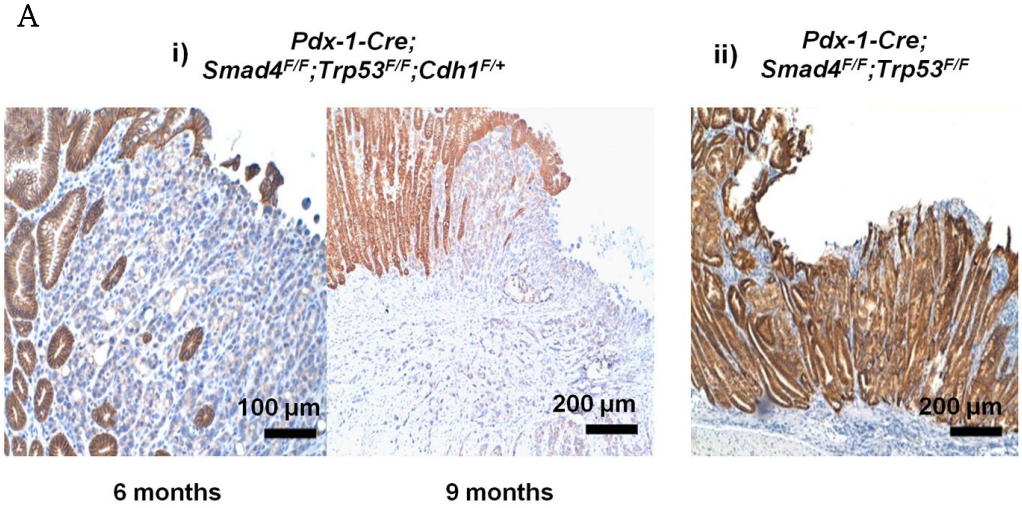
i) Pdx-1-Cre; Smad4F/F;Trp53F/F;Cdh1F/+
ii) Pdx-1-Cre; Smad4F/F;Trp53F/F
100 µm
200 µm
200 µm
6 months
9 months

B

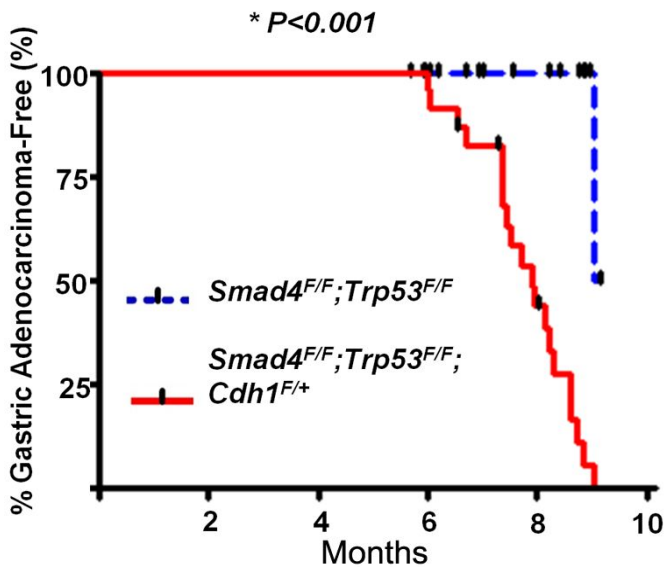
* P<0.001
% Gastric Adenocarcinoma-Free (%)
100
75
50
25
2
4
6
8
10
Months
Smad4F/F;Trp53F/F
Smad4F/F;Trp53F/F; Cdh1F/+

C

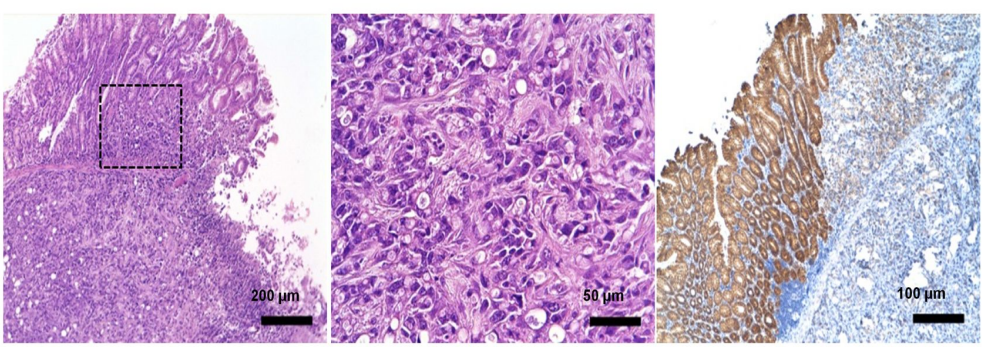
200 µm
50 µm
100 µm

Fig 3. (A) Representative E-cadherin immunohistochemical staining of gastric adenocarcinomas arising in *Pdx-1-Cre;Smad4$^{F/F}$;Trp53$^{F/F}$;Cdh1$^{F/+}$* mice at 6 and 9 months of age *(Ai)*. Gastric adenocaricnoma arising in a *Pdx-1-Cre;Smad4$^{F/F}$;Trp53$^{F/F}$* mouse demonstrates strong membranous staining of E-cadherin *(Aii)*. (B) Gastric adenocarcinoma-free survivals of *Pdx-1-Cre;Smad4$^{F/F}$;Trp53$^{F/F}$;Cdh1$^{F/+}$* (n=25) compared with *Pdx-1-Cre;Smad4$^{F/F}$;Trp53$^{F/F}$* mice (n=28). (C) Loss of E-cadherin expression in stomach cancer arising in *Villin-Cre;Smad4$^{F/F}$;Trp53$^{F/F}$;Cdh1$^{F/+}$* mouse. The boxed region of left panel was shown at higher magnification in middle panel.

E-cadherin was retained in intestinal and mammary adenocarcinomas of Cdh1 heterozygotes

All of the gastric adenocarcinomas arising in *Pdx-1-Cre;Smad4$^{F/F}$;Trp53$^{F/F}$;Cdh1$^{F/+}$* mice were negative for E-cadherin immunostaining, and all of the gastric adenocarcinomas analyzed from this group were also found to express low levels of *Cdh1* mRNA compared with normal tissue (Fig 4A and 4B).

In contrast to the differences in the incidences of gastric adenocarcinomas between the genotypes, duodenal adenocarcinoma-free survival was similar between *Pdx-1-Cre;Smad4$^{F/F}$;Trp53$^{F/F}$;Cdh1$^{F/+}$* and *Pdx-1-Cre;Smad4$^{F/F}$;Trp53$^{F/F}$* mice [9.0 *vs* 9.1 months; Log-rank *P*=0.15] (Fig 5A). E-cadherin was retained in duodenal adenocarcinomas arising in *Pdx-1-Cre;Smad4$^{F/F}$;Trp53$^{F/F}$;Cdh1$^{F/+}$* mice, and, therefore, was relatively overexpressed compared with gastric adenocarcinomas from the same mice (Fig 4A and 4B). Next, we evaluated intestinal and mammary adenocarcinomas in mice created through the loss of the same set of genes using *Villin-Cre* and *MMTV-Cre* transgenes, respectively, to compare the tumor promoting effects of E-cadherin heterozygosity across the different target tissues. Intestinal adenocarcinoma-free survival was similar between *Villin-Cre;Smad4$^{F/F}$;Trp53$^{F/F}$;Cdh1$^{F/+}$* and *Villin-Cre;Smad4$^{F/F}$;Trp53$^{F/F}$* mice [5.2 *vs* 5.4 months; Log-rank *P*=0.27] (Fig 5B). No distant metastases were observed in either genotype, except for one

Villin-Cre;Smad4$^{F/F}$*;Trp53*$^{F/F}$*;Cdh1*$^{F/+}$ mouse developing skin metastasis. E-cadherin was retained in intestinal adenocarcinomas formed in *Villin-Cre;Smad4*$^{F/F}$*;Trp53*$^{F/F}$*;Cdh1*$^{F/+}$ mice (Fig 4A and 4B). *MMTV-Cre;Smad4*$^{F/F}$*;Trp53*$^{F/F}$*;Cdh1*$^{F/+}$ and *MMTV-Cre;Smad4*$^{F/F}$*;Trp53*$^{F/F}$ mice were also not different in the mammary carcinoma-free survival [10.4 *vs* 12.1 months; Log-rank *P*=0.73] and lung metastasis [33.3% (3/9) *vs* 35.7% (5/14), respectively; *P* for Chi-square test=0.91] (Fig 5C). Histologically, *MMTV-Cre;Smad4*$^{F/F}$*;Trp53*$^{F/F}$*;Cdh1*$^{F/+}$ tumors were invasive ductal carcinomas with a squamous component (Fig 6). Mammary adenocarcinomas arising in *MMTV-Cre;Smad4*$^{F/F}$*;Trp53*$^{F/F}$*;Cdh1*$^{F/+}$ mice also retained E-cadherin (Fig 4A and 4B), perhaps accounting for why lobular carcinomas were not observed in this model as has been reported in *K14cre;Trp53*$^{F/F}$*;Cdh1*$^{F/F}$ (Derksen, Liu et al. 2006). These results clearly demonstrate that E-cadherin loss is important for the development of gastric adenocarcinomas, but not for the development of intestinal or mammary adenocarcinomas.

A

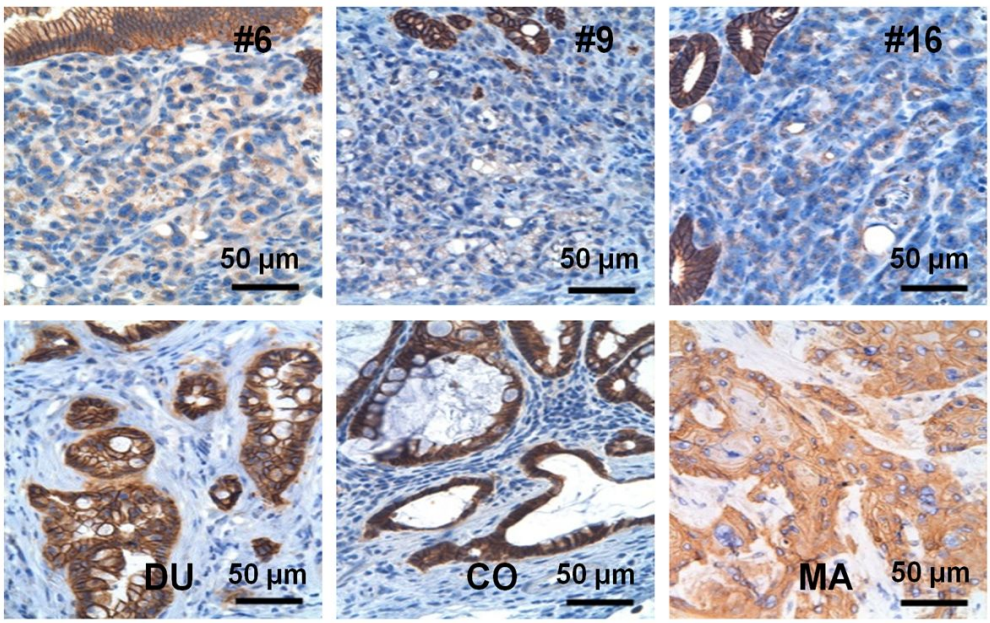
#6
50 μm
#9
50 μm
#16
50 μm
DU
50 μm
CO
50 μm
MA
50 μm

B

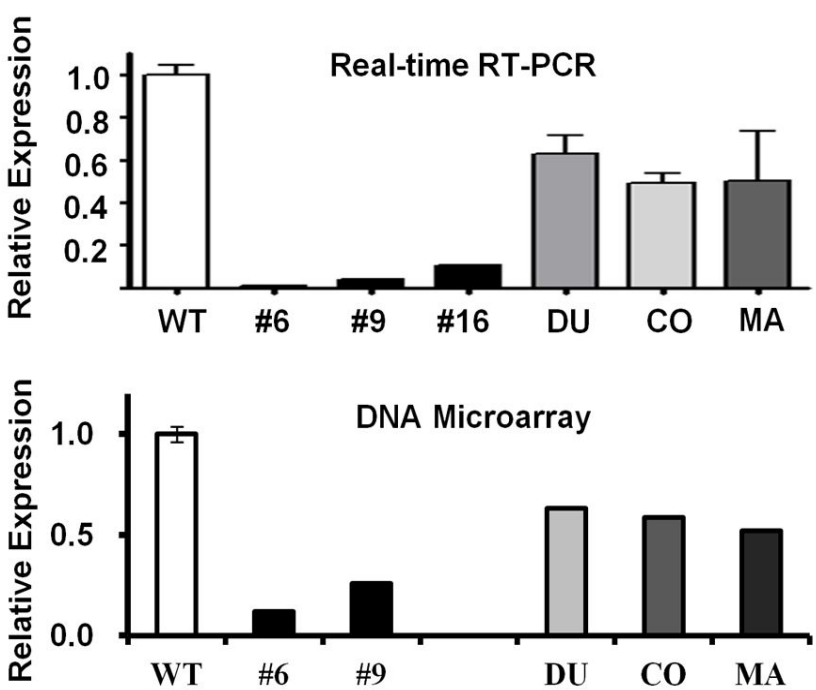
Real-time RT-PCR
Relative Expression
1.0
0.8
0.6
0.4
0.2
WT
#6
#9
#16
DU
CO
MA
DNA Microarray
Relative Expression
1.0
0.5
0.0
WT
#6
#9
DU
CO
MA

Fig 4. (A) E-cadherin immunostaining of gastric adenocarcinomas in upper panels(#6, #9, and #16) arising in three representative *Pdx-1-Cre;Smad4*$^{F/F}$*;Trp53*$^{F/F}$*;Cdh1*$^{F/+}$ mice, duodenal adenocarcinoma (*DU*) from *Pdx-1-Cre;Smad4*$^{F/F}$*;Trp53*$^{F/F}$*;Cdh1*$^{F/+}$ mice, colorectal adenocarcinoma (*CO*) from *Villin-Cre;Smad4*$^{F/F}$*;Trp53*$^{F/F}$*;Cdh1*$^{F/+}$ mice, and mammary adenocarcinoma (*MA*) from *MMTV-Cre;Smad4*$^{F/F}$*;Trp53*$^{F/F}$*;Cdh1*$^{F/+}$ mice. (B) RNA expression levels from Real-time RT-PCR and DNA microarray analysis (in linear scales) for *Cdh1* of tumors relative to normal stomach of *Cre*-negative mice (*WT*). Error bars represent SDs.

A

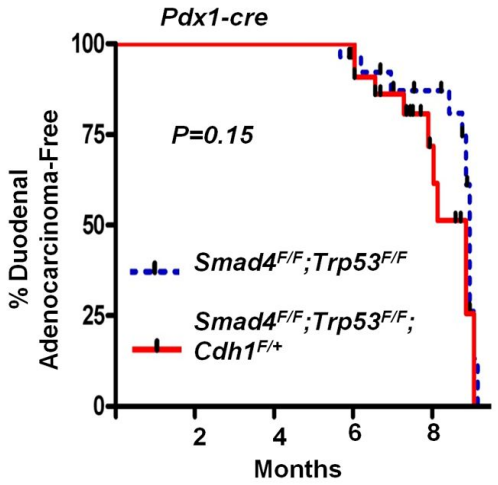
Pdx1-cre
100
75
50
25
0
% Duodenal Adenocarcinoma-Free
P=0.15
Smad4F/F;Trp53F/F
Smad4F/F;Trp53F/F;
Cdh1F/+
2
4
6
8
Months

B

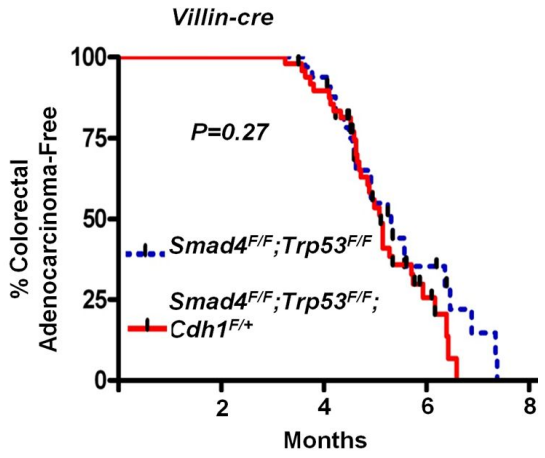
Villin-cre
100
75
50
25
0
% Colorectal Adenocarcinoma-Free
P=0.27
Smad4F/F;Trp53F/F
Smad4F/F;Trp53F/F;
Cdh1F/+
2
4
6
8
Months

C

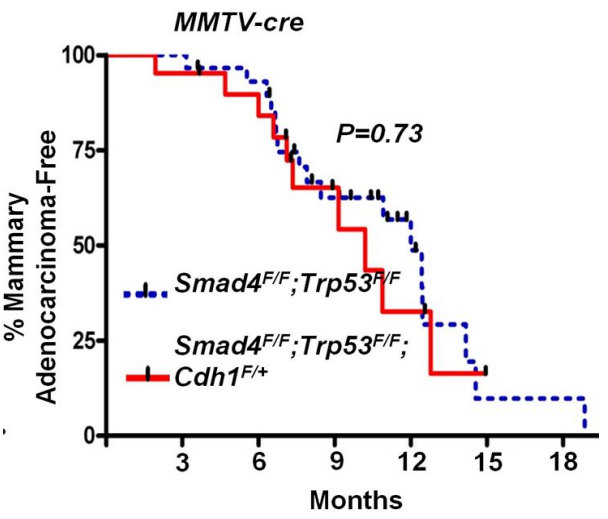
MMTV-cre
100
75
50
25
0
% Mammary Adenocarcinoma-Free
P=0.73
Smad4F/F;Trp53F/F
Smad4F/F;Trp53F/F;
Cdh1F/+
3
6
9
12
15
18
Months

Fig 5. (A) Duodenal adenocarcinoma-free survival of *Pdx-1-Cre;Smad4$^{F/F}$;Trp53$^{F/F}$;Cdh1$^{F/+}$* mice compared with *Pdx-1-Cre;Smad4$^{F/F}$;Trp53$^{F/F}$* mice. (B) Colorectal adenocarcinoma-free survival of *Villin-Cre;Smad4$^{F/F}$;Trp53$^{F/F}$;Cdh1$^{F/+}$* mice compared with *Villin-Cre;Smad4$^{F/F}$;Trp53$^{F/F}$* mice. (C) Mammary adenocarcinoma-free survival of *MMTV-Cre;Smad4$^{F/F}$;Trp53$^{F/F}$;Cdh1$^{F/+}$* mice compared with *MMTV-Cre;Smad4$^{F/F}$;Trp53$^{F/F}$* mice.

A

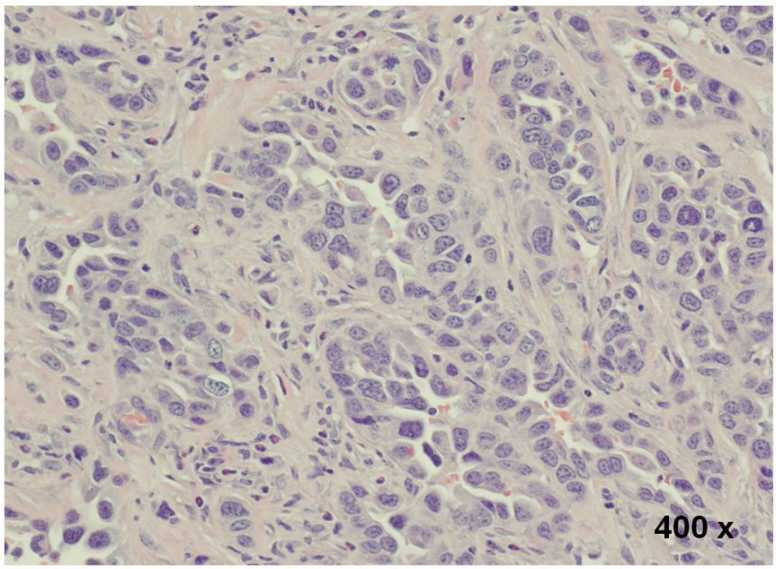

B

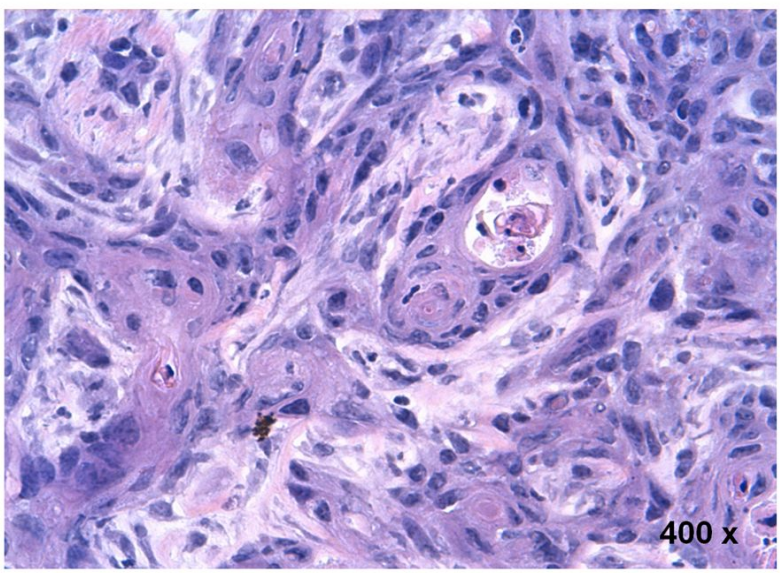

Fig 6. Histopathological findings of mammary adenocarcinoma arising in *MMTV-Cre;Smad4$^{F/F}$;Trp53$^{F/F}$;Cdh1$^{F/+}$*. *(A)* These tumors showed morphological features of invasive ductal adenocarcinoma (B) with a squamous component.

E-cadherin loss was not related to DNA promoter methylation.

First of all, we investigated the promoter hypermethylation of *Cdh1* of these mouse gastric cancers because it is identified in up to 80% of patients with diffuse-type gastric cancers and is the most common second hit in the inactivation of wild type *CDH1* allele. Methylation-specific PCR and bisulfite genomic sequencing analyses of the *Cdh1* promoter in these gastric adenocarcinomas did not show any evidence for *Cdh1* promoter hypermethylation (Fig 7A). Moreover, the treatment with 5-aza-deoxycitidine (5-Aza), a demethylating agent, on these mutant mice bearing gastric cancer did not up-regulate E-cadherin (Fig 7B). Next, we investigated other epigenetic changes leading to the loss of E-cadherin such as histone deacethylation and microRNA regulation. E-cadherin was not up-regulated in the tissue explants of a gastric adenocarcinoma from a *Pdx-1-Cre;Smad4*$^{F/F}$*;Trp53*$^{F/F}$*;Cdh1*$^{F/+}$ mouse after 24-h exposure to TSA, inhibitor of histone deacetylase (Fig 8A). MicroRNA microarray analyses revealed no differences in expression levels of microRNAs targeting *Cdh1*, such as miR-9, between *Pdx-1-Cre;Trp53*$^{F/F}$*;Cdh1*$^{F/+}$ gastric adenocarcinomas and normal tissue (*data not shown*). LOH was not the major cause of E-cadherin loss because LOH at the *Cdh1* locus was identified in 2 of 17 *Pdx-1-Cre;Trp53*$^{F/F}$*;Cdh1*$^{F/+}$ gastric adenocarcinomas tested (11.8%) (Fig 8B). Finally, to investigate the transcriptional repression of *Cdh1* gene by *Snai, Zeb* and *Twist* family members,

we additionally performed DNA microarray analysis of duodenal cancers arising in these Chd1 heterozygous mice. However, mRNA expression levels of these families were high both in the gastric and duodenal tumors compared with normal tissue, and were not different between the gastric cancer tumors which lost E-cad expression and the duodenal cancers which maintained E-cad expression.

A

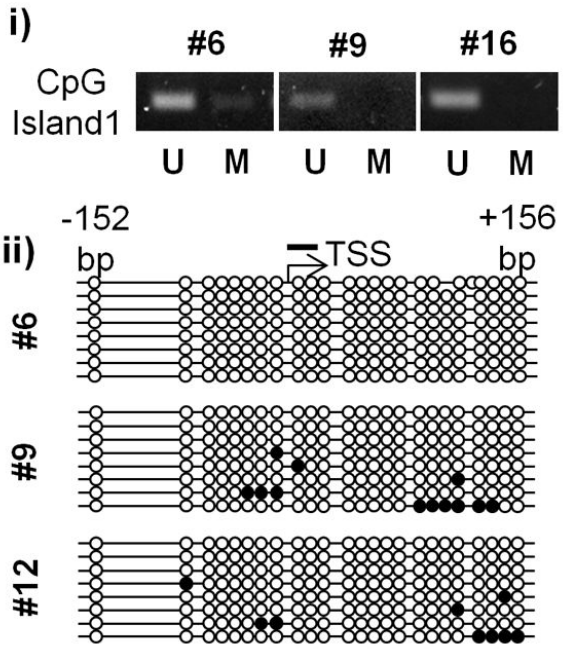
i)
#6
#9
#16
CpG
Island1
U M U M U M
ii)
-152
bp
TSS
+156
bp
#6
#9
#12

B

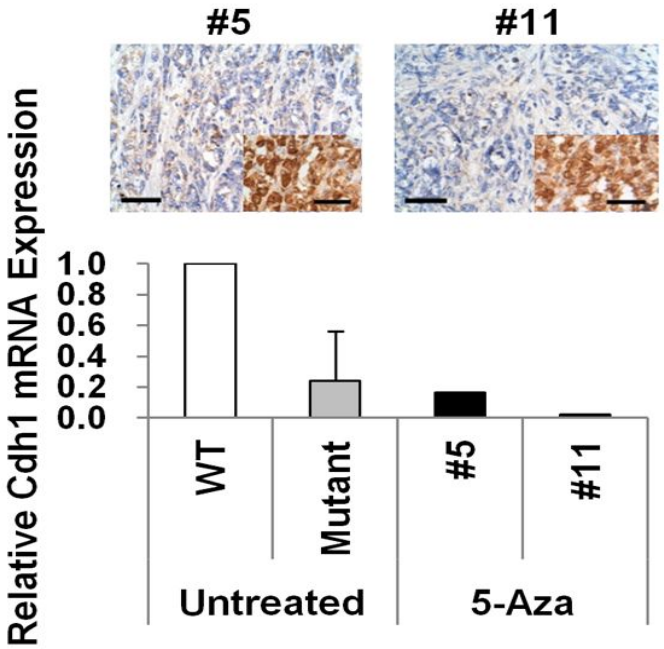
#5
#11
Relative Cdh1 mRNA Expression
1.0
0.8
0.6
0.4
0.2
0.0
WT
Mutant
#5
#11
Untreated
5-Aza

Fig 7. (A*i*) Methylation-specific PCR of the mouse gastric carcinomas shown in Fig 4A. (A*ii*) Bisulfite genomic sequencing analyses of the *Cdh1* promoter in these gastric adenocarcinomas. Open and closed circles represent unmethylated (*U*) and methylated (*M*) CpG sites, respectively (*TSS, transcription start site*). A black bar indicates a CpG site targeted by (A*i*). (B) E-cadherin immunostaining (*top panels; Inset, E-cadherin-positive adjacent normal gastric mucosa*) and real-time RT-PCR for gastric adenocarcinomas from two *Pdx-1-Cre;Smad4*$^{F/F}$*;Trp53*$^{F/F}$*;Cdh1*$^{F/+}$ mice (#5 and #11) treated with 5-aza-deoxycitidine (5-Aza). Mice were sacrificed 3 days after intraperitoneal injections of 2.5mg/kg of 5-aza on days 1 and 3. Gastric mucosa of a *Cre*-negative mouse (*WT*) and a gastric adenocarcinoma from untreated *Pdx-1-Cre;Smad4*$^{F/F}$*;Trp53*$^{F/F}$*;Cdh1*$^{F/+}$ mouse (*Mutant)* were used as references. E-cadherin was not significantly up-regulated after 5-Aza treatment.

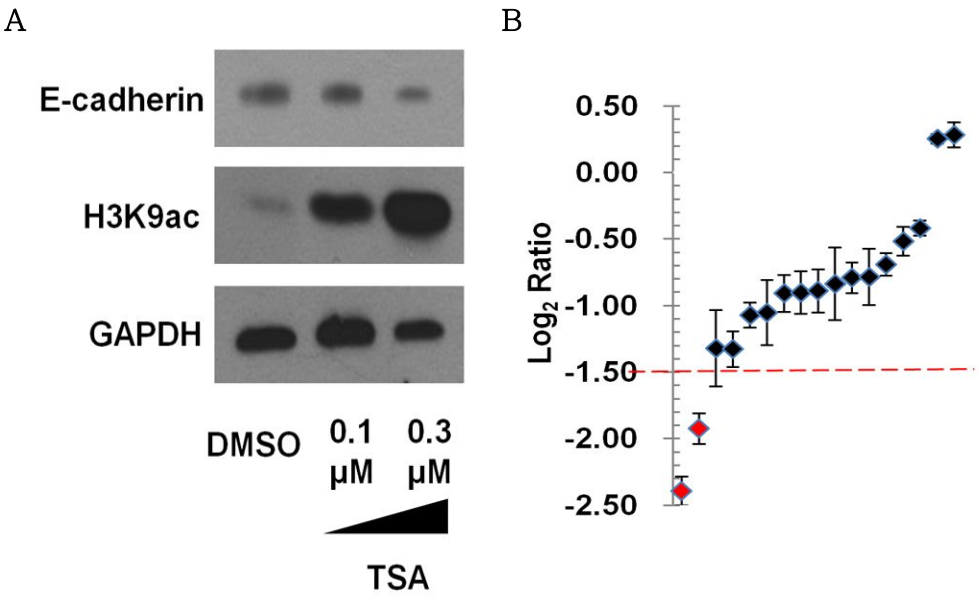

Fig 8. (A) Western blot analysis for E-cadherin of the tissue explants of a gastric adenocarcinoma from a *Pdx-1-Cre;Smad4*$^{F/F}$*;Trp53*$^{F/F}$*;Cdh1*$^{F/+}$ mouse after 24-h exposure to 0.1 μM and 0.3 μM of TSA. Acetyl- histone H3 lysine 9 (H3K9ac) was immunoblotted as a positive control. (B) Genomic DNA real-time PCR for the *Cdh1* gene in adenocarcinomas arising in *Pdx-1-Cre;Smad4*$^{F/F}$*;Trp53*$^{F/F}$*;Cdh1*$^{F/+}$ mice to evaluate LOH. Log_2 ratio of each tumor to *Cre*-negative gastric mucosa is depicted. LOH was defined as the average log_2 ratio of three probes (for exons 6, 8, and 10) of tumor to normal DNA < −1.5 (*broken red line*).

Comparisons with human diffuse-type gastric cancers

It was surprising to us that the *Cdh1* promoter was not significantly methylated in gastric adenocarcinomas formed in our *Cdh1* heterozygous mice. In human diffuse-type gastric cancers, the *CDH1* promoter hypermethylation has been identified in up to 80% of patients. To gain further insight into the clinical relevance of this mouse tumor data, we examined the E-cadherin mutation profiles of 13 young (≤ 40 years old) Korean gastric cancer patients (Table 2). Three of 13 (23.1%) patients demonstrated very low levels of E-cadherin immunostaining and mRNA expression (Fig 9A and 9B), and one of them harbored a germline missense *CDH1* mutation (c.1018A>G (p.T340A)) (Fig 10) that was previously reported in a hereditary diffuse gastric cancer kindred (Oliveira, Bordin et al. 2002). Promoter hypermethylation of the *CDH1* gene was not identified in any of the three E-cadherin-negative patients (Fig 11). Thus, transcriptional repression of *CDH1* possibly due to epigenetic changes other than promoter methylation may be a mechanism for E-cadherin inactivation in humans as in our mutant mice.

Table 2. Clinicopathologic characteristics of young gastric cancer patients

	E-cadherin immunostaining	
	Positive *(n=10)*	Negative *(n=3)*
Median age (yr)	35.5	36.5
Female	6 (60%)	1 (33%)
H. pylori-negative	2 (20%)	2 (66.7%)
Histologic type		
Poorly differentiated tubular	5 (50%)	2 (66.7%)
Signet ring cell carcinoma	5 (50%)	1 (33.3%)
Stage, AJCC		
II	1 (10%)	2 (66.7%)
III	2 (20%)	1 (33.3%)
IV	7 (70%)	0

*AJCC: American Joint Committee on Cancer (7^{th} Edition)

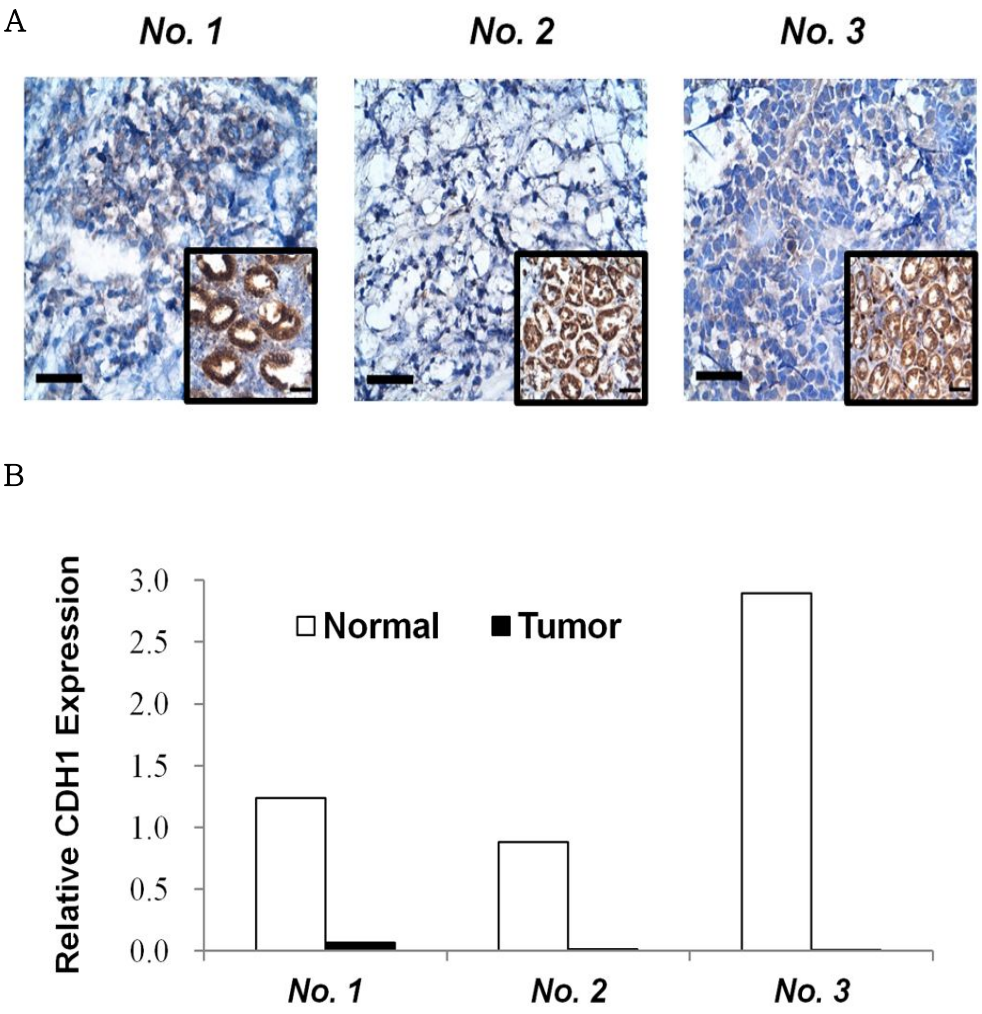

Fig 9. (A) E-cadherin immunostaining of an early-onset human gastric cancer. Adjacent normal tissue of the same patient was positive (*inset*). (B) The *CDH1* real-time RT-PCR expression level of each human gastric cancer relative to adjacent normal tissue.

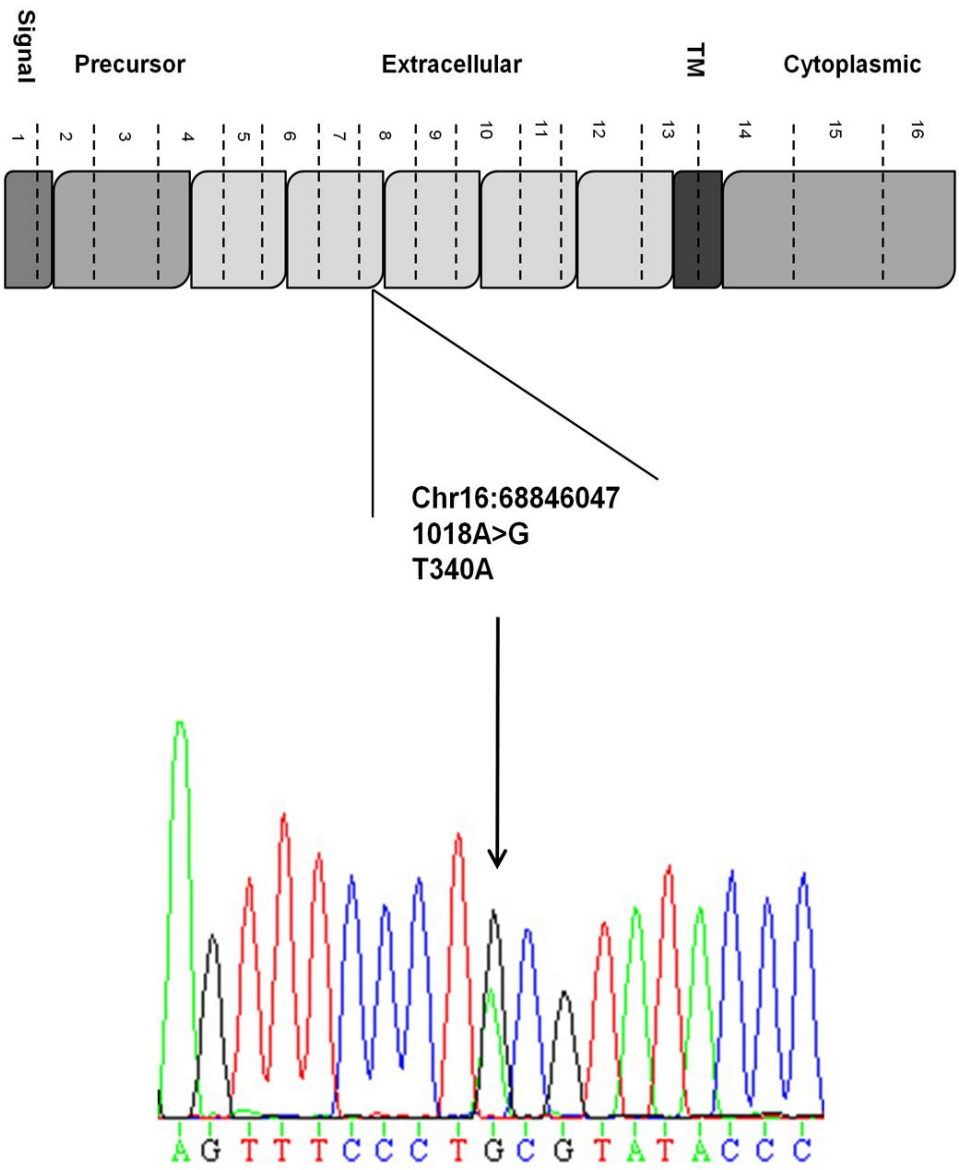

Fig 10. Direct sequencing analysis of the region of the mutation using Buffy coat genomic DNA from the patient with *CDH1* missense germline mutation (c.1018A>G, p.T340A).

A

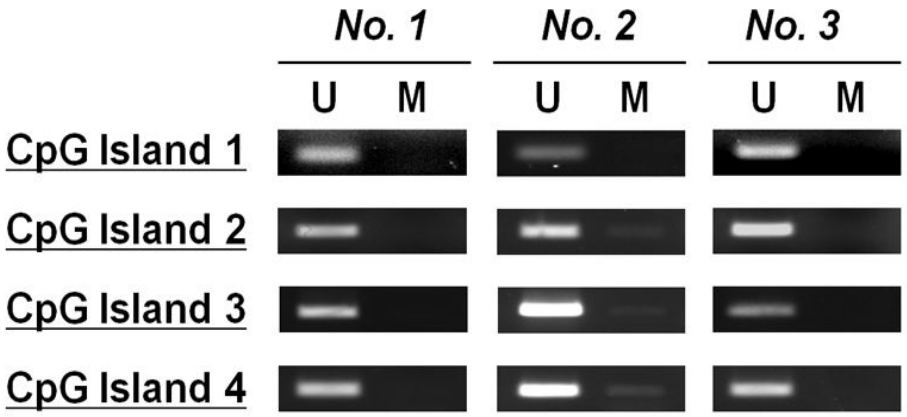

B

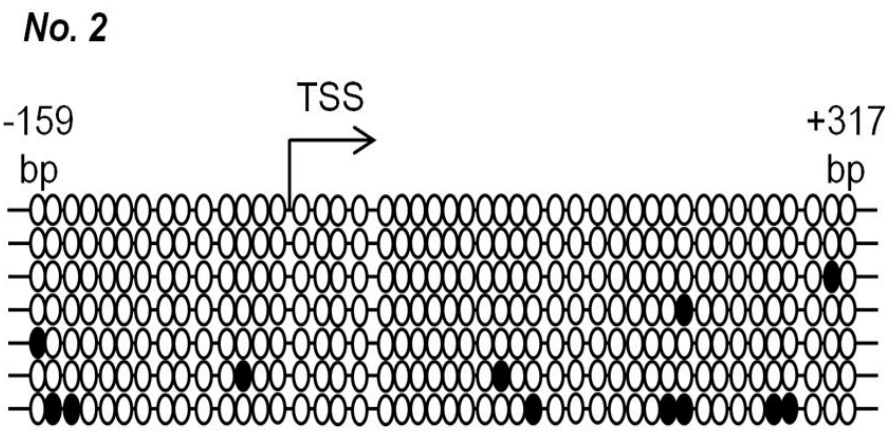

Fig 11. (A) Methylation-specific PCR analysis of human gastric cancers for CpG sites of *CDH1* promoter, demonstrating no evidence of significant *CDH1* promoter hypermethylation (U, unmethylated; M, methylated CpG sites). (B) Bisulfite genomic sequencing analysis of the *Cdh1* promoter in the gastric cancer with a germline missense *CDH1* mutation.

Discussion

Pdx-1-Cre;Smad4$^{F/F}$*;Trp53*$^{F/F}$*;Cdh1*$^{F/+}$ mice described in this study are unique in several aspects. In contrast to previously reported spontaneous murine gastric tumors, which are of parietal cell or neuroendocrine lineage (Graff, Herman et al. 1997; Roussel, Harris et al. 2007; Gutierrez, Dahlberg et al. 2010; Shimada, Mimata et al. 2012), gastric adenocarcinomas formed in these mice are of the mucus-secreting gastric epithelial cell origin. In addition, tumor suppressor genes most commonly inactivated in human diffuse-type gastric adenocarcinomas were targeted to be knocked-out in the gastroduodenal epithelium of this model (Becker, Atkinson et al. 1994; Maesawa, Tamura et al. 1995; Schmierer and Hill 2007; Wang, Kim et al. 2007). While Smad4 is inactivated in 40% of human gastric cancers (Wang, Kim et al. 2007), functional roles of Smad4 in gastric cancer progression have not been fully evaluated using *in vivo* models. This study provides functional evidence for the role of Smad4 in suppressing gastric cancer progression. Although this study focused on gastric adenocarcinomas, it also demonstrates a role of Smad4 in suppressing duodenal carcinomas. While *Pdx-1-Cre;Trp53*$^{F/F}$*;Cdh1*$^{F/F}$ mice developed no duodenal carcinomas, the additional loss of Smad4 significantly promoted duodenal carcinomas (Table 1), confirming that Smad4 loss in the intestinal epithelium promotes carcinogenesis (Takaku, Oshima et al.

1998). Possibly, if *Pdx-1-Cre; Smad4$^{F/F}$;Trp53$^{F/F}$* mice did not die of duodenal obstruction, they might have developed gastric or even pancreatic cancers at later time points.

The specific role of E-cadherin loss in the development of diffuse-type gastric adenocarcinomas was clearly documented by this cross-tissue tumorigenesis study. These results validate and extend a prior study suggesting a role for E-cadherin in the development of gastric cancer (Shimada, Mimata et al. 2012). The inactivation of the wild type *CDH1* allele in germline mutation carriers is generally thought to be promoted by environmental and physiological factors such as diet, carcinogen exposure and inflammation (Sirard, de la Pompa et al. 1998; Machado, Oliveira et al. 2001; Rosivatz, Becker et al. 2002). Humar, *et al.* reported that E-cadherin loss is a consistent finding in the MNU-induced gastric cancer model (Humar, Blair et al. 2009). In contrast, E-cadherin expression was lost in gastric tumors from our mutant mice carrying one mutant allele without any exposure to exogenous carcinogens (Oliveira, Sousa et al. 2009). E-cadherin loss in the stomach epithelium was also identified in a gastric adenocarcinoma arising in our *Villin-Cre*-positive mice (Fig 4), and is therefore not limited to the *Pdx-1* developmental context. In contrast to breast cancers arising in humans with germline E-cadherin mutation, mammary adenocarcinomas arising in *MMTV-Cre;Smad4$^{F/F}$;Trp53$^{F/F}$;Cdh1$^{F/+}$* mice retained E-cadherin

expression, and were not more aggressive than tumors arising in *MMTV-Cre;Smad4*$^{F/F}$*;Trp53*$^{F/F}$ mice. Thus, the selection pressure for E-cadherin loss may be relatively low in the context of the mouse mammary gland, compared with the stomach. This is consistent with the lower lifetime risk for breast cancer than for stomach cancer in germline E-cadherin mutation carriers (Pharoah, Guilford et al. 2001). Studies are ongoing in our laboratory to identify gastric tissue-specific epigenetic events or signaling pathway activation leading to E-cadherin loss that may be promoted by loss of Smad4 or p53.

CHAPTER II.

LOSS OF E-CADHERIN AND SMAD4 COOPERATE TO PROMOTE THE METASTASIS OF DIFFUSE-TYPE GASTRIC ADENOCARCINOMA.

Abstract

To date, only a few genetically-engineered mouse models of gastric cancer have been reported, and none of them develop distant metastasis. Notably, 14.3% of gastric adenocarcinomas arising in *Pdx-1-Cre;Smad4$^{F/F}$;Trp53$^{F/F}$;Cdh1$^{F/+}$* mice metastasized to the lung, which is a highly unique finding for a genetically engineered mouse model for gastric cancers. To dissect the roles of E-cadherin and Smad4 in gastric cancer progression and metastasis, we generated Smad4 intact mutant mice, *Pdx-1-Cre;Trp53$^{F/F}$;Cdh1$^{F/F}$* mice. *Pdx-1-Cre;Smad4$^{F/F}$;Trp53$^{F/F}$;Cdh1$^{F/+}$* mice developed gastric adenocarcinomas more rapidly than *Pdx-1-Cre;$^{F/F}$;Trp53$^{F/F}$;Cdh1$^{F/F}$* mice and the gastric adenocarcinomas formed in *Pdx-1-Cre;Smad4$^{F/F}$;Trp53$^{F/F}$;Cdh1$^{F/+}$* mice were more invasive than those arising in *Pdx-1-Cre; Trp53$^{F/F}$;Cdh1$^{F/F}$* mice. Lung metastases were not identified in *Pdx-1-Cre;Trp53$^{F/F}$;Cdh1^{Ff+}* mice. Nuclear β-catenin accumulation was identified at the invasive tumor front of gastric adenocarcinomas arising in *Pdx-1-Cre;Smad4$^{F/F}$;Trp53$^{F/F}$;Cdh1$^{F/+}$* mice while this phenotype was less prominent in mice with intact E-cadherin or Smad4, indicating that the inhibition of β-catenin signaling by E-cadherin or Smad4 may down-regulate signaling pathways involved in metastases in *Pdx-1-Cre;Smad4$^{F/F}$;Trp53$^{F/F}$;Cdh1$^{F/+}$* mice. Knockdown of β-catenin significantly inhibited migratory activity of *Pdx-1-Cre;Smad4$^{F/F}$;Trp53$^{F/F}$;Cdh1$^{F/+}$* cell lines. Thus, loss of E-cadherin and Smad4 cooperate with p53 loss to promote the metastatic progression of gastric adenocarcinomas.

Introduction

E-cadherin, an epithelial cell adhesion molecule is on protein prominently associated with tumor invasiveness and metastasis on progression of cancers (Fukamachi, Shimada et al. 2011; Qiao and Gumucio 2011; Jaiswal, Breitsprecher et al. 2013). E-cadherin loss in cancer contributes to metastasis by inducing wide-range of transcriptional and functional change as well as disruption of cell to cell contacts (Pharoah, Guilford et al. 2001). E-cadherin loss influenced localization pattern and activation of the E-cadherin binding partner β-catenin (Pharoah, Guilford et al. 2001), which has been associated with the induction of EMTs in various contexts.

Recent study showed that *Atp4b-Cre;Cdh1*$^{F/F}$*;Trp53*$^{F/F}$ mice developed diffuse-type gastric cancers . However this mouse gastric cancers did not metastasize to the distant visceral organs and nuclear β-catenin accumulation was not detected in the tumors (Shimada, Mimata et al. 2012). Thus, gastric cancer metastasis may require a concerted action of key molecular events in addition to loss of E-cadherin.

Smad4 is a co-Smad involved in both branches of the TGF-β/BMP signaling system (Schmierer and Hill 2007). The anti-metastatic role of Smad4 in gastric cancer, which has not been previously demonstrated *in vivo*, is in line with previous data for colorectal and prostate cancers (Takaku, Oshima et al. 1998; Humar, Blair et al. 2009). Possible mechanisms for the anti-metastatic role

of Smad4 may include suppression of proliferation, leading to proliferative dormancy (Oliveira, Sousa et al. 2009).

To date, only a few genetically-engineered mouse models of gastric cancer have been reported, and none of them develop distant metastases. Notably, 14.3% of gastric adenocarcinomas arising in *Pdx-1-Cre;Smad4*$^{F/F}$*;Trp53*$^{F/F}$*;Cdh1*$^{F/+}$ mice metastasized to the lung, which is a highly unique finding for a genetically engineered mouse model for gastric cancers. We demonstrated that the metastatic phenotype of *Pdx-1-Cre;Smad4*$^{F/F}$*;Trp53*$^{F/F}$*;Cdh1*$^{F/+}$ mice may be attributable in part to Smad4 loss-induced β-catenin activation following E-cadherin loss. The metastatic phenotype of our mutant mice provides a unique opportunity to dissect the roles of E-cadherin and Smad4 in gastric cancer progression, and in relation to EMT.

Materials and Methods

Mice

Mouse studies were conducted with the approval of the Animal Care and Use Committees of National Cancer Center of Korea and the National Cancer Institute, Bethesda, MD. *Pdx-1-Cre* mice (B6.FVB-Tg(Ipf1-cre)1Tuv), originally generated by Dr. Lowy (Hingorani, Petricoin et al. 2003), were provided through the Mouse Models of Human Cancers Consortium (MMHCC) repository at the NCI Frederick Cancer Research Center. FVB.129-*Trp53*^{tm1Brn} (Jonkers, Meuwissen et al. 2001) mice were also provided by the MMHCC. B6.129-*Cdh1*^{tm2Kem}/J mice, which have *loxP* sites flanking exons 6-10, were purchased from The Jackson Laboratory (Boussadia, Kutsch et al. 2002). Conditional Smad4 knockout mice (*Smad4*$^{F/F}$) on the Black Swiss, B6 and 129 backgrounds were previously described (Yang, Li et al. 2002).
Compound conditional knockouts of Smad4, p53, and E-cadherin were bred with *Pdx-1-Cre* mice. Offspring mice were genotyped using polymerase chain reaction (PCR) assays for tail DNA. PCR genotyping primers were previously listed in Chapter I.

Quantitative real-time RT-PCR (QRT-PCR)

For mouse samples, total RNA was isolated from fresh frozen tissue using AllPrep DNA/RNA/Protein Mini Kit (Qiagen, Valencia, CA) according to the manufacturer's instructions. Stroma was

trimmed out using an H&E-stained top slide, before RNA isolation. 0.3 μg of total RNA was reverse transcribed using random hexamers and *amfiRivertII* Reverse Transcriptase (GenDEPOT, Barker, TX) according to the manufacturer's standard protocols. For human samples, total RNA was isolated from fresh frozen tissue using *mir*Vana^{TM} Isolation Kit (Ambion), according to the manufacturer's instructions. Stroma was trimmed out using a H&E-stained top slide, before RNA isolation. Isolated RNA was treated with DNase I (Sigma, St. Louis, MO) according to the manufacturer's protocol. Total RNA was reverse transcribed using random hexamers by using SuperScript III First-Strand Synthesis System (Invitrogen) according to the manufacturer's standard protocol. PCR reactions were performed on a Roche LC480 (Roche Diagnostics, Penzberg, Germany) using QuantiTect SYBR Green PCR Master Mix (Qiagen). QRT-PCR primers for mouse gene were

F: 5'-ACGATGAGGACCAGGTGGTAG-3' and

R: 5'-CAGTACAACGAGCTGTCTCTAC-3' for *Ctnnb1,*

F: 5'-GTGCGCCAGCAGTATGAAAG-3' and

R: 5'-GCATCGTTGTTCCGGTTGG-3' for *Vim,*

F: 5'-ACTTACCTCGGATCGTAGTG-3' and

R: 5'-TCTCCATGATCTCTCCTTGC-3' for *Mmp7,*

F: 5'-ATCCTGGTGCCTTGATGTAC-3' and

R: 5'-GTCTGAAGGTCCATAGATTGTC-3' for *Mmp8,*

F: 5'-CCAGCAGATTTCAAGGTGGAC-3' and

R: 5'-TTACAGCTACCTGCCACTTTTC-3' for *Cdh2,*

F: 5'-CACACGCTGCCTTGTGTCT-3' and

R: 5'-GGTCAGCAAAAGCACGGTT-3' for *Snai1,*

F: 5'-CCTTGGGGCGTGTAAGTCC-3' and

R: 5'-TTCTCAGCTTCGATGGCATGG-3' for *Snai2,*

F: 5'-TGATGAAAACGGAACACCAGATG-3' and

R: 5'-GTTGTCCTCGTTCTTCTCATGG-3' for *Zeb1,*

F: 5'-AGCGACACGGCCATTATTTAC-3' and

R: 5'-GTTGGGCAAAAGCATCTGGAG-3' for *Zeb2,*

F: 5'-GGACAAGCTGAGCAAGATTCA-3' and

R: 5'-CGGAGAAGGCGTAGCTGAG-3' for *Twist1,*

F: 5'-ACGAGCGTCTCAGCTACGCC-3' and

R: 5'-AGGTGGGTCCTGGCTTGCGG-3' for *Twist2* and

F: 5'-GGTCGGTGTGAACGGATTTG-3' and

R: 5'-GTGAGTGGAGTCATACTGGAAC-3' for *Gapdh.*

Primary cell culture from mouse cancer tissue

Tumor arising in these mutant mice was minced into small pieces and digested with collagenase for 30 min at 37 ° C. Single tumor cells were seeded into plated on a 60-mm dish in RPMI 1640 media with 20% fetal bovine serum (FBS), 100 U/ml of penicillin, and 0.1 mg/ml of streptomycin in humidified incubator at 37 ° C in an atmosphere of 5% CO_2.

Immunohistochemistry and immunofluorescence

The mouse tissues were fixed in neutral buffered 10% formalin, processed by standard methods and embedded in paraffin. 5 μm cross paraffin sections were dewaxed, rehydrated and subjected to antigen retrieval for immunostaining by heating at 100℃ for 20 minutes in 0.01 M citrate buffer (pH 6.0). The ABC method (Vectastain Elite ABC kit and Vectastain M.O.M. kit, Vector Laboratories, Burlingame, CA) was used according to the manufacturer's protocol. The slides were subjected to colorimetric detection with ImmPact DAB substrate (SK-4105, Vector Laboratories). The slides were counterstained with Meyer' s hematoxylin for 10 seconds. Negative controls were performed by omitting the primary antibody and substitution with diluent. The following antibodies were used in this study; rabbit polyclonal anti E-cadherin antibody (1:200; Cell Signaling, #3195), mouse monoclonal anti β-catenin antibody (1:200; BD, 610154), rabbit monoclonal anti Vimentin antibody (1:100; Cell signaling, #5741), rabbit monoclonal anti MMP7 antibody (1:100; Cell signaling, #3801), and rabbit monoclonal anti MMP8 antibody (1:100; Abcam, ab81286).

Positive cells for β-catenin was defined as tumor cells showing a distinct nuclear staining. Unequivocal immunohistochemical staining in tumor nucleus, as compared with normal gastric mucosa, was considered as the positive nuclear β-catenin staining. A positive

vimentin staining was defined as a strong cytoplasmic signal equivalent to that of normal mesenchymal tissues. A positive MMP7 staining was defined as a strong cytoplasmic signal which was unequivocally deeper than the background. At least three *200x* microscopic fields at the invasive front were examined by a pathologist to determine the average percentage of cells with positive β-catenin, vimentin, and MMP-7 staining. Differences in the percentage of positive immunostaining between genotypes were evaluated using Student *t*-test.

For immunofluorescence analyses, primary antibodies were incubated overnight at 4℃ and secondary antibodies (FITC goat anti-rabbit secondary antibody (1:250; Vector Laboratories FI-1000)) were incubated for 30 minutes at room temperature. Slides were mounted with Vectashield mounting media (Vector Laboratories, H-1200). Rabbit polyclonal anti Ki-67 antibody (1:200; Abcam, ab15580) were used as primary antibodies. At least three *200x* microscopic field was examined to assess the percentage of Ki-67 positive cells.

To stain the β-catenin in primary cultured cells, cells were seeded on coated coverslips with poly-L-lysine (P4707, Sigma, St. Louis, MO) at 1 x 10^5 cells per coverslip. After cells were grown for 24 hours at 37° C, the cells were fixed in ice-cold methanol for 10 minutes and blocked with PBS containing 5% of normal goat serum and 0.5% Triton X-100. Cells were incubated with β-

catenin antibody (1:100) overnight at 4° C, washed with PBS, and then incubated with Alexa Fluor 594 goat anti-mouse antibody (1:100; Life Technologies, A-11005, Carlsbad, CA) for 2 hours. Cells were imaged using using Axiovert 200M (Carl Zeiss, Oberkochen, Germany).

Western blot analysis

Mouse cancer cells were collected and lysed with T-PER Tissue Protein Extraction Reagent (Thermo Fisher Scientific, Hudson, NH, U.S.A) supplemented with protease inhibitors. After removal of cellular debris, protein concentration was quantitated by using a BCA reagent kit (Thermo Fisher Scientific) according to manufacturer's instruction. Equal amounts of protein were separated on SDS-polyacrylamide gel and transferred onto nitrocellulose membrane by electrophoresis and blotting apparatus (Bio-Rad, Hercules, CA). The proteins were probed with the relevant primary antibodies and horseradish peroxidase (HRP)-conjugated secondary antibodies at the recommended dilutions. Rabbit polyclonal anti E-cadherin antibody (1:1000; #3195, Cell Signaling, Danvers, MA), mouse monoclonal anti β-catenin antibody (1:1000; 610154, BD Transduction Laboratories), rabbit monoclonal anti Vimentin antibody (1:100; Cell signaling, #5741), and mouse monoclonal anti GAPDH (1:1000; sc-32233, Santa Cruz, CA) were applied. Immunodetection were performed by using an

enhanced chemiluminescence (ECL) detection kit (Thermo Fisher Scientific).

Measurement of β-catenin activity

β-catenin activities in primary cultured cancer cell lines were evaluated by using Cignal TCF/LEF reporter assay kit (CCS-018L, SA Biosciences, Frederick, MD). Primary cultured cells (2.5 x 10^4 cell per well) were plated in 24 wells 12 h before transfection. These cells were transiently transfected with the TCF/LEF reporter plasmid according to the protocol of the manufacturer using Lipofectamine 2000 transfection reagent (Life Technologies). 24 hours after the transfection, Opti-MEM medium was changed to RPMI 1640 containing 10% FBS. The cells were allowed to grow for one more day and luciferase assays were carried out using the dual luciferase reporter assay system (Promega, Madison, WI) according to the manufacturer's protocol. Light emission was quantified with a Victor 3 1420 luminescence microplate reader (Perkin-Elmer, Waltham, MA). The signals were normalized for transfection efficiency to the internal *Renilla* control.

Establishment of stable β-catenin knock down cells

The lentiviral Ctnnb1 shRNA constructs were purchased from Sigma-Aldrich (St. Louis, MO) with pLKO.1-puro eGFP control vector (Sigma, SHC005). The target set was generated from

accession number NM_007614.2: (1) CCGGGCGTTATCAAACCCTAGCCTTCTCGAGAAGGCTAGGGTTTGATAACGCTTTTT(2) CCGGCCCAAGCCTTAGTAAACATAACTCGAGTTATGTTTACTAAGGCTTGGGTTTTT. Lentiviruses were produced by cotransfecting shRNA-expressing vector and pMD2.G and psPAX2 constructs (Addgene) into 293T cells by using lipofectamine 2000 (Invitrogen). Viral supernatants were harvested 48 hours after transfection, filtered though a 0.45 μm filter, titered, and used to infect primary cultured cancer cells with 10 μg/mL polybrene. Cells were treated by 2 μg/mL puromycin at 48 hours after viral transduction and were selected for 3 days.

To measure monolayer growth rates of these cells, the cells were seeded on tissue culture 24 well plates at 2.5 x 104 cells/well in RPMI 1640 media containing 10% FBS. At 24 hours after seeding, the growth rates were evaluated by manual cell counting.

Migration assay

Primary cultured cells were plated on 24-well inserts with 8 μm pore (353097, BD) at 2.5 x 10^4/well in serum-free RPMI 1640 media. Media containing 10% FBS was added to 24-well insert plate (354578, BD) and cells were cultured at 37°C and 5% CO_2. At 24 h after plating, remaining cells were removed by gently scrapping the upper chamber with a wet cotton swab. Migrated cells

were fixed with 10% formalin for 10 min and washed with PBS once. The inserts were soaked in hematoxylin for 1 min and eosin for 5 min and then washed with tap water several times. Membranes were cut from inserts and moved to a glass slide. A few drops of Permount (Fisher Scientific, Waltham, MA) were added onto the membrane and the glass side was covered with cover slide evenly. The number of migrated cells was averaged by counting 3 high power fields (200x) and compared using Student t−test.

Results

Smad4 cooperates with E-cadherin in constraining the development of gastric adenocarcinoma by inhibiting cell cycle progression

No neoplastic lesions were found at the time of necropsy of *Pdx-1-Cre;Trp53*$^{F/F}$*;Cdh1*$^{F/+}$ mice (Fig 1A). These results suggest that loss of Smad4 was required for the development of gastric adenocarcinoma in *Pdx-1-Cre;Trp53*$^{F/F}$*;Cdh1*$^{F/+}$ mice [Log-rank *P*=0.005]. Since all of the *Pdx-1-Cre;Smad4*$^{F/F}$*;Trp53*$^{F/F}$*;Cdh1*$^{F/+}$ mice analyzed were found to develop E-cadherin-negative gastric adenocarcinomas, tumors from those mice were compared with tumors from *Pdx-1-Cre;Trp53*$^{F/F}$*;Cdh1*$^{F/F}$ mice. Six mice in the *Pdx-1-Cre;Trp53*$^{F/F}$*;Cdh1*$^{F/F}$ cohort (n=15) developed gastric adenocarcinomas with a median tumor-free survival of 9.4 months for this group (Fig 1A), but did not develop distant metastases. This phenotype is consistent with that of the previously reported *Atb4-Cre;Trp53*$^{F/F}$*;Cdh1*$^{F/F}$ mice (Shimada, Mimata et al. 2012). Gastric adenocarcinoma-free survival was significantly longer in *Pdx-1-Cre;Trp53*$^{F/F}$*;Cdh1*$^{F/F}$ mice than in *Pdx-1-Cre;Smad4*$^{F/F}$*;Trp53*$^{F/F}$*;Cdh1*$^{F/+}$ mice [median, 9.4 *vs* 8.0 months; Log-rank *P*=0.007], demonstrating the role of Smad4 in constraining gastric cancer progression (Fig 1A). Gastric adenocarcinomas formed in *Pdx-1-Cre;Trp53*$^{F/F}$*;Cdh1*$^{F/F}$ mice were less invasive than those arising in *Pdx-1-*

Cre;Smad4$^{F/F}$*;Trp53*$^{F/F}$*;Cdh1*$^{F/+}$ mice (Fig 1B). Gastric adenocarcinomas formed in *Pdx-1-Cre;Trp53*$^{F/F}$*;Cdh1*$^{F/F}$ mice exhibited lower Ki-67 positivity than *Pdx-1-Cre;Smad4*$^{F/F}$*;Trp53*$^{F/F}$*;Cdh1*$^{F/+}$ mice [median, 42.8% *vs* 71.7%, respectively; $P<0.001$], suggesting that Smad4 constrains tumor progression through the inhibition of the cell cycle (Fig 2A and 2B).

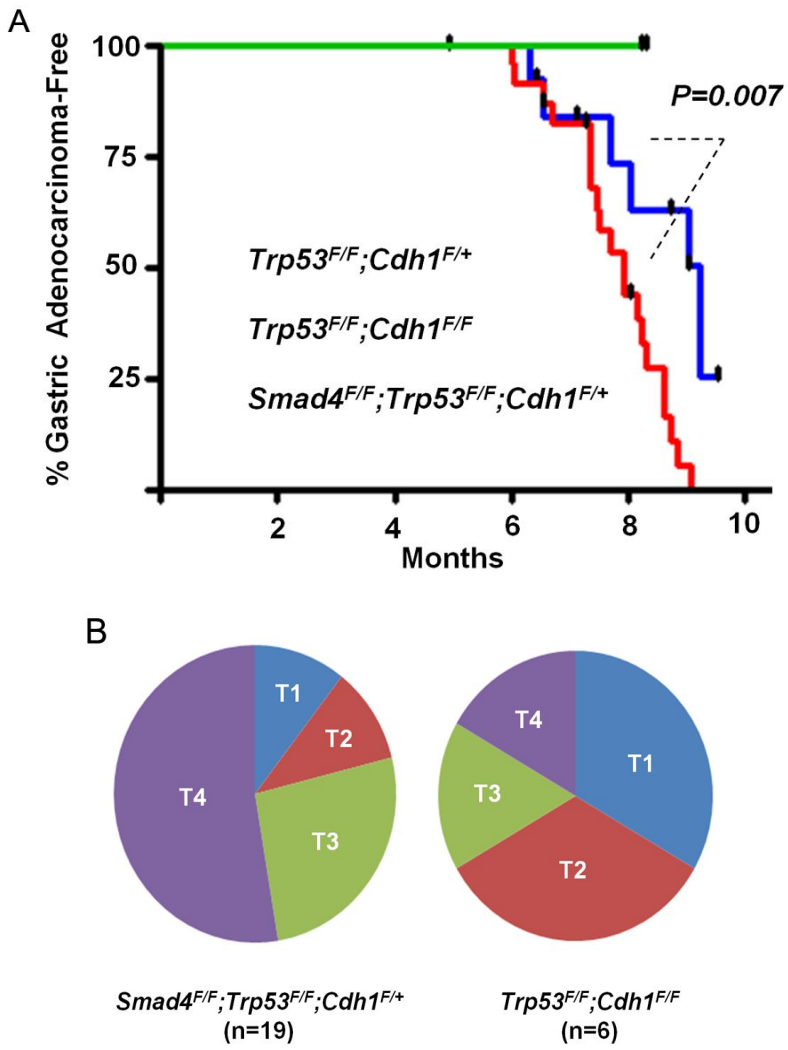

Fig 1. (A) Gastric adenocarcinoma-free survival of *Pdx-1-Cre;Smad4$^{F/F}$;Trp53$^{F/F}$;Cdh1$^{F/+}$* mice (n=25) compared with *Pdx-1-Cre;Trp53$^{F/F}$;Cdh1$^{F/F}$* mice (n=15) and with *Pdx-1-Cre;Trp53$^{F/F}$;Cdh1$^{F/+}$* mice which developed no tumors (n=7) (B) Depth of invasion between gastric adenocaricnomas arising in *Pdx-1-Cre;Smad4$^{F/F}$;Trp53$^{F/F}$;Cdh1$^{F/+}$* mice and *Pdx-1-Cre;Trp53$^{F/F}$;Cdh1$^{F/F}$* mice at 7 to 9 months of age. -, T1;Mucosa and Submucosa, T2; Muscularis propria, T3; Subserosa, T4;Serosa and adjacent structure infiltrating.

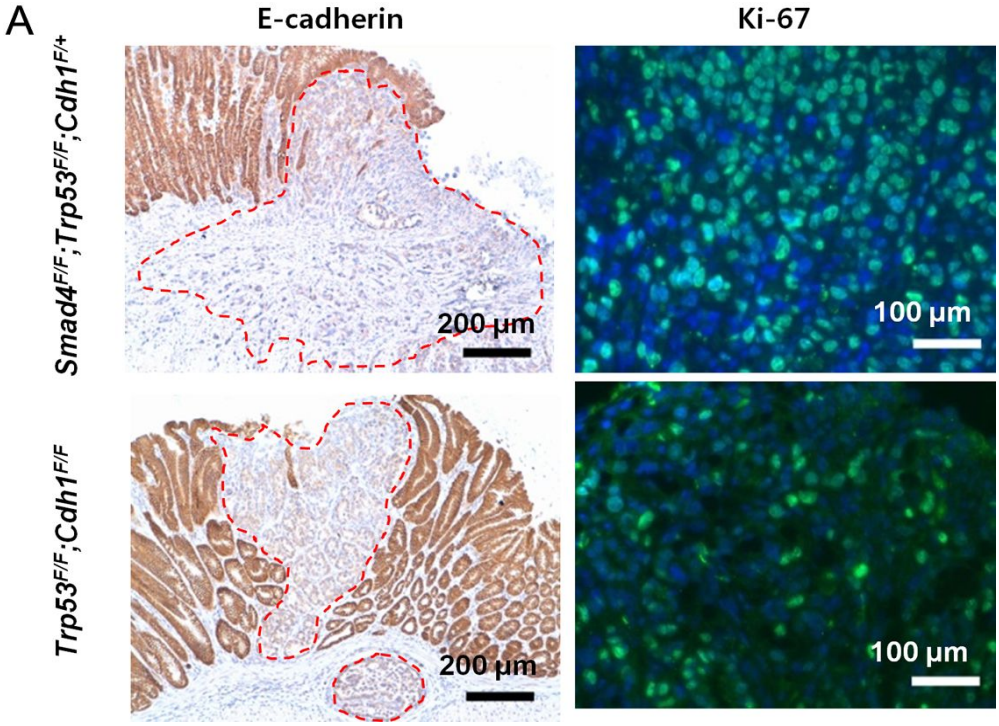
A
E-cadherin
Ki-67
Smad4F/F;Trp53F/F;Cdh1F/+
Trp53F/F;Cdh1F/F
200 µm
200 µm
100 µm
100 µm

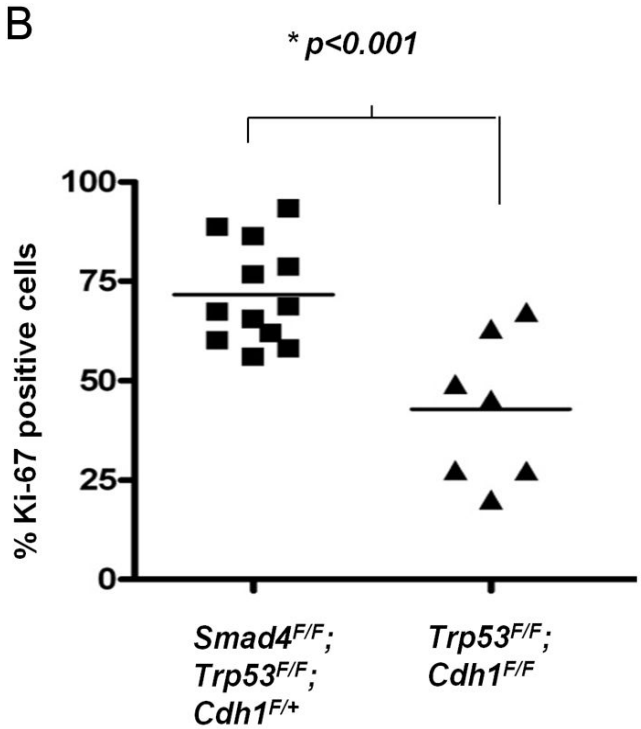
B
* p<0.001
% Ki-67 positive cells
100
75
50
25
0
Smad4F/F; Trp53F/F; Cdh1F/+
Trp53F/F; Cdh1F/F

Fig 2. (A) E-cadherin and Ki-67 immunoreactivity across genotypes. Representative E-cadherin immunohistochemical and Ki-67 immunofluoresence staining of gastric adenocarcinomas arising in *Pdx-1-Cre;Smad4*$^{F/F}$*;Trp53*$^{F/F}$*;Cdh1*$^{F/+}$ and *Pdx-1-Cre;Trp53*$^{F/F}$*;Cdh1*$^{F/F}$. Dotted red lines indicate tumor margins. (B) The percentage of Ki-67-positive cells in gastric adenocarcinomas arising in *Pdx-1-Cre;Trp53*$^{F/F}$*;Cdh1*$^{F/F}$ mice was lower than that of *Pdx-1-Cre;Smad4*$^{F/F}$*;Trp53*$^{F/F}$*;Cdh1*$^{F/+}$ mice.

Loss of E-cadherin and Smad4 cooperate to promote lung metastasis through the accumulation of nuclear β-catenin

Importantly, three of 21 *Pdx-1-Cre;Smad4*$^{F/F}$*;Trp53*$^{F/F}$*;Cdh1*$^{F/+}$ mice with gastric adenocarcinomas (14.2%) developed lung metastases (Fig 4). The metastatic lesions had similar histopathological features to the primary gastric tumors, including the lack of E-cadherin immunostaining (Fig 3). Prompted by the GSEA analyses showing the enrichment of *Lef1* target genes in the gastric cancers arising in *Pdx-1-Cre;Smad4*$^{F/F}$*;Trp53*$^{F/F}$*;Cdh1*$^{F/+}$ mice (Table 1), we sought to evaluate β-catenin immunostaining in the mutant mouse tumors. Nuclear β-catenin accumulation was identified at the invasive front of gastric adenocarcinomas from *Pdx-1-Cre;Smad4*$^{F/F}$*;Trp53*$^{F/F}$*;Cdh1*$^{F/+}$ mice, suggesting the association of nuclear β-catenin accumulation with tumor progression [*P* for *t*-test between the invasive front and tumor center<0.001] (Fig 5). β-catenin target genes, such as MMP7 and Vimentin, were focally overexpressed among nuclear β-catenin-positive carcinoma cells at the invasive front, suggesting an EMT (Fig 5). Ki-67 immunostaining was decreased at the invasive front of these mice, compared with the tumor center (Fig 5).

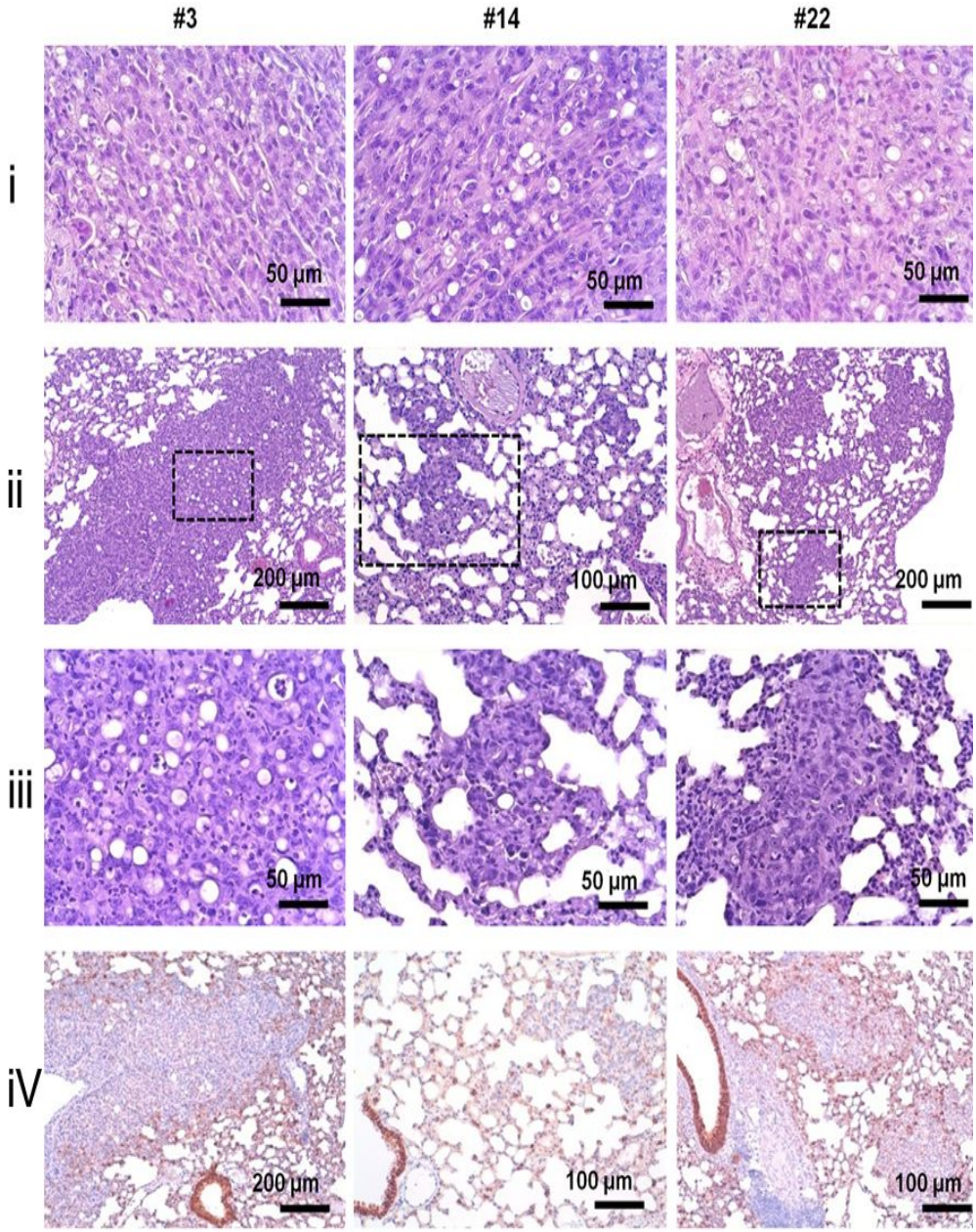

Fig 3. H&E (*Aii , Aiii*) and E−cadherin immunostaining (*Aiv*) of lung metastases of gastric carcinomas arising in three *Pdx−1−Cre;Smad4*$^{F/F}$*;Trp53*$^{F/F}$*;Cdh1*$^{F/+}$ mice (#3, #14, and #22). Corresponding primary tumors are shown in (*Ai*).

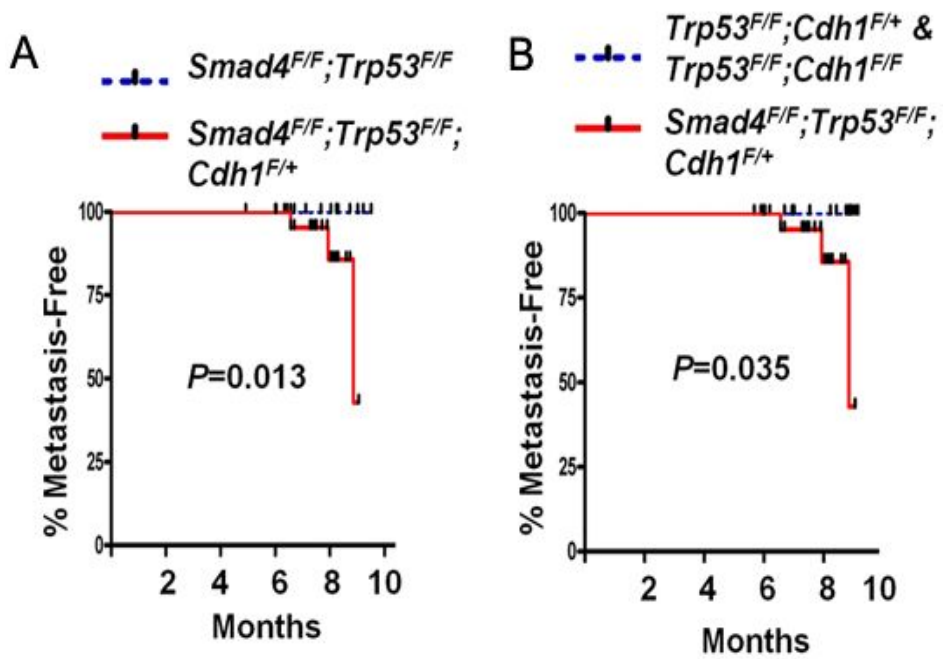

Fig 4. (A) Metastasis-free survival of *Pdx-1-Cre;Smad4$^{F/F}$;Trp53$^{F/F}$;Cdh1$^{F/+}$* compared with *Pdx-1-Cre;Smad4$^{F/F}$;Trp53$^{F/F}$* mice. (B) Metastasis-free survival of *Pdx-1-Cre;Smad4$^{F/F}$;Trp53$^{F/F}$;Cdh1$^{F/+}$* compared with *Pdx-1-Cre;Trp53$^{F/F}$;Cdh1$^{F/F}$ and Pdx-1-Cre; Trp53$^{F/F}$;Cdh1$^{F/+}$* mice

Table 1. Gene sets most enriched in 1,096 genes upregulated in gastric adenocarcinomas at $P < 0.001$

Gene set	Transcription Factor	*P* Value	*No.* genes in gene set	*No.* overlapping Genes
CAGGTG_V$E12_Q6	*Tcf3*	$<10^{-16}$	2485	162
CAGCTG_V$AP4_Q5	*Repin1*	$<10^{-16}$	1524	106
GATTGGY_V$NFY_Q6_01		$<10^{-16}$	1160	81
TTGTTT_V$FOXO4_01	*Mllt7*	$<10^{-16}$	2061	151
CTTTGA_V$LEF1_Q2	*Lef1*	$<10^{-16}$	1232	92
TATAAA_V$TATA_01	*Taf*	$<10^{-16}$	1296	100
GGGCGGR_V$SP1_Q6	*Sp1*	$<10^{-16}$	2940	229
GGGAGGRR_V$MAZ_Q6	*Maz*	$<10^{-16}$	2274	178
TGACAGNY_V$MEIS1_01	*Meis1*	$<10^{-16}$	827	65
GGGTGGRR_V$PAX4_03	*Pax4*	$<10^{-16}$	1294	102
AACTTT_UNKNOWN		$<10^{-16}$	1890	151
CTGCAGY_UNKNOWN		$<10^{-16}$	765	65
RNGTGGGC_UNKNOWN		$<10^{-16}$	766	66
TGGAAA_V$NFAT_Q4_01	*Nfat*	$<10^{-16}$	1896	164
TGANTCA_V$AP1_C	*Jun*	$<10^{-16}$	1121	99
CTTTGT_V$LEF1_Q2	*Lef1*	$<10^{-16}$	1972	182
RYTTCCTG_V$ETS2_B	*Ets2*	$<10^{-16}$	1085	111
TTTNNANAGCYR_UNKNOWN		$<10^{-16}$	133	29
KRCTCNNNNMANAGC_UNKNOWN		$<10^{-16}$	66	25
CACGTG_V$MYC_Q2	*v-Myc*	1.1×10^{-16}	1032	73

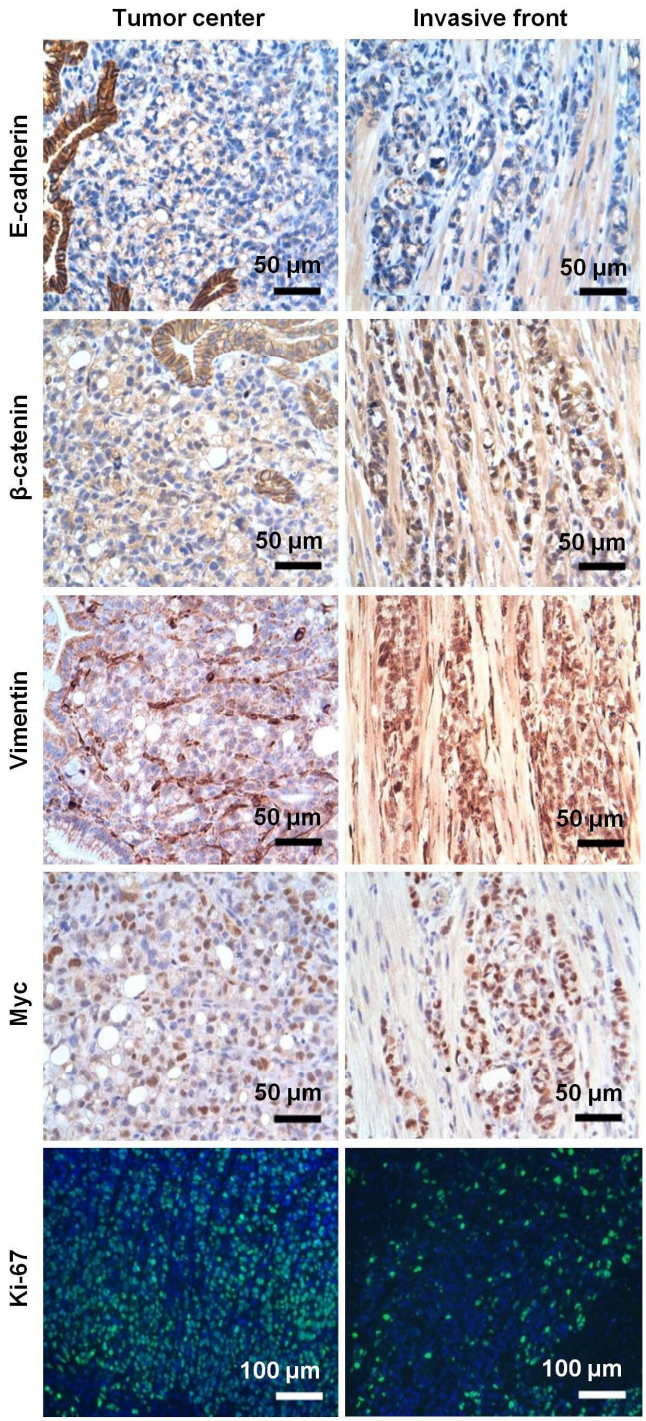

Fig 5. Immunohistochemistry for the tumor center and invasive front of gastric cancers formed in *Pdx-1-Cre;Smad4*$^{F/F}$*;Trp53*$^{F/F}$*;Cdh1*$^{F/+}$ mice.

The loss of E-cadherin and Smad4 expression cooperate to promote lung metastasis partly through the β-catenin activation

A gastric carcinoma from a *Pdx-1-Cre;Smad4*$^{F/F}$*;Trp53*$^{F/F}$ mouse did not demonstrate nuclear β-catenin staining (Fig 6A). Duodenal carcinomas from *Pdx-1-Cre;Smad4*$^{F/F}$*;Trp53*$^{F/F}$*;Cdh1*$^{F/+}$ mice (n=4), with intact E-cadherin expression, also demonstrated significantly lower nuclear β-catenin positivity at the invasive front than gastric carcinomas from mice with the same genotype (n=14) [median, 8.5% *vs* 29.3%; *P* for *t*-test<0.001] (Fig 6B). Invasive fronts of these tumors with E-cadherin expression did not express vimentin (*data not shown*). Thus, complete loss of E-cadherin may be a prerequisite for nuclear β-catenin accumulation across the different epithelial tumor types. The *Pdx-1-Cre;Smad4*$^{F/F}$*;Trp53*$^{F/F}$ mouse with a gastric adenocarcinoma had no distant metastases [Log-rank *P* value for metastasis-free survival between *Pdx-1-Cre;Smad4*$^{F/F}$*;Trp53*$^{F/F}$ and *Pdx-1-Cre;Smad4*$^{F/F}$*;Trp53*$^{F/F}$*;Cdh1*$^{F/+}$=0.013] (Fig 4A). Given the low nuclear β-catenin positivity of the duodenal adenocarcinomas from *Pdx-1-Cre;Smad4*$^{F/F}$*;Trp53*$^{F/F}$*;Cdh1*$^{F/+}$ mice which do not metastasize (Fig 6B), these results suggest the metastatic propensity of *Pdx-1-Cre;Trp53*$^{F/F}$*;Cdh1*$^{F/+}$ mice may be attributable, at least in part, to the activation of the β-catenin signaling pathway following E-cadherin loss.

Since no distant metastases were identified in mice with intact

Smad4 (*Pdx-1-Cre;Trp53*$^{F/F}$*;Cdh1*$^{F/+}$ and *Pdx-1-Cre;Trp53*$^{F/F}$*;Cdh1*$^{F/F}$) [Log-rank *P*=0.035], we investigated possible mechanisms for the role of Smad4 in suppressing metastasis. Gastric adenocarcinomas arising in *Pdx-1-Cre;Trp53*$^{F/F}$*;Cdh1*$^{F/F}$ (n=4) demonstrated nuclear β-catenin accumulation at the invasive front, but not as frequently as gastric adenocarcinomas from *Pdx-1-Cre;Smad4*$^{F/F}$*;Trp53*$^{F/F}$*;Cdh1*$^{F/+}$ mice (n=14), consistent with a prior report (Shimada, Mimata et al. 2012) [*P* for *t*-test= 0.047] (Fig 6B). Gastric cancers formed in *Pdx-1-Cre;Smad4*$^{F/F}$*;Trp53*$^{F/F}$*;Cdh1*$^{F/+}$ mice demonstrated lower expression of Vimentin and MMP7 at the invasive front than those arising from *Pdx-1-Cre;Smad4*$^{F/F}$*;Trp53*$^{F/F}$*;Cdh1*$^{F/+}$ mice [*t*-test *P* values for the positivity, 0.021 and 0.037 for vimentin and MMP7, respectively] (Fig 7A and 7B). MMP8 expression also tended to be higher in *Pdx-1-Cre;Smad4*$^{F/F}$*;Trp53*$^{F/F}$*;Cdh1*$^{F/+}$(Fig 7A and 7B).

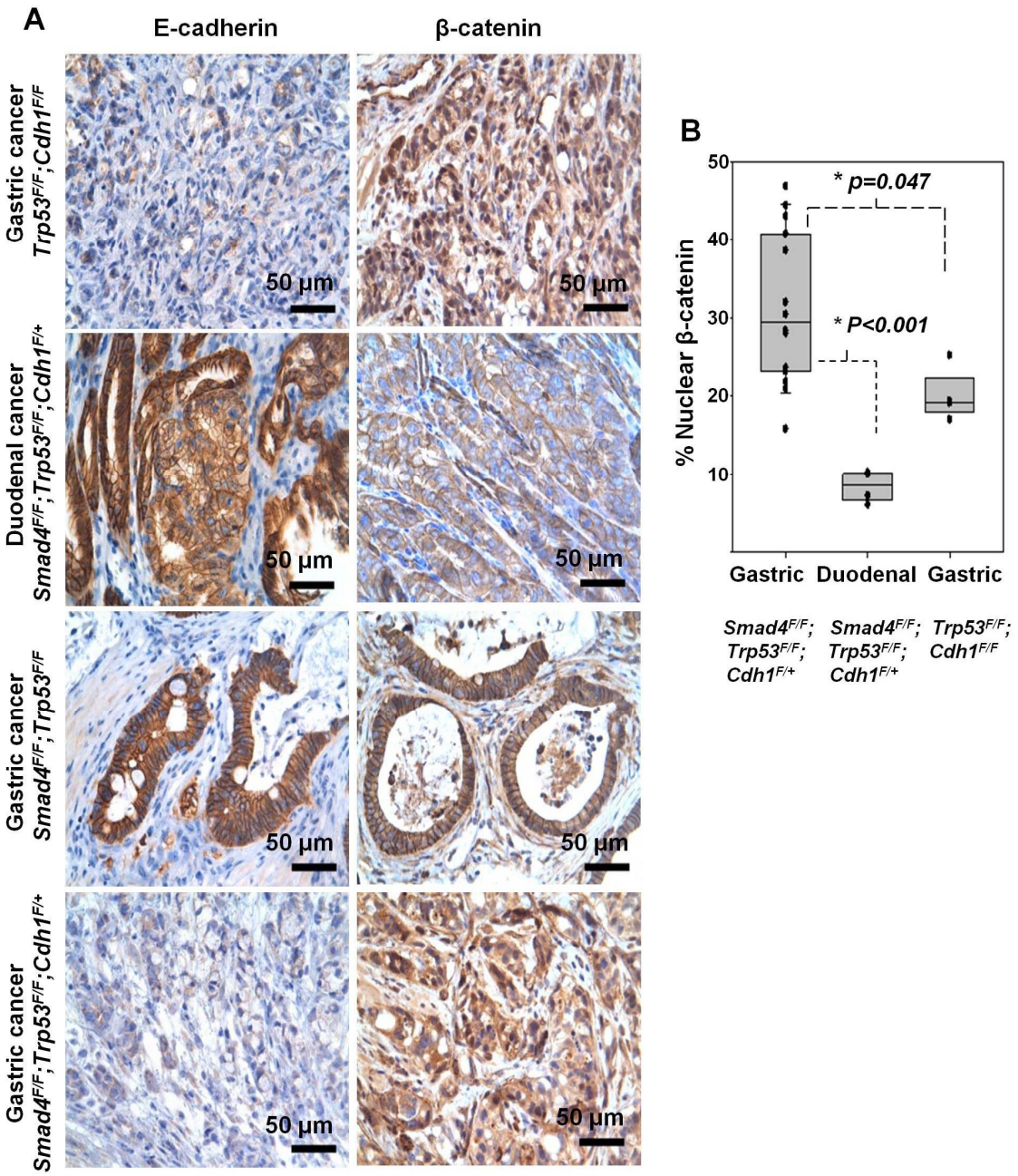
A
E-cadherin
β-catenin
Gastric cancer
Trp53F/F;Cdh1F/F
Duodenal cancer
Smad4F/F;Trp53F/F;Cdh1F/+
Gastric cancer
Smad4F/F;Trp53F/F
Gastric cancer
Smad4F/F;Trp53F/F;Cdh1F/+
50 μm
B
% Nuclear β-catenin
* p=0.047
* P<0.001
Gastric
Duodenal
Gastric
Smad4F/F; Trp53F/F; Cdh1F/+
Smad4F/F; Trp53F/F; Cdh1F/+
Trp53F/F; Cdh1F/F

Fig 6. (A) Representative immunohistochemistry findings for E-cadherin and β-catenin at the invasive front of tumors across genotypes. (B) Percentage of gastric adenocarcinoma cells at the invasive front with nuclear β-catenin immunostaining in *Pdx-1-Cre;Smad4*$^{F/F}$*;Trp53*$^{F/F}$*;Cdh1*$^{F/+}$ cohort (n=14) and *Pdx-1-Cre;Trp53*$^{F/F}$*;Cdh1*$^{F/F}$ cohort (n=4) [*P* for *t*-test=0.047]. Nuclear β-catenin positivity was lower in duodenal carcinomas from *Pdx-1-Cre;Smad4*$^{F/F}$*;Trp53*$^{F/F}$*;Cdh1*$^{F/+}$ mice that retained E-cadherin than gastric adenocarcinomas with the same genotype [*P* for *t*-test<0.001]. Box indicates interquartile range with median.

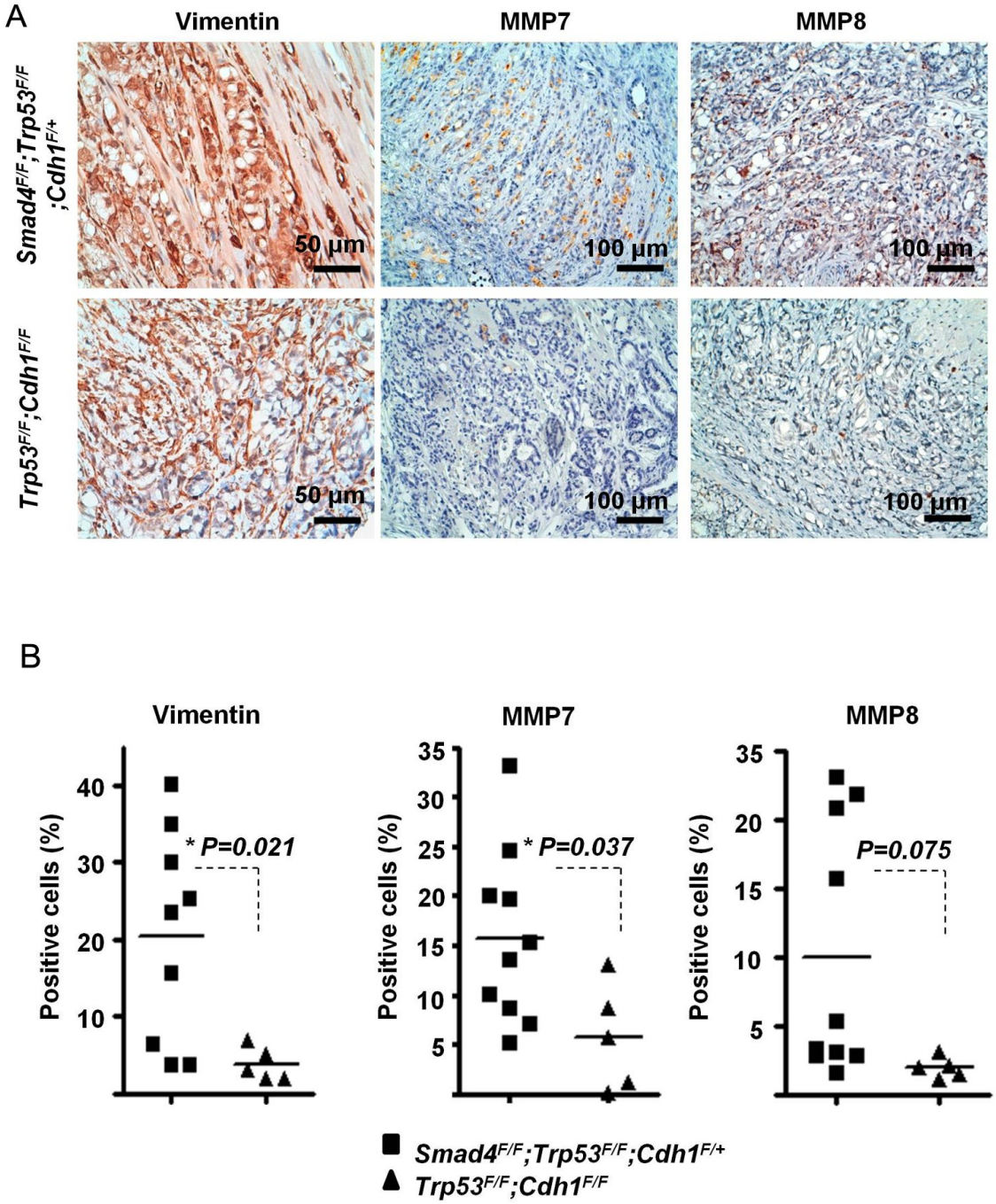
A
Vimentin
MMP7
MMP8
Smad4F/F;Trp53F/F;Cdh1F/+
Trp53F/F;Cdh1F/F
50 µm
100 µm
B
Positive cells (%)
* P=0.021
* P=0.037
P=0.075
Smad4F/F;Trp53F/F;Cdh1F/+
Trp53F/F;Cdh1F/F

Fig 7. (A) Vimentin and MMP7 immunohistochemistry at the tumor invasive front between *Pdx-1-Cre;Smad4$^{F/F}$;Trp53$^{F/F}$;Cdh1$^{F/+}$* and *Pdx-1-Cre;Trp53$^{F/F}$;Cdh1$^{F/F}$* mice. (B) Percentage of Vimentin- and MMP7-positive cells were higher in gastric cancer tissues arising in *Pdx-1-Cre;Smad4$^{F/F}$;Trp53$^{F/F}$;Cdh1$^{F/+}$* mice (n=10) than those in *Pdx-1-Cre;Trp53$^{F/F}$;Cdh1$^{F/F}$* mice (n=5).
MMP8 expression at the invasive front of gastric cancer of *Pdx-1-Cre;Smad4$^{F/F}$;Trp53$^{F/F}$;Cdh1$^{F/+}$* mice as compared with that of *Pdx-1-Cre;Trp53$^{F/F}$;Cdh1$^{F/+}$* mice.

Knockdown of β-catenin significantly inhibited migratory activity of primary cultured gastric cancer cell lines

To further evaluate the effect of Smad4 loss on β-catenin activity, we established primary cultured cells from gastric adenocarcinomas arising from *Pdx-1-Cre;Smad4$^{F/F}$;Trp53$^{F/F}$;Cdh1$^{F/+}$* and *Pdx-1-Cre;Trp53$^{F/F}$;Cdh1$^{F/F}$* mice. *Pdx-1-Cre;Smad4$^{F/F}$;Trp53$^{F/F}$;Cdh1$^{F/+}$* gastric cancer cell lines showed higher expression of mesenchymal markers than that of *Pdx-1-Cre;Trp53$^{F/F}$;Cdh1$^{F/F}$* gastric cancer cell lines (Fig 8A and 8B). Consistent with our *in vivo* results, *Ctnnb1* mRNA expression [P<0.001], β-catenin reporter activity [P<0.001], and nuclear β-catenin immunoflourescence were higher in *Pdx-1-Cre;Smad4$^{F/F}$;Trp53$^{F/F}$;Cdh1$^{F/+}$* cells than *Pdx-1-Cre;Trp53$^{F/F}$;Cdh1$^{F/F}$* cells (Fig 9A and 9B). Results using the Boyden chamber migration assay revealed that *Pdx-1-Cre;Smad4$^{F/F}$;Trp53$^{F/F}$;Cdh1$^{F/+}$* cells demonstrated higher migratory activity than *Pdx-1-Cre;Trp53$^{F/F}$;Cdh1$^{F/F}$* cells [P<0.001] (Fig 10A).

Based upon these results, we performed β-catenin knockdown experiments on 2 independent *Pdx-1-Cre;Smad4$^{F/F}$;Trp53$^{F/F}$;Cdh1$^{F/+}$* cell lines. Knockdown of β-catenin in *Pdx-1-Cre;Smad4$^{F/F}$;Trp53$^{F/F}$;Cdh1$^{F/+}$* cells led to mesenchymal-to-epithelial switch in morphology and gene expression , without significant change in monolayer growth rates (Fig 10A and Fig 10B).

Importantly, knockdown of β-catenin, using two different short hairpin RNAs, significantly inhibited migratory activity of both of *Pdx-1-Cre;Smad4*$^{F/F}$*;Trp53*$^{F/F}$*;Cdh1*$^{F/+}$ cells [P<0.001] (Fig 11). These results collectively suggest that the loss of E-cadherin and Smad4 expression cooperate to promote lung metastasis partly through the β-catenin activation.

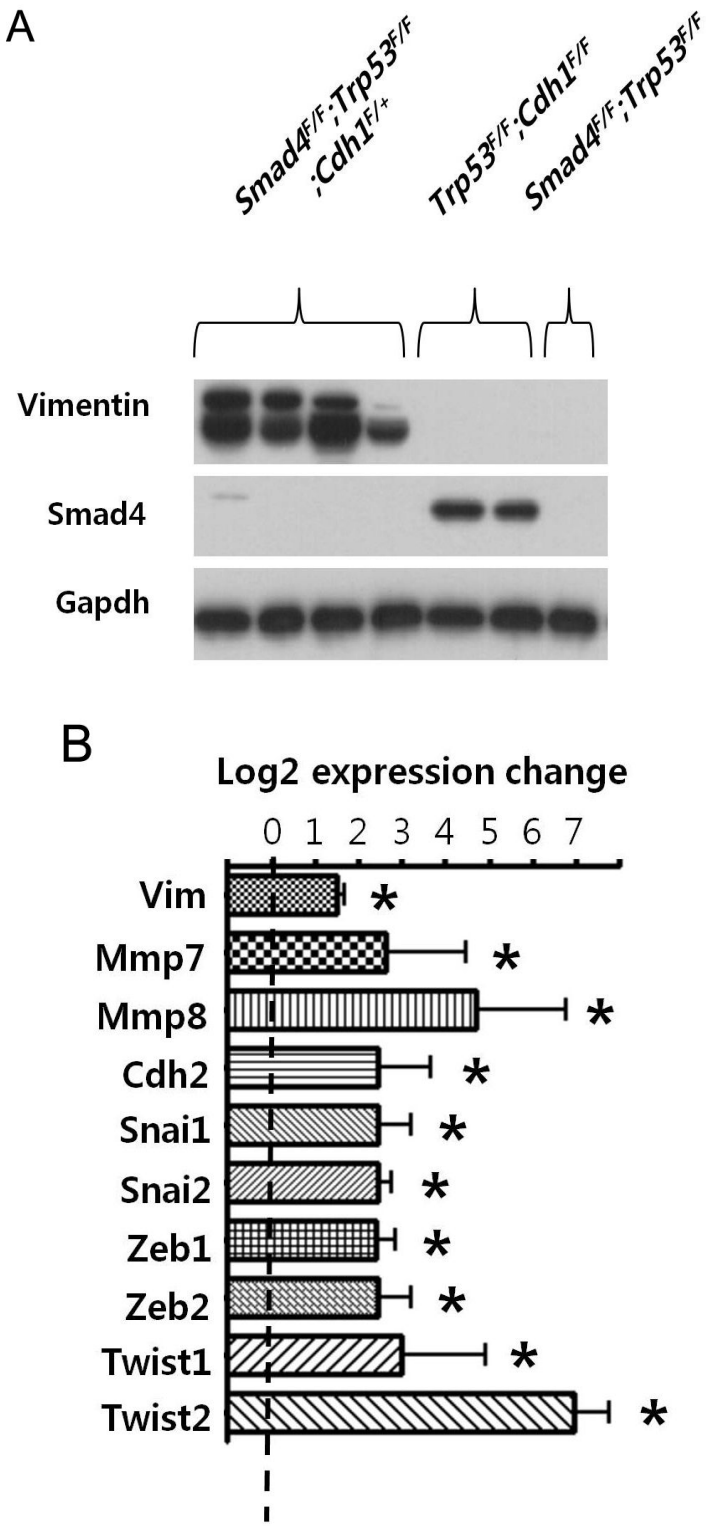
A
Smad4F/F;Trp53F/F;Cdh1F/+
Trp53F/F;Cdh1F/F
Smad4F/F;Trp53F/F
Vimentin
Smad4
Gapdh
B
Log2 expression change
0 1 2 3 4 5 6 7
Vim
Mmp7
Mmp8
Cdh2
Snai1
Snai2
Zeb1
Zeb2
Twist1
Twist2

Fig 8. (A) Mesenchymal marker, Vimentin expression of *Pdx-1-Cre;Smad4$^{F/F}$;Trp53$^{F/F}$;Cdh1$^{F/+}$* gastric cancer cell lines by western blotting. (B) The expression of mesenchymal markers, Vimentin (Vim), and N-cadherin (Cdh2), and epithelial to mesenchymal transition regulators, Snail (Snai1), Slug (Snai2), Zeb1, Zeb2, Twist1, and Twist2, and matrix metalloproteinases (*Mmp7* and *Mmp8)* of *Pdx-1-Cre;Smad4$^{F/F}$;Trp53$^{F/F}$;Cdh1$^{F/+}$* gastric cancer cell lines as compared with that of *Pdx-1-Cre;Trp53$^{F/F}$;Cdh1$^{F/F}$* gastric cancer cell lines.

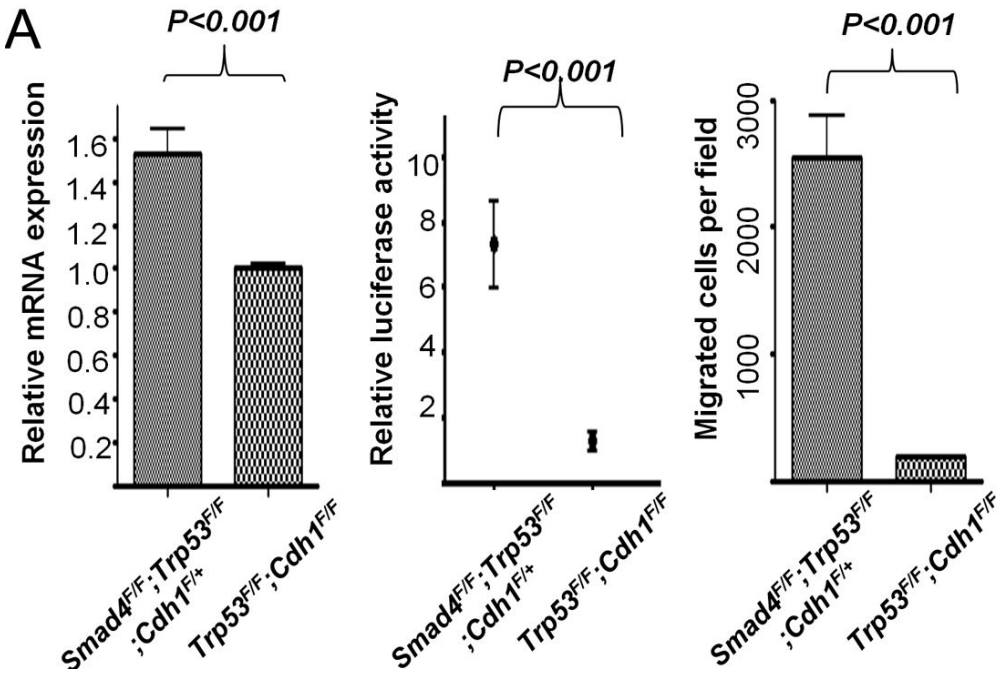
A
P<0.001
Relative mRNA expression
1.6
1.4
1.2
1.0
0.8
0.6
0.4
0.2
Smad4F/F;Trp53F/F ;Cdh1F/+
Trp53F/F;Cdh1F/F
P<0.001
Relative luciferase activity
10
8
6
4
2
Smad4F/F;Trp53F/F ;Cdh1F/+
Trp53F/F;Cdh1F/F
P<0.001
Migrated cells per field
3000
2000
1000
Smad4F/F;Trp53F/F ;Cdh1F/+
Trp53F/F;Cdh1F/F

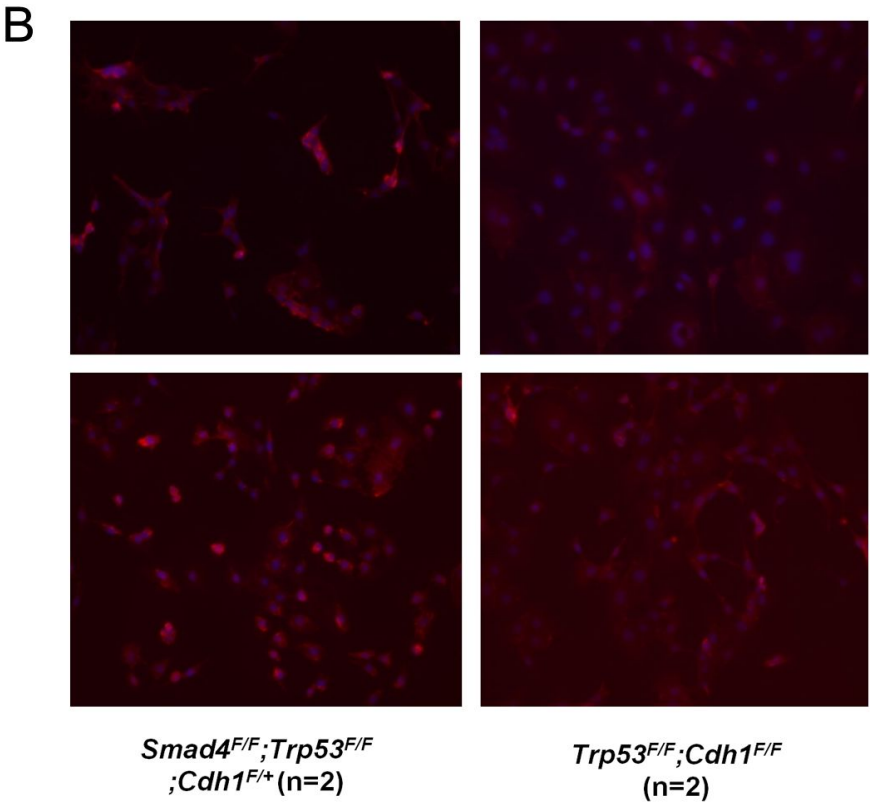
B
Smad4F/F;Trp53F/F ;Cdh1F/+ (n=2)
Trp53F/F;Cdh1F/F (n=2)

Fig 9. (A) Representative mRNA expression (real-time RT-PCR), β-catenin reporter activity, and migratory activity of primary cultured cells from gastric adenocarcinomas arising from *Pdx-1-Cre;Smad4*$^{F/F}$*;Trp53*$^{F/F}$*;Cdh1*$^{F/+}$ (n=4) and *Pdx-1-Cre;Trp53*$^{F/F}$*;Cdh1*$^{F/F}$ mice (n=2) from multiple experiments. (B) Nuclear β-catenin immunoflourescence of primary cultured cells from gastric adenocarcinomas arising from *Pdx-1-Cre;Smad4*$^{F/F}$*;Trp53*$^{F/F}$*;Cdh1*$^{F/+}$ and *Pdx-1-Cre;Trp53*$^{F/F}$*;Cdh1*$^{F/F}$ mice.

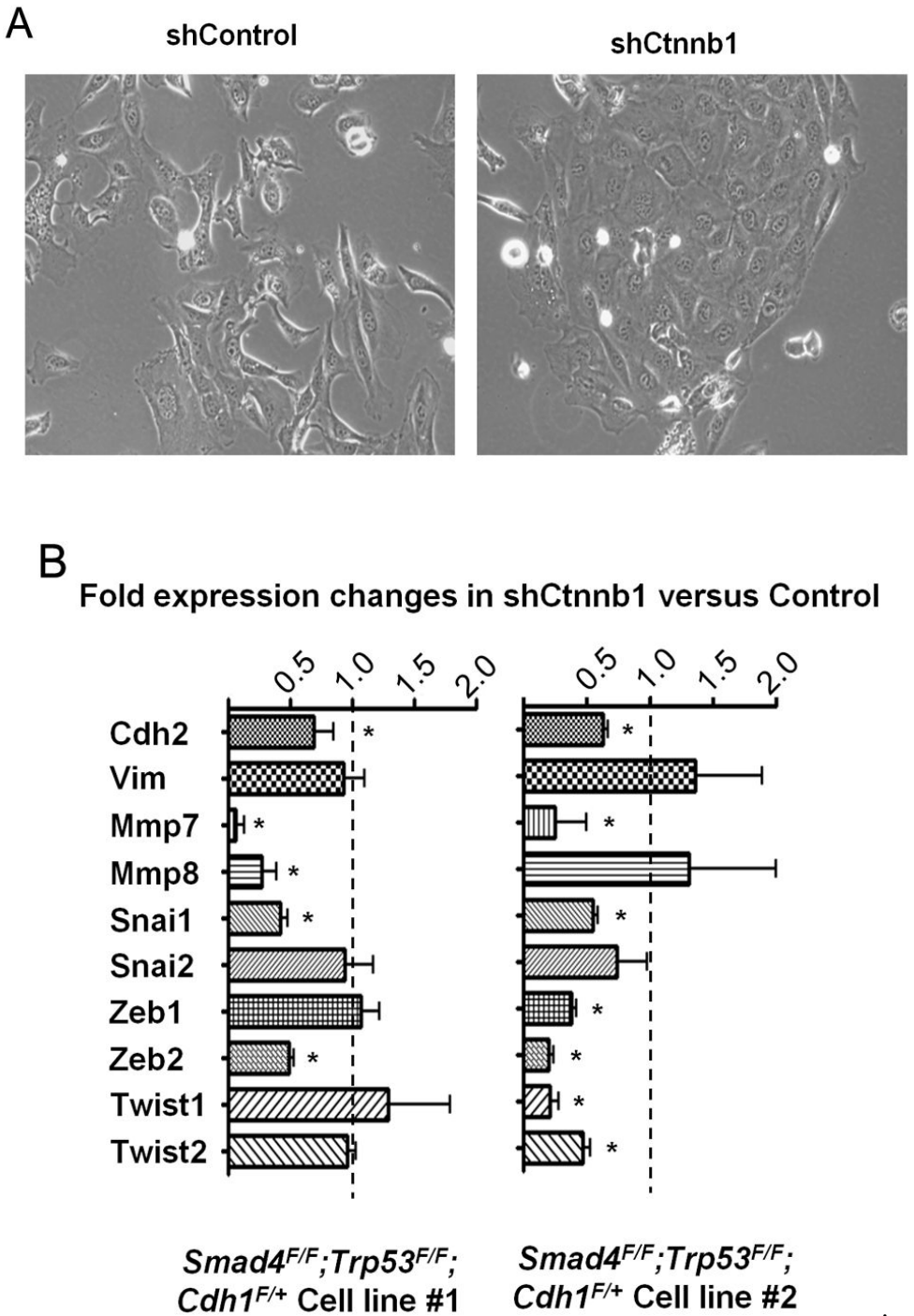
A
shControl
shCtnnb1
B
Fold expression changes in shCtnnb1 versus Control
0.5
1.0
1.5
2.0
Cdh2
Vim
Mmp7
Mmp8
Snai1
Snai2
Zeb1
Zeb2
Twist1
Twist2
Smad4F/F;Trp53F/F; Cdh1F/+ Cell line #1
Smad4F/F;Trp53F/F; Cdh1F/+ Cell line #2

Fig 10. (A) *Pdx-1-Cre;Smad4*$^{F/F}$*;Trp53*$^{F/F}$*;Cdh1*$^{F/+}$ cells, that originally exhibited a fibroblast, spindle-like shape, acquired epithelial, cuboidal cell morphology, after knockdown of β-catenin. (B) mRNA expression of *MMP7* and *MMP8* as well as that of mesenchymal markers and EMT regulators after β-catenin knockdown.

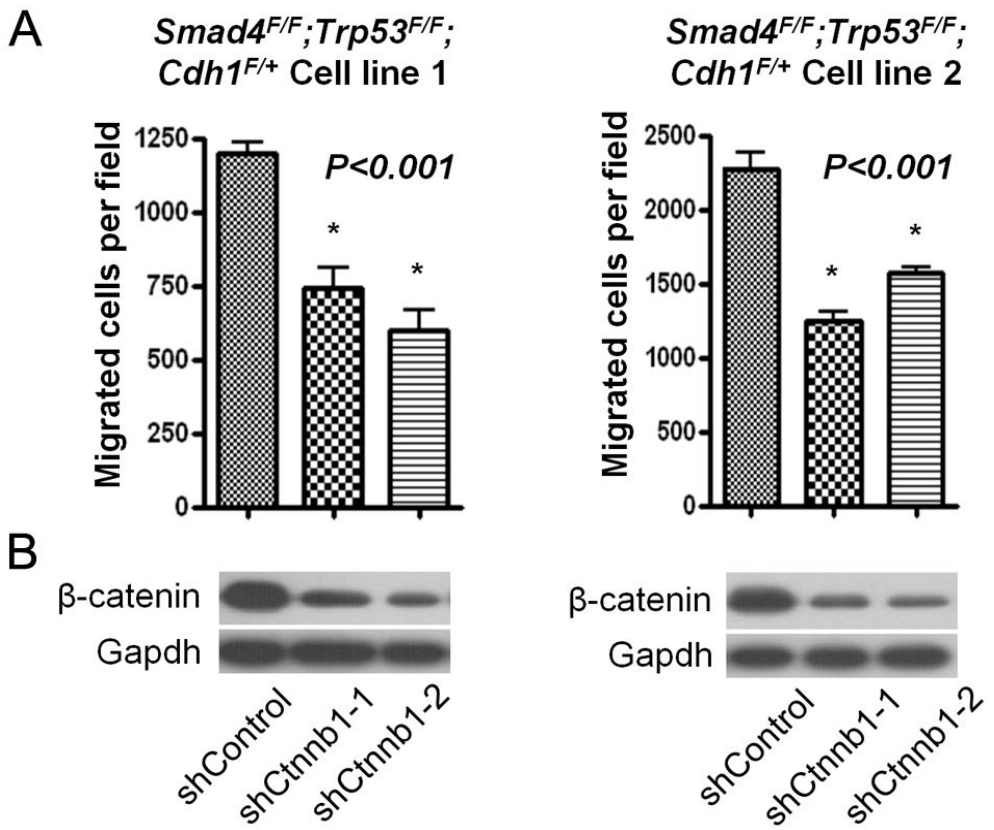

Fig 11. (A) Migratory activity of two independent primary cultured cells from gastric adenocarcinomas arising from *Pdx-1-Cre;Smad4$^{F/F}$;Trp53$^{F/F}$;Cdh1$^{F/+}$* mice, after knockdown of β-catenin using two different short hairpin RNAs. (B) Western blot analysis to assess the efficiency of β-catenin knockdown.

Discussion

Gastric adenocarcinomas arising in *Pdx-1-Cre;Smad4$^{F/F}$;Trp53$^{F/F}$;Cdh1$^{F/+}$* mice metastasized to the lung, which is a highly unique finding for a genetically engineered mouse model for gastric cancers. To date, only a few genetically-engineered mouse models of gastric cancer have been reported, and none of them develop distant metastases (Graff, Herman et al. 1997; Derksen, Liu et al. 2006; Roussel, Harris et al. 2007; Gutierrez, Dahlberg et al. 2010; Shimada, Mimata et al. 2012). After Helicobacter inoculation, insulin-gastrin (INS-GAS) transgenic mice develop invasive gastric carcinomas with a frequency of 75% (Roussel, Harris et al. 2007), but without distant metastases. Thirty percent of mice deficient in pS2 trefoil factor develop multifocal intraepithelial or intramucosal carcinomas, but no distant metastases (Gutierrez, Dahlberg et al. 2010). *Gp130$^{F/F}$* mice lacking in the SHP2-binding site on the IL-6 family receptor gp130 develop gastric cancer with submucosal invasion only (Graff, Herman et al. 1997). The K19-C2mE mice expressing COX-2 and microsomal prostaglandin E synthase-1 in the stomach develop dysplastic tumors in the gastric epithelium (Derksen, Liu et al. 2006). *Atp4b-Cre;Cdh1$^{F/F}$;Trp53$^{F/F}$* mice develop diffuse-type gastric cancers which frequently metastasize to lymph nodes but not to the distant visceral organs (Shimada, Mimata et al. 2012). Thus, gastric cancer metastasis may require a concerted action of

key molecular events, including losses of E-cadherin and Smad4, as demonstrated in this study.

The metastatic phenotype of our mutant mice provides a unique opportunity to dissect the roles of E-cadherin and Smad4 in gastric cancer progression, and in relation to EMT. Without exposure to carcinogens, the gastric epithelium of *Pdx-1-Cre;Smad4$^{F/F}$;Trp53$^{F/F}$;Cdh1$^{F/+}$* mice lost E-cadherin expression and developed adenocarcinomas that progressed through EMT, suggesting the importance of EMT in gastric cancer progression. Nuclear β-catenin accumulation, suggesting activation of the canonical Wnt/β-catenin pathway, was accompanied by EMT phenotype such as vimentin overexpression (Oliveira, Bordin et al. 2002). Given that this phenotype was not observed in gastrointestinal tumors of our mutant mice that retained E-cadherin, the unique metastatic phenotype of *Pdx-1-Cre;Smad4$^{F/F}$;Trp53$^{F/F}$;Cdh1$^{F/+}$* mice may be attributable in part to the activation of the β-catenin signaling pathway following E-cadherin loss (Shimada, Mimata et al. 2012). Our study also provides functional evidences for the causal role of β-catenin for the migration process related to metastasis of gastric cancer, consistent with data in the literature suggesting that β-catenin promotes the metastatic progression of breast and colorectal cancers by transcriptional activation of vimentin, MMP7, fibronectin, and other pro-metastatic genes (Lefebvre, Chenard et

al. 1996; Wang, Dangler et al. 2000; Judd, Alderman et al. 2004; Shimada, Mimata et al. 2012).

The anti-metastatic role of Smad4 in gastric cancer, which has not been previously demonstrated *in vivo*, is in line with previous data for colorectal and prostate cancers (Takaku, Oshima et al. 1998; Humar, Blair et al. 2009). Notably, nuclear β-catenin accumulation at the invasive front was more prominent in our *Pdx-1-Cre;Smad4*$^{F/F}$*;Trp53*$^{F/F}$*;Cdh1*$^{F/+}$ mice than in *Pdx-1-Cre;Trp53*$^{F/F}$*;Cdh1*$^{F/F}$, which is partly consistent with a report by Shimada, *et al.* that E-cadherin-/-; p53-/- mice do not overexpress β-catenin (Shimada, Mimata et al. 2012). In addition, *Pdx-1-Cre;Smad4*$^{F/F;}$ *Trp53*$^{F/F}$*;Cdh1*$^{F/+}$ cells demonstrated enhanced β-catenin activity and migratory activity compared with *Pdx-1-Cre;Trp53*$^{F/F}$*;Cdh1*$^{F/+}$ cells. Thus, our study is the first to demonstrate the Smad4 loss-induced β-catenin activation in gastric cancer, and is consistent with a prior report that Smad4 mediates canonical BMP signaling by repressing the transcription of β-catenin in SW480 colon cancer cells (Oliveira, Sousa et al. 2009). Therefore, inhibition of β-catenin may be a converging node for the anti-metastatic signaling pathways driven by E-cadherin and Smad4 in *Pdx-1-Cre;Smad4*$^{F/F}$*;Trp53*$^{F/F}$*;Cdh1*$^{F/+}$ mice. Other possible mechanisms for the anti-metastatic role of Smad4 may include suppression of proliferation, leading to proliferative dormancy (Oliveira, Sousa et al. 2009).

Taken together, we conclude that loss of E-cadherin and Smad4 cooperate to promote the metastatic progression of p53-null diffuse-type gastric carcinoma. By performing gastroduodenal epithelium-specific knockout of one allele of *Cdh1* and both alleles of p53 and Smad4, which are frequently inactivated in human gastric cancers, we have created a genetically-engineered mouse model that develops distant metastasis. Gastric adenocarcinomas that formed in this genetic context, but not intestinal or mammary adenocarcinomas, lose E-cadherin expression and undergo EMT. These results closely recapitulate human diffuse-type gastric cancers, and sharpen our understanding of the interaction between E-cadherin and Smad4, two commonly inactivated tumor suppressors in gastric cancer. Additionally, the *Pdx-1-Cre;Smad4*$^{F/F}$*;Trp53*$^{F/F}$*;Cdh1*$^{F/+}$ will be extremely useful for preclinical studies given its similarities with human diffuse-type gastric carcinoma and its metastatic propensity.

CHAPTER III.

SCA-1 IS IDENTIFIED AS A POTENTIAL CANCER STEM CELL MARKER IN METASTATIC DERIVATIVES OF A MURINE GASTRIC CANCER CELL LINE

Abstract

There are no genetically defined murine gastric cancer cell lines or mouse models. A primary cell line (NCC-S1) was established from a gastric cancer that developed from a mouse deficient in Smad4, p53, and one copy of E-cadherin. NCC-S1 closely recapitulated, histologically and genetically, human diffuse-type gastric cancer. Furthermore, a cancer subpopulation of NCC-S1 cells was isolated from lung metastases that developed from heterotopic tumors transplanted into severe combined immunodeficiency mice. The metastasis derived cells, designated NCC-S1M, formed orthotopic tumors and exhibited a significant improvement in *in vivo* metastatic potential compared with the parental cell line, showing EMT features. NCC-S1M cells demonstrated many features of cancer stem cells, including the ability to initiate tumor formation and chemoresistance. Importantly, Sca-1 was found to be more overerexpressed in NCC-S1M cells than NCC-S1 cells. Sca-1 positive cells demonstrated increased ability to initiate tumor formation and *in vivo* chemoresistance than Sca-1 negative cells, showing upregulation of interleukin 1 signaling pathway. Genes overexpressed in Sca-1 highly positive NCC-S1 cells, compared with Sca-1 negative cells, clustered in 123 metastatic gastric cancer patients according to overall survival following cisplatin/fluorouracil chemotherapy. Taken together, we have identified Sca-1 as a murine gastric cancer stem cell marker using unique metastatic cell line models.

Introduction

Gastric cancer is the fourth most common cancer and the second most common cause of cancer-related death in the world (Alberts, Cervantes et al. 2003). Despite the overall decline in gastric cancer prevalence, many patients who undergo surgical resection develop regional recurrences and distant metastasis and show anticancer drug resistance (Jemal, Siegel et al. 2008). It is postulated that tumors are composed of heterogenous cancer cells and that only a rare subpopulation of cells, known as cancer stem cells (CSC) is responsible for sustaining tumorigenesis and establishing the heterogeneity inherent in tumors (Visvader and Lindeman 2012). CSCs are promising for the development of anticancer drugs because it could explain resistance to chemotheraphy and eventual tumor relapse. The existence of a CSC in gastric cancer have been investigated in several reports and Takaishi et al identified putative cancer initiating cells within a CD44 positive cellular fraction in gastric cancer cells (Takaishi, Okumura et al. 2009). Although, several markers have proven useful for the isolation of CSCs in solid tumor, including CD133, Epcam, and CD44 (Visvader and Lindeman 2012), robust CSC markers have not been identified in human and mouse gastric cancers.

In the scientific and pharmaceutical communities, there is a need for genetically defined, murine gastric cancer cell models that closely recapitulate human gastric cancer. In addition, there are no

metastatic cell line models that can be used to study mechanisms of gastric cancer metastasis in immunocompetent mice. To address these issues, we have established primary cultured murine gastric cancer cell lines and their metastatic derivatives from *Villin-cre;Smad4*$^{F/F}$*;Trp53*$^{F/F}$*;Cdh1*$^{F/+}$ mice. These metastatic derivatives predictably form orthotopic tumors in syngeneic mice which predictably metastasize to liver and lung. In addition, these cells display several cancer stem cell-like features such as increased tumorigenic potential and chemoresistance.

Importantly, our mRNA sequencing comparisons between these metastatic derivatives and parental cells identified Sca-1 as one of the overexpressed genes acquired during the metastasis process. Sca-1 is a marker of mouse hematopoietic stem cells, and is thought to be a cancer stem cell marker in murine breast cancer (Cohn, Kramerov et al. 1997; Treister, Sagi-Assif et al. 1998; Xin, Lawson et al. 2005; Grange, Lanzardo et al. 2008). It is upregulated on murine mammary cells undergoing carcinogen driven transformation, and in spheres generated from oncogene driven murine tumors (Li, Welm et al. 2003). Overexpression of Sca-1 is commonly associated with an aggressive phenotype in mouse tumors (Witz 2000). Sca-1 regulates mammary tumor development and cell migration, but its role in gastrointestinal carcinogenesis is not fully elucidated (Batts, Machado et al. 2011).

Using novel mouse cell line models, we demonstrate that Sca-1

high gastric cancer cells have cancer stem cell-like features. In addition, a gene expression signature for Sca-1 high cells was found to be associated with clinical chemoresistance. Sca-1 high cells showed upregulation of interleukin 1-related signaling. Collectively, we showed here for the first time Sca-1 might be murine gastric cancer stem cell marker.

Materials and Methods

Mice

B6.Cg−Tg(Vil−Cre)20Sy mice and FVB.129−*Trp53*^{tm1Brn} mice (Jonkers, Meuwissen et al. 2001) were provided by the Mouse Models of Human Cancers Consortium repository at the NCI Frederick Cancer Research Center. B6.129−*Cdh1*^{tm2Kem}/J mice were purchased from The Jackson Laboratory (Derksen, Liu et al. 2006). *Pdx−1−Cre* mice (B6.FVB−Tg(Ipf1−cre)1Tuv), originally generated by Dr. Lowy, were provided through the Mouse Models of Human Cancers Consortium (MMHCC) repository at the NCI Frederick Cancer Research Center. Conditional Smad4 knockout mice (*Smad4*$^{F/F}$) on the Black Swiss and B6 and 129 backgrounds were generously provided by Dr. Chu−Xia Deng (NIH, Bethesda, MD) (Yang, Li et al. 2002). Compound conditional knockouts for Smad4, p53, and E−cadherin were bred with B6.Cg−Tg(Vil−Cre)20Sy mice to delete transgenes in the gastrointestinal epithelium. Offspring mice were genotyped using polymerase chain reaction (PCR) assays on tail DNA. Genotyping primers were previously listed in Chapter 1.

Severe combined immunodeficiency (SCID) mice were purchased from Orient Bio (Korea). Mice were anesthetized with isoflurane and sacrificed by cervical dislocation. Mouse studies were conducted with the approval of the Animal Care and Use

Committees of National Cancer Center of Korea and the National Cancer Institute, Bethesda, MD.

Primary cell culture of NCC-S1 and NCC-S1M cells

For primary culture, a gastric tumor arising in a *Villin-cre;Smad4$^{F/F}$;Trp53$^{F/F}$;Cdh1$^{F/wt}$* mouse was minced into small pieces that were digested with collagenase digestion for 30 min at 37 ° C. Single tumor cells were seeded into plated on a 60-mm dish in RPMI 1640 media with 20% fetal bovine serum (FBS), 100U/ml penicillin and 0.1 mg/ml streptomycin in humidified incubator at 37 ° C in an atmosphere of 5% CO_2. Initial passage was performed when heavy tumor cell growth was observed. Two tumor cell populations showing different morphology and growth rate were observed and each population was isolated. These cell lines were designated as NCC-S1 and NCC-S2, respectively. After establishment, the culture was maintained in RPMI 1640 with 10% FBS.

To establish the metastatic variant cell line, 5 x 10^4 EpCam-positive subpopulation of NCC-S1 cells were subcutaneously injected into SCID mice. After 80 days, mice were sacrificed and the lung metastasis of a mouse was transplanted to another SCID mice. After 55 days, the lung metastasis was primary cultured and this cell line was designated as NCC-S1M. All functional experiments were performed during early-passage cells (passage

11-15).

In vivo tumor cell injections

For orthotopic injection, SCID and syngenic mice were anesthetized using isoflurane. A small incision was made in the skin overlying the abdomen, and the stomach was exposed. 1 x 10^6 tumor cells in 25 μl of RPMI and 25 μl of Matrigel (BD Bioscience) were injected into the serous side of the stomach using 0.5 ml insulin syringe. The necropsy was performed 4 weeks after injection.

For splenic injection, SCID mice were anesthetized using isoflurane. A small incision was made in the skin overlying the abdomen, and the spleen was exposed. 0.5 x 10^6 tumor cells in 25 μl of RPMI and 25 μl of Matrigel were injected into spleen. The necropsy was performed 3 weeks after injection. For tail vein injection, 0.1 x 10^6 tumor cells were injected into tail vein of SCID mice and the necropsy was performed 5 weeks after injection.

Limiting dilution assay

Tumor cells (10^6, 10^5, 10^4, and 10^3 cells) were suspended in 100 μl of RPMI and 100 μl of Matrigel and were injected into the flank subcutaneous tissue of syngenic or SCID mice, using a 26-gauge needle and syringe. Data were analyzed using the Extreme Limiting Dilution Analysis (Hu and Smyth 2009).

In vitro chemoresistance ssay

1 x 10^5 tumor cells were seeded into triplicate 12-well plate and cultured for 12 hours. After washing with fresh culture medium containing no antibiotics, cells were treated with 0.5, 1, 4, 6 μM cisplatin and 1, 10, 100, 1000 μM fluorouracil. 48 hours after drug treatment, 200 μl of MTT solution (5mg/ml in PBS) was added to each well in 1 ml of media. Formazane formation was terminated after 2 hours by removing the MTT solution. 500 μl DMSO was added into each well to dissolve the precipitation. The absorbance was detected at 570 nm with a Microplate Reader.

In vivo chemoresistance assay

Fluorouracil (5-Fu) and Cisplatin, two anticancer drugs, were purchased from Sigma Aldrich (Buchs, Switzerland). The drugs were dissolved in 10% DMSO. The mice were intraperitoneally injected with 5-Fu (25 mg/kg) once daily for four days. Cisplatin (5mg/kg) was administered at the last day of 5-Fu treatment.

Sca-1 high- and negative-sorted tumor cells (5 x 10^5 cells in 100 μl of serum-free RPMI) were mixed with equal volumes of Matrigel (BD Biosciences, Bedford, MA) and injected into the subcutaneous flank tissue of the nonobese diabetic/severe combined immunodeficiency (NOD/SCID) mice. When the tumors reached approximately 100 mm^3, the drugs were treated. There were 5 mice

per drug-treated group. The responses of the tumors to the drugs were evaluated using percent treated/control (% T/C), as determined by dividing the median tumor volume of the treatment group (T) by that of the negative control group (C) on the day of measurement. If a tumor regressed, % T/C was defined by the negative of the percentage of decrease in the median tumor volume of the treatment group (T) relative to the baseline volume on the day of measurement.

Quantitative real-time RT-PCR (QRT-PCR)

Total RNA was isolated from mouse gastric cancer cells using AllPrep DNA/RNA/Protein Mini Kit (Qiagen, Valencia, CA) according to the manufacturer's instructions. Total RNA (0.3 μg) was reverse transcribed using random hexamers and *amfiRivertII* Reverse Transcriptase (GenDEPOT, Barker, TX) according to the manufacturer's standard protocols. PCR reactions were performed on a Roche LC480 (Roche Diagnostics, Penzberg, Germany) using 5 μl of 2× QuantiTect SYBR Green PCR Master Mix (Qiagen), 400 nM of each primer, and 2 μl of cDNA sample which was diluted 1:5 in water in a total volume of 10 μl. Cycling conditions were as follows: 15 min at 95℃, followed by 55 cycles each consisting of 20 s at 94℃, 20 s at 57℃ and 20 s at 72℃. Data were analyzed using the LC480 software (Roche Diagnostics). QRT-PCR primers were previously listed in chapter 1. The $2^{-\Delta\Delta CT}$ method was used to

calculate relative changes.

Immunohistochemistry and immunofluorescence

The excised gastric tumor was fixed in neutral buffered 10% formalin, processed by standard methods and embedded in paraffin. 5-μm cross sections were cut and then stained with H&E for histopathological examination. The ABC method (Vectastain Elite ABC kit and Vectastain M.O.M. kit, Vector Laboratories) was used for immunohistochemical detection of c-myc, p53, Smad4 and ki-67. The following antibodies were used in this study; rabbit polyclonal anti E-cadherin antibody (1:200; Cell Signaling, #3195), rabbit polyclonal anti c-Myc antibody (1:50; Abcam, ab32072), rabbit polyclonal anti p53 antibody (1:100; Santa Cruz, sc-6243), mouse monoclonal anti Smad4 (1:50; sc-7966) and rabbit polyclonal anti Ki-67 (1:200; Abcam, ab15580). The slides were subjected to colorimetri detection with ImmPact DAB substrate (Vector Laboratories, SK-4105). The slides were counterstained with Mayer' s hematoxylin for 10 seconds. Negative controls were performed by omitting the primary antibody and substitution with diluent.

Western blot anaylsis

Cells were collected 48 hours after seeding 3 x 10^5 cells in 100 mm dish and lysed with T-PER Tissue Protein Extraction Reagent

(Thermo Fisher Scientific, Hudson, NH, U.S.A) supplemented with protease inhibitors. After removal of cellular debris, protein concentration was quantitated by using a BCA reagent kit (Thermo Fisher Scientific, Hudson, NH, U.S.A) according to manufacturer's instruction. Protein sample was prepared by making a 3 in 4 dilution with 4x Laemmli sample buffer (250 mM Tris-HCl (pH 6.8), 4% SDS, 40% glycerol, 0.05% bromphenol blue, 4% 2-mercaptoethanol) and boiling for 5 minute. Equal amounts of protein were separated on SDS-polyacrylamide gel and transferred onto nitrocellulose membrane by electrophoresis and blotting apparatus (Bio-Rad, Hercules, CA, U.S.A). The proteins were probed with the relevant primary antibodies and horseradish peroxidase (HRP)-conjugated secondary antibodies at the recommended dilutions. The rabbit polyclonal anti E-cadherin antibody (1:1000; Cell Signaling, #3195), rabbit polyclonal anti c-Myc antibody (1:1000; Abcam, ab32072), rabbit polyclonal anti p53 antibody (1:1000; Santa Cruz, sc-6243), mouse monoclonal anti Smad4 (1:1000; sc-7966), rabbit monoclonal anti JNK1/2/3 antibody (1:1000; Abcam, ab124956), rabbit monoclonal anti phosphor-IkBa antibody (1:1000, Cell signaling, #2859), and rabbit monoclonal anti phosphor-p44/42 MAPK (Erk1/2) (1:1000, Cell signaling, #4370), and were applied. Immunodetection were performed. by using an enhanced chemiluminescence (ECL) detection kit (Thermo Fisher Scientific, Hudson, NH, U.S.A).

Flow cytometry (FACS) analysis and fluorescence-activated cell sorting

Tumor cells were detached with trypsin and stained with anti-mouse Ly6a PE (sca-1, 1:800; BD pharminogen, 553336), anti-mouse CD133 PE (1:300; ebioscience, 12-1331-82) and anti-mouse Epcam PE (1:200; ebioscience, 12-5791-82) for 30 minutes at 4℃ in the dark room with gentle agitation. The stained cells were resuspended with FACS sorting buffer (1 mM EDTA, pH 7.0 25 mM HEPES, 1% FBS,Ca2+ and Mg2+ free PBS). The cells were sorted on an Aria cell sorter (BD biosciences, San Jose, CA).

In vivo tumor cell injection after IL-1β treatment

NCC-S1 cells were seeded on 6 well plates. 12 hours after seeding, the cells were treated with 25 ng/ml recombinant mouse IL-1β (R&D systems, 401-ML-025) in serum free RPMI 1640. 24 hours after the treatment, tumor cells were detached with trypsin and 0.5 x 106 tumor cells in 100 μl of RPMI and 100 μl of Matrigel were injected into the flank subcutaneous tissue of SCID mice.

Measurement of β-catenin activity

Primary cultured cells (2.5 x 10^4 cell/well) were plated in 24 wells 12 h before transfection. These cells were transiently transfected

with the TCF/LEF reporter plasmid according to the protocol of the manufacturer using Lipofectamine 2000 transfection reagent (Life Technologies). 24 hours after the transfection, Opti-MEM medium was changed to RPMI 1640 containing 10% FBS. The cells were allowed to grow for one more day and luciferase assays were carried out using the dual luciferase reporter assay system (Promega, Madison, WI) according to the manufacturer's protocol. Light emission was quantified with a Victor 3 1420 luminescence microplate reader (Perkin-Elmer, Waltham, MA). The signals were normalized for transfection efficiency to the internal *Renilla* control.

RNA sequencing and DNA microarray

Total RNAs (1 μg), isolated from NCC-S1 and NCC-S1M cells, were subjected to RNA sequencing using HiSeq2000 sequencer and TruSeq protocol, according to the manufacturer's recommendation (Illumina Hayward, CA). Quantile-normalized FPKM (fragments per kilobase of exon per million fragments mapped) was used as the expression level of each gene. 1 μg of total RNAs, isolated from NCC-S1 cells and normal epithelial mucosa, were subjected to Mouse Gene 1.0 ST array, according to the manufacturer's recommendation (Affymetrix, Sanat Clara, CA). BRB-ArrayTools (ver 4.1) was used for gene set comparison and hierarchical clustering analyses. After gene centering, average linkage hierarchical clustering was performed using centered correlation as

a distance metric. Survival difference was evaluated by a log rank test using SAS software (*proc lifetest*, Cary, NC). The Sca-1 signature was annotated using DAVID functional annotation tool (http://david.abcc.ncifcrf.gov/).

CGH array analyses

CGH array analyses were performed using Mouse GE 4x44K v2 Microarrays and 0.5 μg of tumor genomic DNA samples and the same amount of tail genomic DNA of each mouse, according to the manufacturer's recommendation (Agilent Technologies, Santa Clara, CA). Using Agilent's CGH Analytics software, the data were mapped to mm8 mouse genome and analyzed using the ADM-2 algorithm (Threshold of ADM-2: 6.0; Centralization: ON; Fuzzy Zero: ON; Aberration Filters: ON (minProbes = 3 AND minAvgAbsLogRatio = 0.25 AND maxAberrations = 10000000 AND percentPenetrance = 0)). An average tumor/normal $\log_2$ ratio > 0.5 for 5 or more consecutive probes in a genomic locus was identified as the amplification.

Results

Establishment of primary cultured NCC-S1 cells recapitulating human diffuse-type gastric cancer

One of 45 *Villin-cre;Smad4*$^{F/F}$*;Trp53*$^{F/F}$*;Cdh1*$^{F/wt}$ mice developed spontaneous gastric adenocarcinoma in the glandular stomach at 28 weeks of age (Fig 1A). Histology of the primary tumor recapitulated human diffuse-type gastric carcinoma (Fig 1B and 1C). Immunohistochemisty demonstrated that the tumor lost expression of Smad4 and Trp53 as predicted (Fig 1D). The gastric adenocarcinoma showed high Ki-67 proliferative index and overexpression of Myc oncogene (Fig 1E and 1F).

NCC-S1 was primarily cultured and established from this gastric cancer. *In vitro* morphology of the cell lines was epithelial cell type (Fig 2A). Western blotting analyses indicated that NCC-S1 showed overexpression of Myc as observed in the primary gastric tumor (Fig 2B). Array-comparative genomic hybridization revealed copy number gains of chromosomes 19q and 15q harboring *Myc* (log ratio, 0.92 and 0.55, respectively, data not shown). A survey of key regulators of G1/S transition revealed significant induction of Cyclin D1 with down regulation of p21 (Fig 2B). p21 is one of target genes for TGF-β pathway and tightly controlled by p53 (Elston and Inman 2012). p21 acts to induce a G1 arrest via the inhibition of Cyclin D1 and Cyclin E (Elston and Inman 2012).

Gene expression profiles of NCC-S1, as identified by RNA sequencing analysis, showed significant overlaps with human gastric cancers. There were 3,742 overexpressed and 1,378 underexpressed genes in NCC-S1 cells compared with normal gastric epithelium (by > 3-fold). Both overexpressed genes (4,322 Affymetrix probe sets) and underexpressed genes (1,241 Affymetrix probe sets) significantly overlapped with genes differentially expressed between 123 gastric cancer patients and 21 normal tissue samples (LS p values, 0.043 and < 0.001, respectively). These data indicate that NCC-S1 recapitulated human gastric cancers.

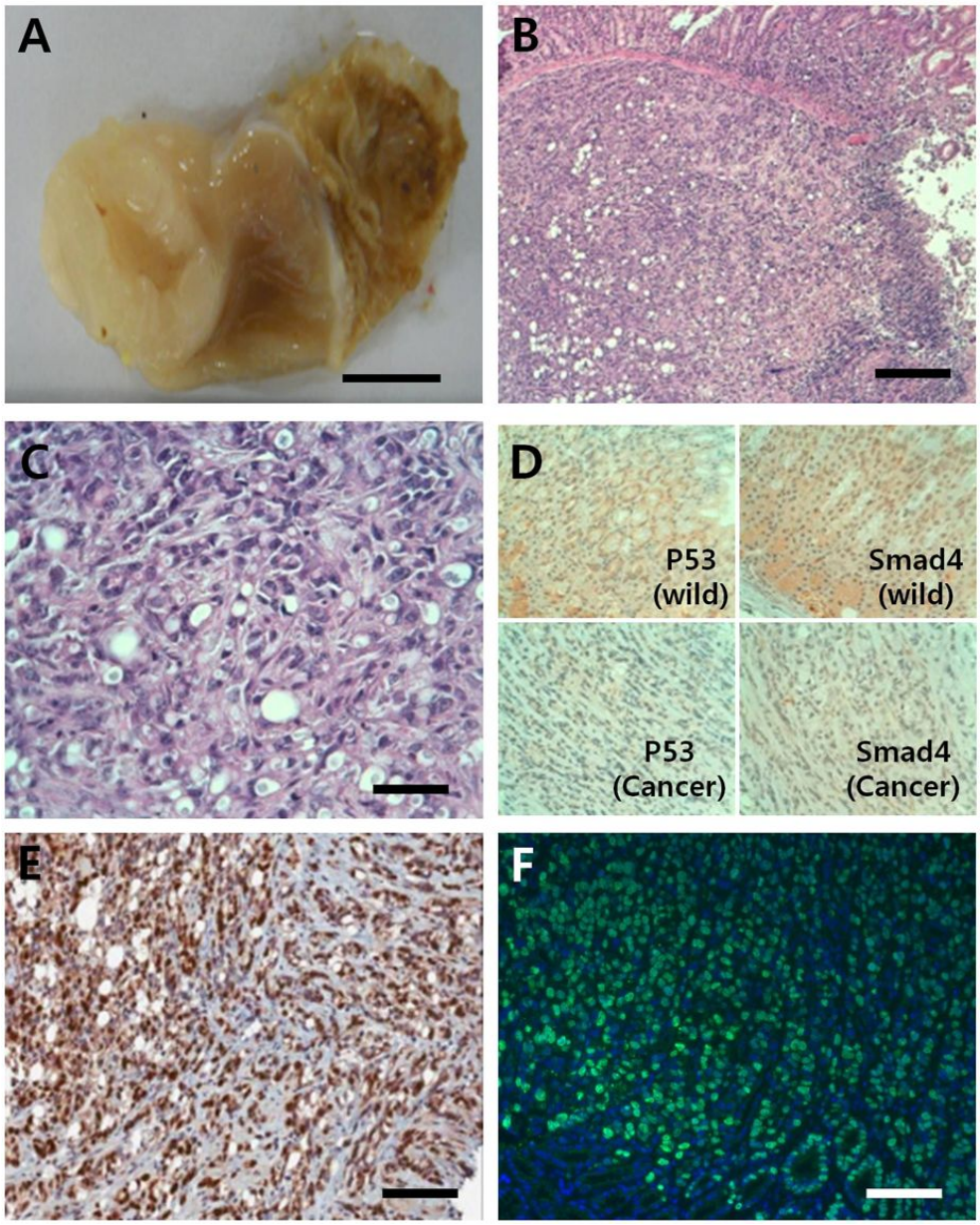

Fig 1. (A) Gross findings of a gastric cancer, an ulceroinfiltrative mass in the antral mucosa, arising in *Villin−Cre;Smad4*$^{F/F}$*;Trp53*$^{F/F}$*;Cdh1*$^{F/+}$ mice. (B and C) Histopathological findings of the gastric cancer. H&E. (D) Immunohistochemistry for the confirmation of loss of Smad4 and p53 in the gastric cancer. (E) Myc and (F) Ki−67 immunostaining of the primary gastric cancer.

A

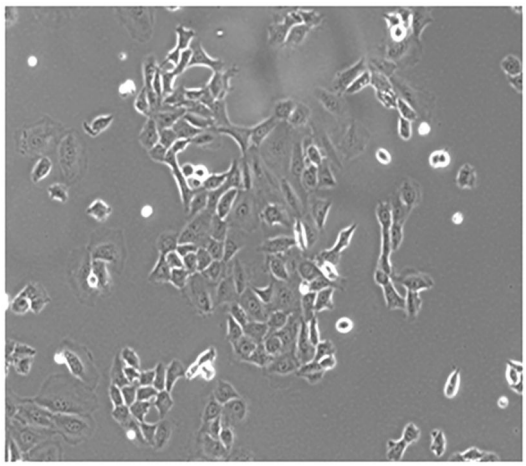

B

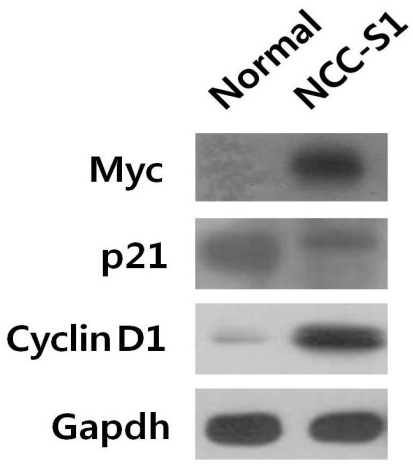

Fig 2. (A) *In vitro* morphology of NCC-S1. (B) Western blot analysis showing upregulated expression of Myc and Cyclin D1 and reduced expression of p21 in NCC-S1 compared to normal gastric mucosa.

Establishment of metastatic variant NCC-S1M

A cancer subpopulation was then isolated from lung metastatic foci that developed from heterotopic tumors of NCC-S1cells on SCID mouse. This metastatic derivative, designated as NCC-S1M, grew like mesenchymal cells in terms of *in vitro* morphology (Fig 3A). Consistent with mesenchymal morphology, E-cadherin protein was down-regulated in NCC-S1M cells compared to NCC-S1 (Fig 3Bi), but the *Cdh1* promoter hypermethylation was not identified (*data not shown*). Although expression of Vimentin, a widely used epithelial to mesenchymal transition (EMT) marker, did not change in NCC-S1M compared to NCC-S1 cells, this marker is not suitable for evaluation of the EMTs in NCC-S1M cells because NCC-S1 cells already exhibited strong expression of Vimentin (Fig 3Bi). mRNA expression of EMT regulators was elevated in NCC-S1 M cells compared to NCC-S1 cells (Fig 3Bii). In addition, NCC-S1M cells showed higher activity of a Wnt signaling reporter than that of NCC-S1 cells (Fig 3Ciii). NCC-S1M cells consistently developed lung metastasis after the heterotopic, splenic, and tail vein injection in SCID mice, much more rapidly than parental cells (Table 1).

A

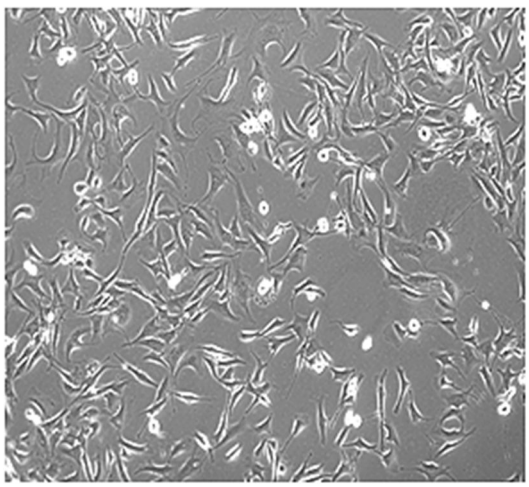

B

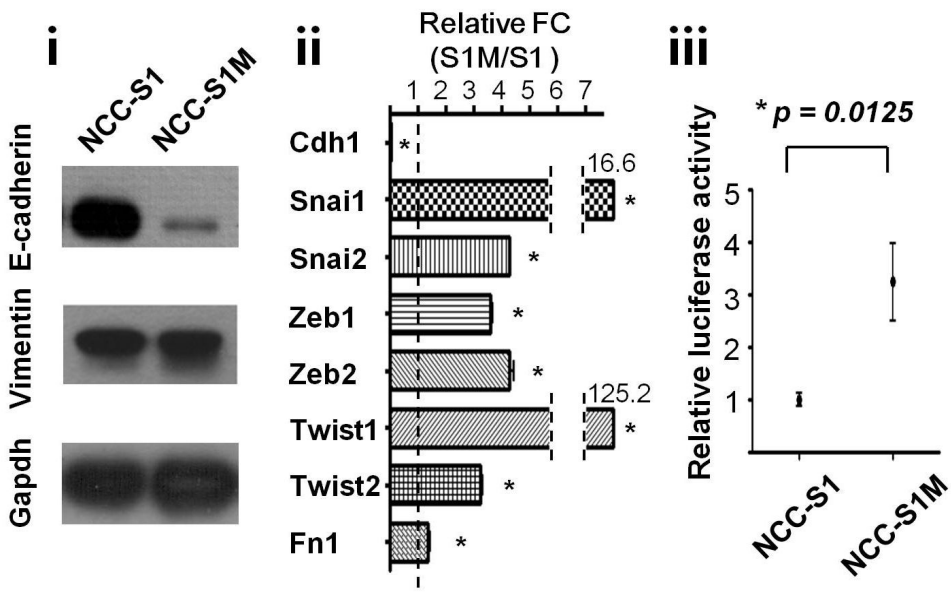

Fig 3. (A) *In vitro* morphology of NCC-S1M. (B)). (Bi) Western blot analyses showing down-regulated E-cadherin expression in NCC-S1M. (Bii) The mRNA expression of mesenchymal markers and EMT regulators of NCC-S1M as compared with that of NCC-S1. (Biii) Increased β-catenin reporter activity of NCC-S1M compared to NCC-S1.

Table 1. Frequency of gross or microscopic metastasis of NCC-S1 and NCC-S1M following experimental procedures

	Orthotopic injection[1]		Splenic injection[2]		Tail vein injection[3]	
	S1	S1M	S1	S1M	S1	S1M
Frequency of metastasis	0 / 8 (0%)	5 / 5 (100%)	0 / 5 (0%)	5 / 5 (100%)	0 / 5 (0%)	4 / 5 (80%)

[1]According to the necropsy findings 4 weeks after injection
[2]According to the necropsy findings 3 weeks after injection
[3]According to the necropsy findings 5 weeks after injection

NCC-S1M showed uniform cancer stem cell-like characteristics.

NCC-S1M proliferated much more rapidly than parental S1cells *in vivo* (Fig 4Ai). All of SCID mice harboring NCC-S1M tumors showed lung metastasis when the volume of the primary tumor in the flank reached 1,700 mm^3, while NCC-S1 didn't showed any lung metastasis at the same volumes (Fig 4Aii). NCC-S1M cells overexpressed EpCam and CD133, putative cancer stem cell markers (Fig 4B). NCC-S1M cells also demonstrated the increased tumorigenic potential in syngeneic mice (Table 2). In addition, NCC-S1M cells were more resistant to fluorouracil and cisplatin than NCC-S1 cells (Fig 5, cisplatin IC_{50} of S1 and S1M = 0.97 μM and 2.10 μM, fluorouracil IC_{50} of S1 and S1M = 1.60 μM and 3.50 μM). In addition, these results show that this metastatic variant cell line demonstrates uniform cancer stem cell-like characteristics.

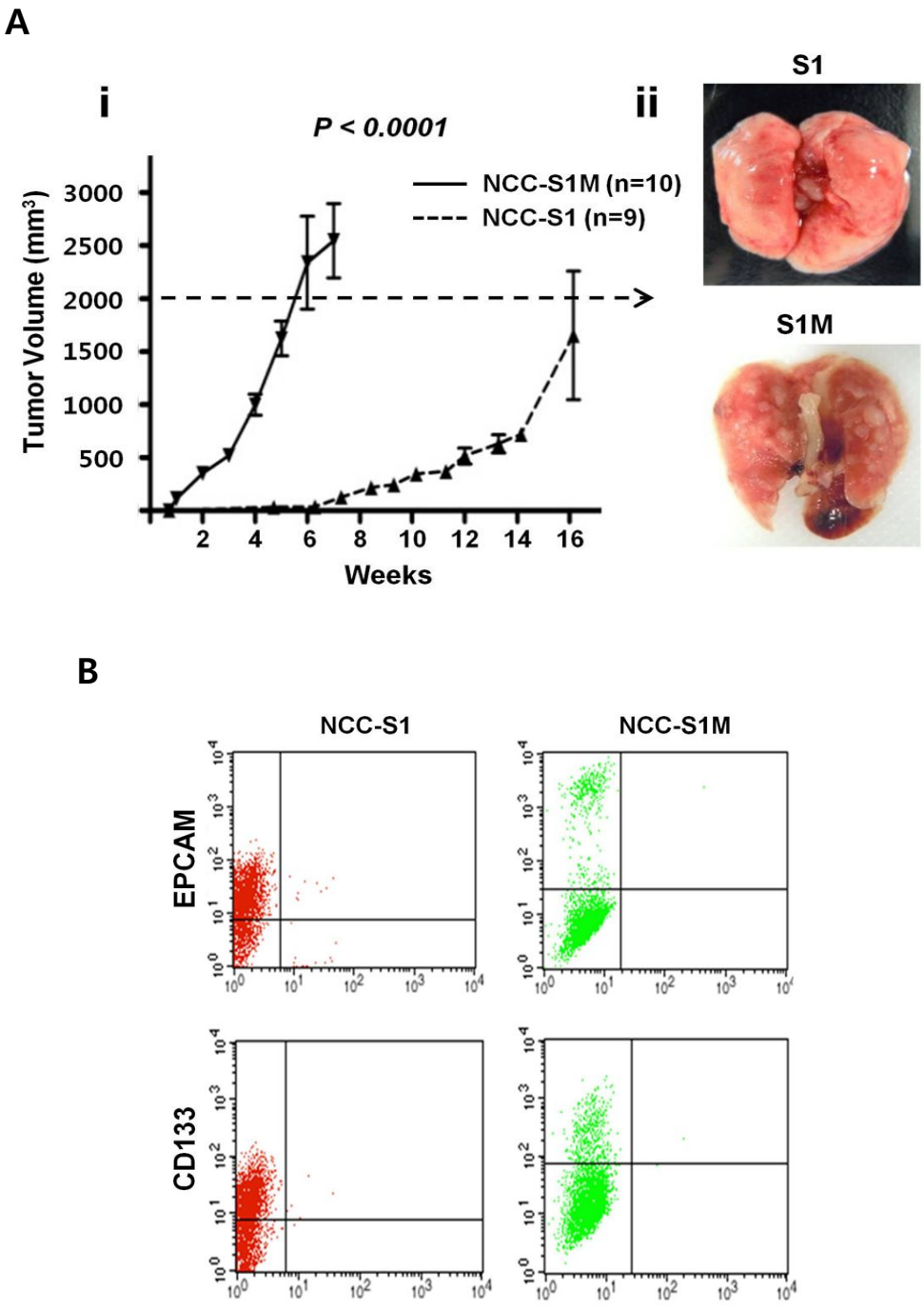

Fig 4. (A) *In vivo* growth for NCC-S1M and NCC-S1. (B) FACS findings demonstrating overexpression of EpCam and CD-133 in NCC-S1M cells compared to NCC-S1 cells.

Table 2. Comparison of tumorigenic potential between NCC-S1 and NCC-S1M in syngenic mice.

Cell	Cell dose	*No.* mice with tumors (%)	*P*
NCC-S1M	1 X 10^6	7 / 7 (100)	
	1 X 10^5	6 / 6 (33.3)	
	1 X 10^4	4 / 6 (16.7)	
	1 X 10^3	3 / 6 (16.7)	
			<0.001
NCC-S1	1 X 10^6	4 / 7 (14.3)	
	1 X 10^5	2 / 6 (0)	
	1 X 10^4	1 / 6 (0)	
	1 X 10^3	0 / 6 (0)	

A

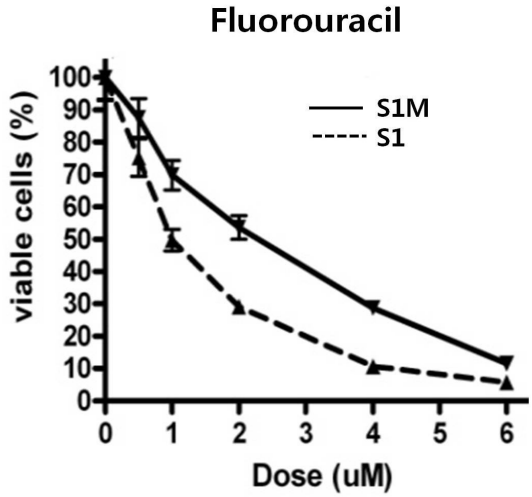

B

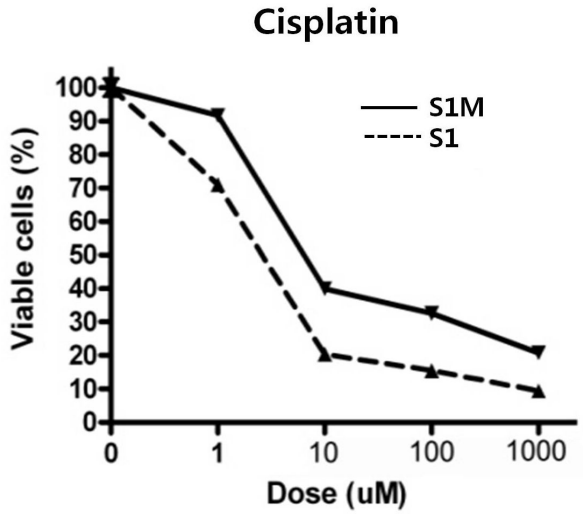

Fig 5. Decreased IC_{50} for fluorouracil (A) and cisplatin (B) in NCC-S1M compared with NCC-S1 cells

Sca-1 was upregulated in NCC-S1M cells and Sca-1 postive cells showed cancer stem cell-like characteristics

Given that NCC-S1M cells showed cancer stem cell-like features, it was hypothesized that gene expression profiling of these cells may provide clues for the identification of putative stem cell markers in our cell line model. An mRNA sequencing comparison between NCC-S1M and NCC-S1 identified Sca-1 as one of the most significantly overexpressed genes. Overexpression of Sca-1 protein in NCC-S1M cells was validated using FACS analyses (Fig 6A) and immunofluorescence (Fig 6B). FACS-sorted Sca-1 high population was compared with Sca-1 negative population for the tumorigenic potential using the limiting dilution assay. After 3 weeks, SCID mice injected with 10^5 Sca-1 high NCC-S1 and NCC-S2 cells formed subcutaneous tumors, while mice injected with the same number of Sca-1 negative cells did not. After 8 weeks, there was significant difference in tumors formed according to the Sca-1 (Table 3). Once formed, Sca-1 high cells also grew much faster *in vivo* (data not shown). Sca-1 FACS analysis using Sca-1 high cell-forming tumors showed that they consisted of tumor cells with a wide range of expression pattern of Sca-1 similar to that of original cell line (data not shown). The limiting dilution assay using two primary gastric cancer cell lines from gastric cancers arising in *Pdx-1-Cre;Smad4*$^{F/F}$*;Trp53*$^{F/F}$*;Cdh1*$^{F/+}$ mice also demonstrated that Sca-1 high populations possessed higher tumorigenic potential than

Sca-1 negative population as observed in NCC-S1 and NCC-S2 (Table 4). In addition, Sca-1 high cell-forming tumors showed higher rates of drug resistance than Sca-1 negative cell-forming tumors (Fig 7A and 7B).

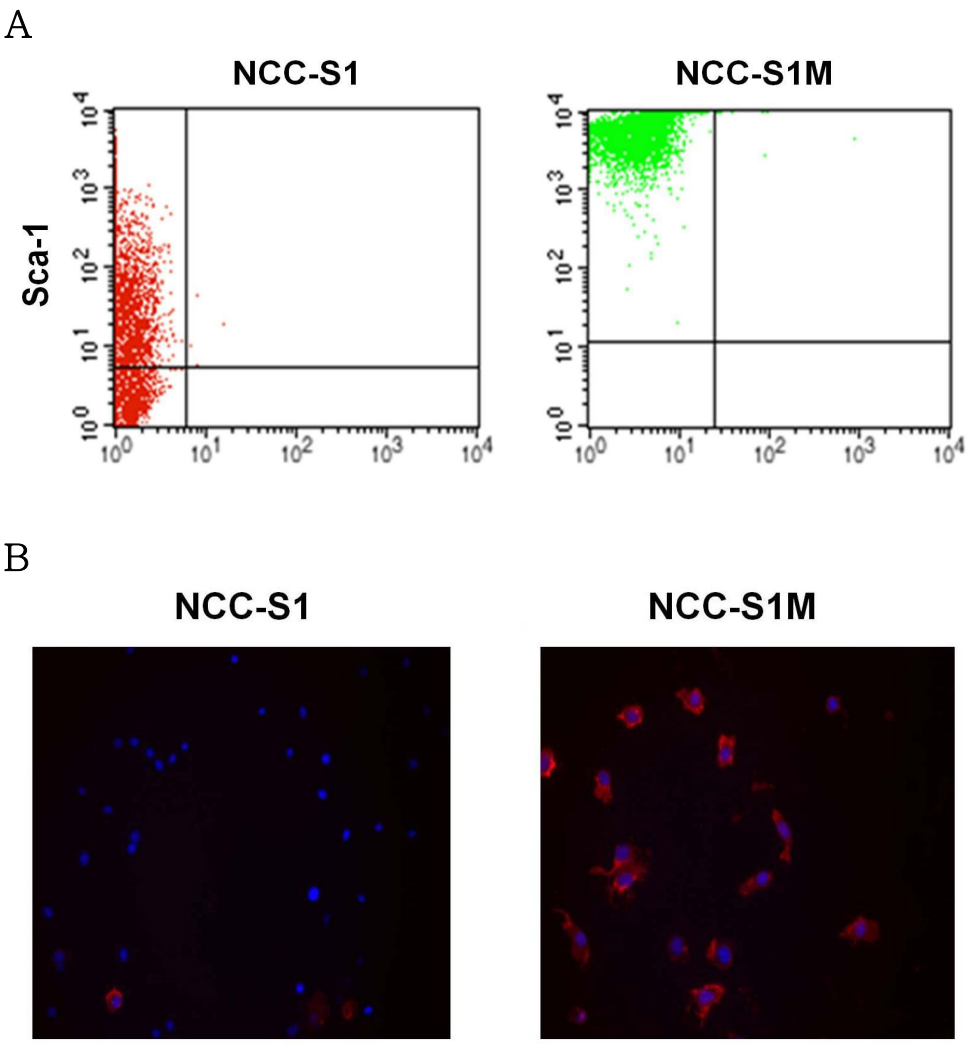

Fig 6. (A) Sca-1 FACS finding for NCC-S1M and S1 cells and (B) Sca-1 immunofluorescent images of NCC-S1 and S1M cells.

Table 3. Limiting dilution assays for NCC-S1 and S2 in Nude mice according to Sca-1 expression, measured 8 weeks after injection

Cell	Cell dose	No mice with tumors (%)	p-value
NCC-S1			
Sca-1 high	1 X 10^5	5 / 5 (100.0)	
	1 X 10^4	5 / 5 (100.0)	
	1 X 10^3	4 / 5 (80.0)	
			<0.001
Sca-1 negative	1 X 10^5	4 / 5 (80.0)	
	1 X 10^4	4 / 5 (80.0)	
	1 X 10^3	2 / 5 (40.0)	
NCC-S2			
Sca-1 high	1 X 10^5	5 / 5 (100.0)	
	1 X 10^4	5 / 5 (100.0)	
	1 X 10^3	4 / 5 (80.0)	
			<0.001
Sca-1 Low	1 X 10^5	5 / 5 (100.0)	
	1 X 10^4	4 / 5 (80.0)	
	1 X 10^3	0 / 5 (40.0)	

Table 4. Limiting dilution assays for *Pdx-1-Cre;Smad4$^{F/F}$;Trp53$^{F/F}$;Cdh1$^{F/+}$* gastric cancer cell lines in Nude mice according to Sca-1 expression, measured 8 weeks after injection

Cell	Cell dose	Number of mice with tumors (%)	P-value
Cell line 1			
	1×10^5	5 / 5 (100.0)	
High	1×10^4	5 / 5 (100.0)	
	1×10^3	3 / 5 (60.0)	
			<0.001
	1×10^5	5 / 5 (100.0)	
Negative	1×10^4	3 / 5 (60.0)	
	1×10^3	0 / 5 (0.0)	
Cell line 2			
	1×10^5	5 / 5 (80.0)	
High	1×10^4	4 / 5 (0.0)	
	1×10^3	4 / 5 (0.0)	
			<0.001
	1×10^5	5 / 5 (0.0)	
Negative	1×10^4	4 / 5 (0.0)	
	1×10^3	1 / 5 (0.0)	

A

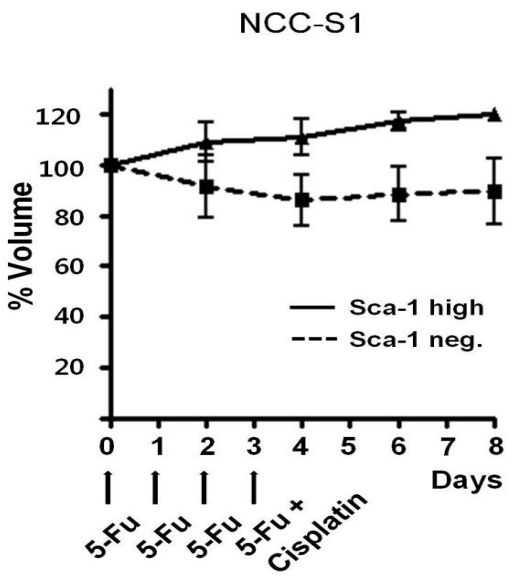

B

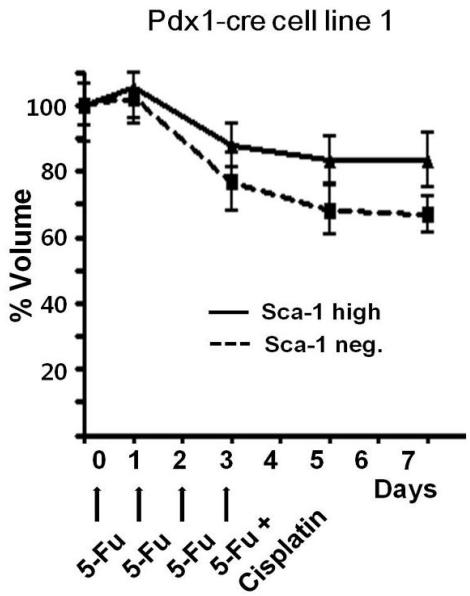

Fig 7. Gastric cancer cells with high Sca-1 expression showed higher *In vivo* chemoresistance to 5-Fu (25 mg/kg) and Cisplatin (5 mg/kg) combination treatment on SCID mice than Sca-1 negative gastric cells.

Sca-1 gene expression signature predicts survival following chemotherapy

According to the DNA microarray analysis, 85 genes were overexpressed by greater than 1.5-fold in Sca-1 high NCC-S1 cells compared with Sca-1 negative NCC-S1 cells (Table 5). These 85 genes overexpressed in Sca-1 high cells were designated as the *Sca-1* signature. Interestingly, CD133, a potential cancer stem cell marker in gastric cancer, was included in these 85 genes (Fukamachi, Shimada et al. 2011; Qiao and Gumucio 2011). *Fscn1 (Chen, Yang et al. 2010; Sun, He et al. 2011), Lox* (El-Haibi, Bell et al. 2012) and *Tnc* (Oskarsson, Acharyya et al. 2011), known to be critical for metastasis, were included among these 85 genes. Nestin, a neural stem cell marker, which was also known to promote metastasis, was also included (Lendahl, Zimmerman et al. 1990; Matsuda, Naito et al. 2011). Embryonic stem cell markers, such as SOX9 (Matheu, Collado et al. 2012), and others involved in the stem cell niche, such as Cxcl7 (Liu, Ginestier et al. 2011), were also included in the *Sca-1* signature. As shown in Table 5, most of these 85 genes were also overexpressed in NCC-S1M cells compared with Sca-1 negative NCC-S1 cells.

Because Sca-1 does not have human homologs, human homologs of these 85 mouse genes in the *Sca-1* signature (88 Affymetrix probe sets) were evaluated for clinical relevance. Using these 88 probe sets in the *Sca-1* signature, hierarchical clustering analysis

was performed on DNA microarray data for pretreatment biopsy samples collected from gastric cancer patients who were treated with cisplatin/fluorouracil chemotherapy (Kim, Choi et al. 2012). The *Sca-1* signature clustered 123 patients into 2 subsets (Fig 8A). Patients who overexpressed genes in the *Sca-1* signature had significantly shorter overall survival following cisplatin/fluorouracil chemotherapy compared with those who underexpressed these genes {7.6 months [95% confidence interval (CI), 6.1-9.2] *vs* 11.9 months (95% CI, 8.1-16.8); log-rank *p* value = 0.005; hazards ratio = 1.7 (95% CI, 1.2-2.5)} (Fig 8B), while 2 patient subsets clustered using all Affymetrix probe sets were not different in overall survival (*data not shown*). *Ifitm3*, *Fscn1*, *Wnt7a*, and *Cldn6* were representative genes in the *Sca-1* signature that were associated with poor survival following chemotherapy. Thus, overexpression of the *Sca-1* signature was associated with the clinical chemoresistance.

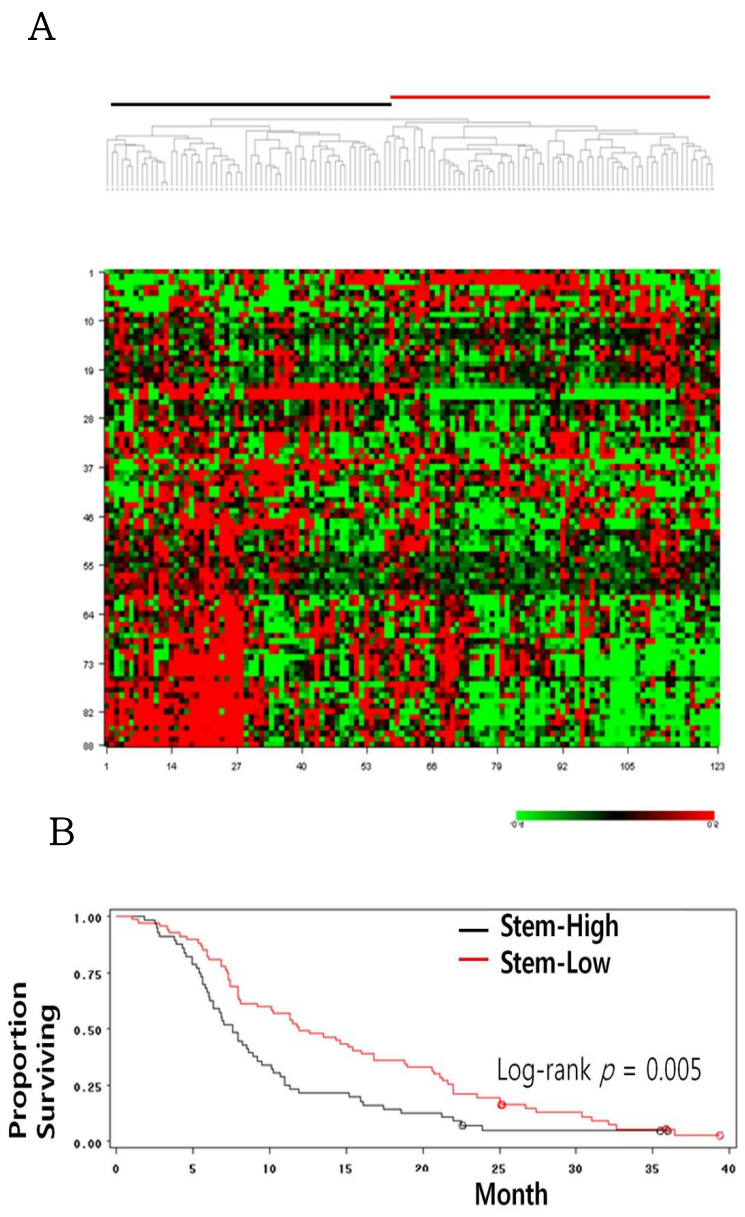

Fig 8. (A) A hierarchical clustering dendrogram for pretreatment biopsy samples of chemotherapy-treated gastric cancer patients, which was generated using genes overexpressed in Sca-1 high S1 cells (*Sca-1* signature) (B) Overall survival of 2 clusters generated by (A). Patients who overexpressed the *Sca-1* signature had significantly shorter overall survival (Log-rank p = 0.005).

Table 5. Sca-1 signature (*shown in the order of decreasing fold change*)

Gene	Sca-1 Negative	Sca-1 High	NCC-S1M
Ly6c1	1213	4979	9587
Ifitm3	449	1805	11824
Vmn1r93	53	185	79
Dcn	299	1022	1064
Ly6a	3020	10046	14630
Ly6c2	652	2094	4017
Rhox4e	33	104	34
2310007B03Rik	515	1480	537
Rhox4a	52	135	70
Serpine2	475	1208	3138
Fscn1	739	1853	5673
C87414	28	69	41
Rpl21	63	153	106
Fstl1	704	1673	4448
Prrx1	324	736	5700
Fgf7	459	992	1095
D5Ertd577e	29	62	37
Lox	1212	2550	2948
Cldn2	314	637	174
Nes	394	778	1297
Pcolce	1739	3354	9013
Sox9	709	1367	1881
C1s	91	175	340
Prom1	359	676	1355
6330406I15Rik	197	370	1598
Igf2bp3	257	483	477
Enpp2	447	834	424
Lcn2	418	775	1168
Tnc	579	1063	2495
Tead2	751	1373	2331

Gjc1	412	748	887
Ccbe1	634	1147	3342
Pdzrn3	267	476	541
Thbs1	2505	4427	10678
5730471H19Rik	760	1340	2392
Tmem173	389	683	3525
Vmn2r43	85	149	118
Sox11	347	607	266
AI451617	75	130	950
Gprc5c	405	700	272
Lrrk2	286	489	293
Angpt1	116	197	740
Ott	236	399	329
Ppap2b	833	1398	2934
Acan	488	817	1835
Hmcn1	117	195	420
Wnt7a	353	585	1243
Grasp	695	1145	2104
Ebf1	230	379	811
Plac9	237	390	444
Ccl7	517	843	3220
Xlr4b	148	239	142
Pmp22	2345	3783	5895
Gpr176	1113	1792	2349
Saa3	183	294	458
Igfbp4	888	1425	8755
2610528A11Rik	1411	2252	431
C3	3061	4874	7550
Cldn6	4456	7067	6177
Cda	1187	1878	2540
Acaa1b	109	173	116

Amd1	142	224	106
Masp1	493	776	3624
Pramel3	108	169	96
Osmr	1303	2041	3855
Tgm2	1378	2151	1671
Sema6a	445	694	1247
Cmbl	409	638	218
Fndc4	580	901	1555
Nox4	169	261	855
Gm4907	137	211	154
Il1rl1	485	748	11874
Plxdc2	377	579	3891
Pcdh18	567	871	571
Hmgb1	466	713	691
Ifi203	231	354	911
Sdc3	476	726	606
Olfr1331	110	167	152
Speer4d	129	195	106
Olfr963	124	188	116
Sirpa	807	1222	2081
Il1r1	554	837	1140
Rcn1	762	1149	2212
EG381936	72	109	69
Rhoq	343	516	1357

Upregulated Interleukin-1 signaling pathway in Sca-1 postive cells

Because DAVID functional annotation chart analyses on the Sca-1 signature demonstrated that Sca-1 high cells exhibited accentuated inflammatory response associated with interleukin 1 signaling such as higher expression of interleukin 1 receptor type 1 (*IL1R1*) than Sca-1 negative cells (Table 6), we hypothesized that Sca-1 high cancer cells acquired the cancer stem cell-like properties via activation of interleukin 1 pathway.

Actually, Sca-1 high cells consistently showed higher gene expression levels of interleukin 1-related genes such as *IL1R1*, *IL1RL1*, and *IL1RAP* compared to Sca-1 negative cells as NCC-S1M cells did compared to NCC-S1 cells (Fig 9). Western blot analysis demonstrated that Sca-1 high cells showed upregulated JNK and higher expression of phosphorylated c-Jun and Bcl-xl than Sca-1 negative cells as observed in NCC-S1M cells (Fig 10). JNK, which could be activated by interleukin 1, phosphorylates and regulates the activity of proto-oncogene c-Jun (Davis 2000). Bcl-xL protects against apoptotic cell death and results in survival of cancer cells, thus confers resistance to multiple chemotherapy agents (Minn, Rudin et al. 1995). The activity of Bcl-xL could be regulated by JNK (Liu and Lin 2005).

To determine whether Interleukin 1 signaling pathway plays an important roles in tumorigenesis, we activated Interleukin 1 pathway in NCC-S1 cells by IL-1β treatment. NCC-S1 cells

treated by IL-1β showed enhanced tumorigenic potential compared to untreated NCC-S1 cells (Fig 11A). These cells also enhanced JNK pathway and Bcl-xL level (Fig 11B). FACS analysis demonstrated that IL-1β treatment on NCC-S1 cells didn't change Sca-1 expression level (data not shown).

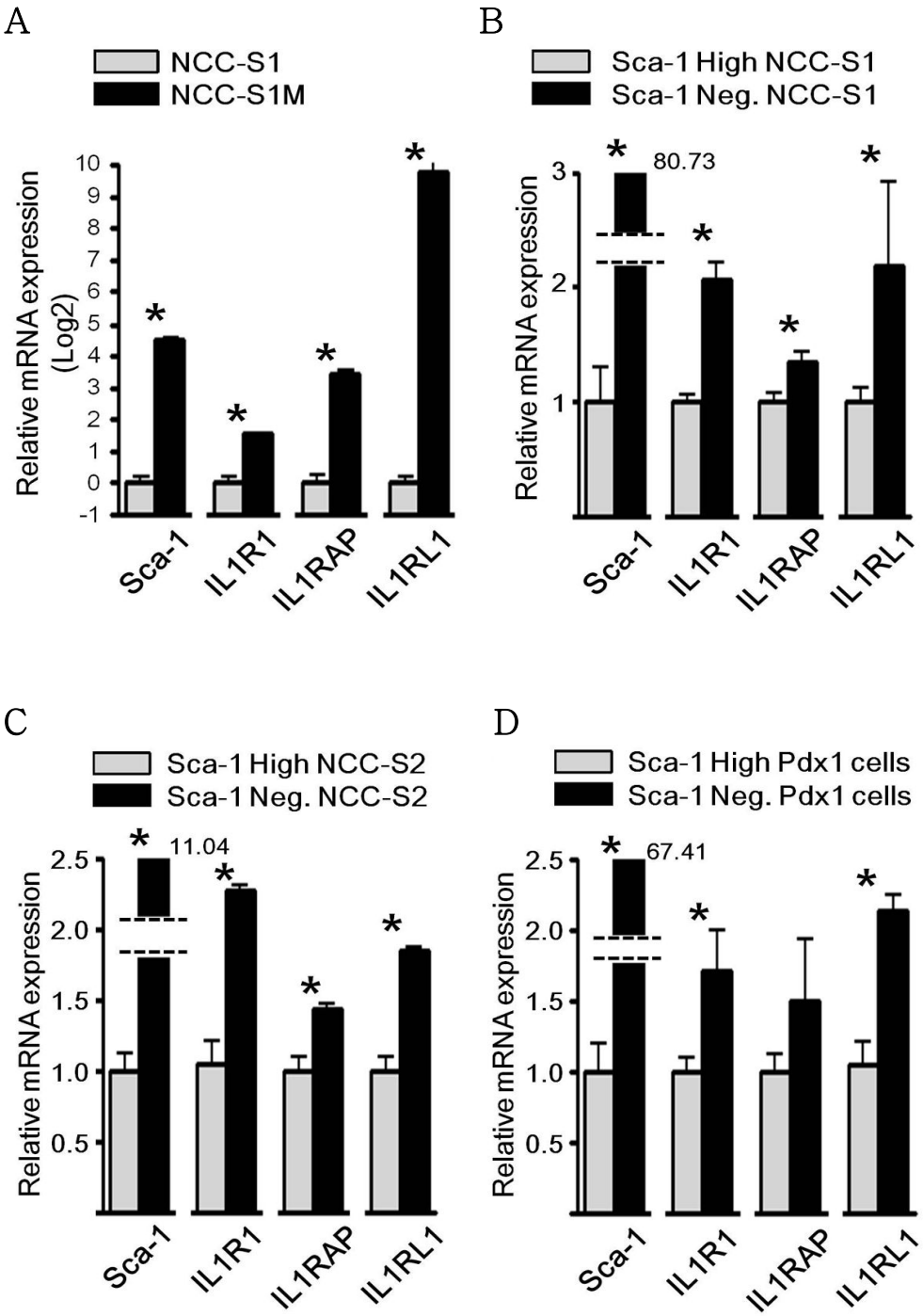
A
NCC-S1
NCC-S1M
Relative mRNA expression (Log2)
10
9
8
7
6
5
4
3
2
1
0
-1
Sca-1
IL1R1
IL1RAP
IL1RL1
B
Sca-1 High NCC-S1
Sca-1 Neg. NCC-S1
Relative mRNA expression
3
2
1
80.73
Sca-1
IL1R1
IL1RAP
IL1RL1
C
Sca-1 High NCC-S2
Sca-1 Neg. NCC-S2
Relative mRNA expression
2.5
2.0
1.5
1.0
0.5
11.04
Sca-1
IL1R1
IL1RAP
IL1RL1
D
Sca-1 High Pdx1 cells
Sca-1 Neg. Pdx1 cells
Relative mRNA expression
2.5
2.0
1.5
1.0
0.5
67.41
Sca-1
IL1R1
IL1RAP
IL1RL1

Fig 9. mRNA expression of interleukin 1-related genes (*IL1R1*, *IL1RL1*, and *IL1RAP*) in NCC-S1M cells compared to NCC-S1 cells (A), in Sca-1 high NCC-S1 cells compared to Sca-1 negative NCC-S1 cells (B), in Sca-1 high NCC-S2 cells compared to Sca-1 negative NCC-S2 cells (C), and in Sca-1 high Pdx1-cre gastric cancer cells compared to Sca-1 negative cells (D).

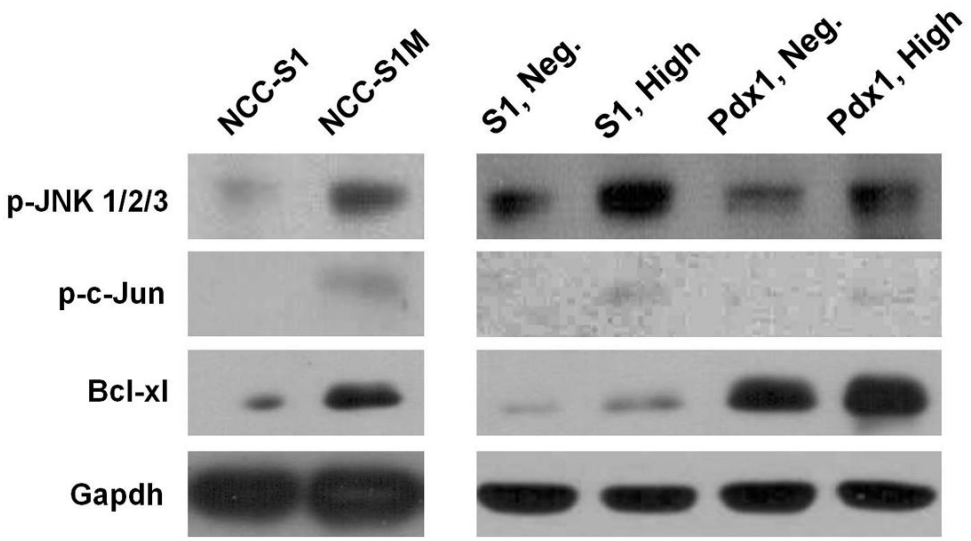

Fig 10. Western blot analyses showing the overexpression of JNK, phospholylated c-Jun, and Bcl-xL in NCC-S1M cells compared to NCC-S1 cells and in Sca-1 high gastric cancer cells compared to Sca-1 negative cells.

A

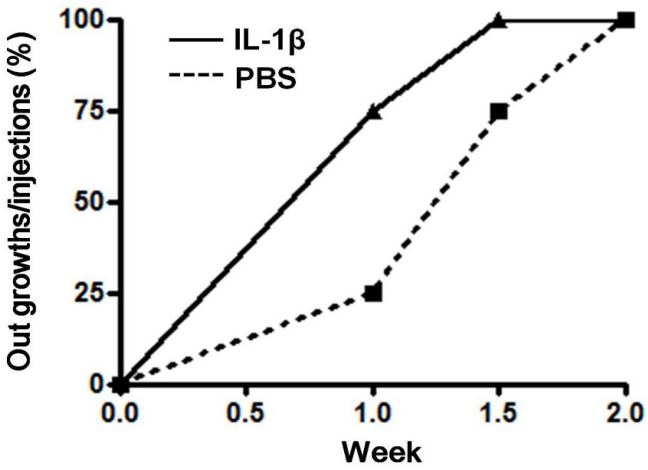

B

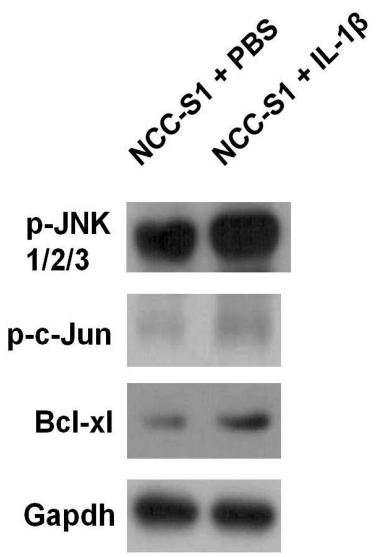

Fig 11. (A) Enhanced tumorigenic potential in NCC-S1 cells treated by IL-1β in subcutaneously tumor cell-injected SCID mice. (B) Western blot analyses showing upregulated expression of JNK, phospholylated c-Jun, and Bcl-xL in IL-1β-treated NCC-S1 cells compared to PBS-treated cells.

Table 6. DAVID functional annotation chart analyses on the genes upregulated by >1.5-fold in Sca-1 high S1cells (*Sca-1* signature)

Term	*P*	Genes
GO:0045087~innate immune response	0.0001	IL1R1, TMEM173, MASP1, IL1RL1, C3, C1S
GO:0006952~defense response	0.0001	IL1R1, TMEM173, MASP1, IL1RL1, C3, SAA3, C1S, THBS1, CCL7, IGFBP4
GO:0006954~inflammatory response	0.0003	MASP1, C3, SAA3, C1S, THBS1, CCL7, IGFBP4
GO:0001568~blood vessel development	0.0005	CCBE1, TGM2, PRRX1, ANGPT1, LOX, PPAP2B, GJC1
GO:0032103~positive regulation of response to external stimulus	0.0005	HMGB1, C3, TGM2, THBS1
GO:0001944~vasculature development	0.0005	CCBE1, TGM2, PRRX1, ANGPT1, LOX, PPAP2B, GJC1
GO:0048584~positive regulation of response to stimulus	0.0010	HMGB1, MASP1, C3, TGM2, C1S, THBS1
GO:0009611~response to wounding	0.0029	MASP1, C3, SAA3, C1S, THBS1, CCL7, IGFBP4
GO:0006955~immune response	0.0031	IL1R1, TMEM173, MASP1, IL1RL1, C3, ENPP2, C1S, CCL7
GO:0002526~acute inflammatory response	0.0045	MASP1, C3, SAA3, C1S
GO:0022612~gland morphogenesis	0.0050	FGF7, TNC, TGM2, SOX9
GO:0007155~cell adhesion	0.0079	CLDN6, TNC, ACAN, CLDN2, THBS1, SOX9, SIRPA, PCDH18
GO:0022610~biological adhesion	0.0080	CLDN6, TNC, ACAN, CLDN2, THBS1, SOX9, SIRPA, PCDH18
GO:0032101~regulation of response to external stimulus	0.0088	HMGB1, C3, TGM2, THBS1
GO:0048514~blood vessel morphogenesis	0.0089	CCBE1, TGM2, PRRX1, ANGPT1, GJC1
GO:0002541~activation of plasma proteins involved in acute inflammatory response	0.0096	MASP1, C3, C1S
GO:0006956~complement activation	0.0096	MASP1, C3, C1S
GO:0016337~cell-cell adhesion	0.0161	CLDN6, ACAN, CLDN2, SOX9, PCDH18
GO:0048705~skeletal system morphogenesis	0.0164	ACAN, PRRX1, SOX9, WNT7A

GO:0006959~humoral immune response	0.0208	MASP1, C3, C1S
GO:0042127~regulation of cell proliferation	0.0228	NOX4, HMGB1, FGF7, IFITM3, TGM2, PRRX1, SOX9
GO:0043062~extracellular structure organization	0.0235	TNC, ACAN, LOX, WNT7A
GO:0060638~mesenchymal–epithelial cell signaling	0.0245	FGF7, TNC
GO:0051605~protein maturation by peptide bond cleavage	0.0294	MASP1, C3, C1S
GO:0051216~cartilage development	0.0410	ACAN, PRRX1, SOX9
GO:0050921~positive regulation of chemotaxis	0.0444	HMGB1, THBS1
GO:0048732~gland development	0.0475	FGF7, TNC, TGM2, SOX9
GO:0048520~positive regulation of behavior	0.0484	HMGB1, THBS1
GO:0050920~regulation of chemotaxis	0.0484	HMGB1, THBS1
GO:0002253~activation of immune response	0.0489	MASP1, C3, C1S

Discussion

There are only a few murine gastric cancer cell lines available in the scientific community, neither of which is genetically defined because tumors were carcinogen-induced. Several genetically engineered mouse models for gastric cancer have been reported, these models have been generated in the lineage of parietal cells using K14 and Atb6 promoters (Wang, Dangler et al. 2000; Oshima, Matsunaga et al. 2006; Shimada, Mimata et al. 2012), from which no human gastric cancer ever originate. On the other hand, we have developed a spontaneous mouse gastric cancer deficient in Smad4 and p53, which represent most frequently mutated genes/pathways in gastric cancer (Wang, Kim et al. 2007), using Villin-cre mice. The *Villin* promoter is active in quiescent cells in the antrum until E16 (Qiao, Ziel et al. 2007). In this regard, this mouse gastric cancer of ductal origin uniquely recapitulates human gastric adenocarcinomas from both histological and molecular perspectives.

Only one of 45 *Villin-cre*;*Smad4*$^{F/F}$;*Trp53*$^{F/F}$;*Cdh1*$^{F/wt}$ mice have developed the gastric cancer primarily because they had obstructive intestinal tumors at an early age. Even so, we were able to establish one cell line, NCC-S1, primarily cultured from the *Villin-cre;Smad4*$^{F/F}$;*Trp53*$^{F/F}$;*Cdh1*$^{F/wt}$ gastric cancer. Significant overlap between human and mouse gastric cancer signatures was observed in NCC-S1. *Myc,* one of the frequently amplified genes in human

gastric cancer, was also found to be amplified in our cells (data not shown). NCC-S1M cells were primarily cultured from lung metastases of NCC-S1 cells. Interestingly, NCC-S1M cells showed EMT phenotype including morphology and molecular perspectives, showing enhanced Wnt signaling. EMT is crucially involved in cancer metastasis and Wnt signaling has been linked to the process of EMT (Vincan and Barker 2008; Kahlert, Maciaczyk et al. 2012). Thus, EMT features of NCC-S1M are partially explainable by the EMTs.

NCC-S1M cells consistently developed lung metastases more rapidly than parental clones. Moreover, NCC-S1M cells provide an orthotopic gastric cancer model that predictably metastasizes to lung and liver. For the first time to our knowledge, these cells can serve as unique models to evaluate the metastatic potential of gastric cancer. In addition, NCC-S1M cells are very useful to test efficacy and toxicity of immunotherapeutic agents because this cell line readily formed tumor in syngeneic host mice. Actually anti-4-1BB mAb, novel immunotherapeutic agent, significantly suppressed the growth of NCC-S1M compared with controls.

NCC-S1M cells demonstrate cancer stem cell-like features such as increased tumorigenicity, metastasis, and chemoresistance. Sca-1 was found to be one of the most highly upregulated genes in NCC-S1M cells. Our findings are consistent with data in the literature that overexpression of Sca-1 or other Ly6 family

members are commonly associated with an aggressive tumor phenotype (Cohn, Kramerov et al. 1997; Treister, Sagi-Assif et al. 1998; Witz 2000; Li, Welm et al. 2003; Xin, Lawson et al. 2005; Grange, Lanzardo et al. 2008; Batts, Machado et al. 2011). Sca-1 is associated with increased tumorigenicity or metastasis in breast or prostate cancers but not in gastrointestinal tract cancers. Although Sca-1 is murine-specific, our gastric cancer patient database indicates that the Ly6 gene family (8q24.3) is frequently amplified (9%), and associated with poor response to cisplatin/fluorouracil chemotherapy (hazard ratios of LY6E and LY6D=1.2 and 1.2; p=0.025 and 0.042, respectively). Moreover, we observed the similar association between the poor clinical response to chemotherapy and the high expression of Sca-1 gene expression signature (Fig 4D). In addition, several putative stem cell markers such as CD133 and SOX9 were included in the Sca-1 gene expression signature (Table 5).

Sca-1 high populations in our gastric cancer cell lines showed higher tumorigenic potential and chemoresistance. FACS analysis demonstrated that Sca-1 high population comprises about 5% of our primary gastric cancers arising in *Pdx-1-Cre;Smad4*$^{F/F}$*;Trp53*$^{F/F}$*;Cdh1*$^{F/+}$ mice and Sca-1 high cell-forming tumors consisted of tumor cells with a wide range of expression pattern of Sca-1 similar to that of original cell line (data not

shown). Collectively, these results suggest that Sca-1 might be a murine gastric cancer stem cell marker.

In normal mammary cells, the mechanism of action of Sca-1 involves the inhibition of TGF-β signal transduction pathway (Upadhyay, Yin et al. 2011). Because our Smad4-null cells are deficient in the TGF-β pathway, other signal transduction pathways may play important roles in Sca-1 high cells. Interestingly, the DNA microarray analysis demonstrated that the Sca-1 signature is significantly enriched in genes involved in the immune system and immune response, especially upregulation of interleukin 1 signaling-related genes such as *IL1R1* and *IL1RL1*. In addition, Sca-1 high cells consistently showed higher gene expression levels of *IL1R1*, *IL1RL1*, and *IL1RAP* compared to Sca-1 negative cells and IL-1β-treated NCC-S1 cells showed enhanced tumorigenic potential compared to untreated NCC-S1 cells. This finding provides the possibility that cancer stem cell like phenotype in Sca-1 high cells might be explained by enhanced interleukin 1 signaling pathway. Inflammatory cytokines play a key role in malignant progression of various cancers (Germano, Allavena et al. 2008). Although dual roles for activated interleukin 1 signaling pathway have been proposed, activation of this pathway been associated with a aggressive tumor phenotype such as growth, invasion, and metastasis in several types of mouse or human cancers (Gemma, Takenaka et al. 2001; Elaraj, Weinreich et al.

2006). Interleukin 1 gene cluster polymorphisms suspected of enhancing production of interleukin 1 beta are associated with an increased risk of gastric cancer (El-Omar, Carrington et al. 2000). Recent study revealed the effects of IL-1beta on the promotion of stemness such as increased tumorigenic potential and drug resistance in glioma and colon cancer cells (Li, Wang et al. 2012; Wang, Liu et al. 2012).

Western blot analysis showed that Sca-1 high cells up-regulated JNK, a mitogen-activated protein kinase (MAPK) family member, compared to Sca-1 negative cells. Increased JNK expression in Sca-1 high cells might be associated with enhanced interleukin 1 pathway because its enzymatic activity is induced in response to diverse stimuli including cytokine such as interleukin 1 and tumor necrosis factor (TNF) (Li, Commane et al. 2001; Seki, Brenner et al. 2012). Expectedly, phosphorylated c-jun, a representative target of JNKs (Seki, Brenner et al. 2012), was overexpressed in Sca-1 high cells. Although roles of JNK in cancer are unclear, several mouse cancer models revealed the oncogenic roles in gastrointestinal cancers (Sakurai, Maeda et al. 2006; Shibata, Maeda et al. 2008). Mice lacking JNK1 exhibited a marked decrease in gastric carcinogenesis induced by N-methyl-N-nitrosourea compared to their wild-type counterparts (Shibata, Maeda et al. 2008). Bcl-xL, antiapoptotic protein, also increased in Sca-1 high cells. Bcl-xL confers resistance to multiple chemotherapy agent

(Minn, Rudin et al. 1995) and multiple kinases, including JNKs, mediate phosphorylation of Bcl-xL (Kharbanda, Saxena et al. 2000; Upreti, Galitovskaya et al. 2008). Thus, drug resistance observed in Sca-1 high cells is partially explainable by overexpression of Bcl-xL.

In summary, our NCC-S1M cells serve as a good gastric cancer cell line model for the identification of candidate cancer stem cell markers as well as for testing immunotherapeutics and, possibly, anti-metastasis agents. Sca-1 is identified as a potential cancer stem cell marker in metastatic derivatives of a murine gastric cancer cell line. Although the Sca-1 results may not explain all aggressive behavior of the NCC-S1M cells, it suggests that Interleukin 1 - JNK - Bcl-xL axis observed in Sca-1 signature may play an important role in gastric cancer stem cell pathways.

GENAERAL DISCUSSION AND CONCLUSION

Gastric cancer is the second most common cause of cancer death, but, in the scientific and pharmaceutical communities, there are no genetically defined, murine metastatic gastric cancer models that closely recapitulate human gastric cancer. *Pdx-1-Cre;Smad4$^{F/F}$;Trp53$^{F/F}$;Cdh1$^{F/+}$* mice described in this study are unique in several aspects. Gastric adenocarcinomas formed in these mice are of the mucus-secreting gastric epithelial cell origin, which is relevant for human gastric adenocarcinomas. In addition, tumor suppressor genes most commonly inactivated in human diffuse-type gastric adenocarcinomas were targeted to be knocked-out in the gastroduodenal epithelium of this model. In this regard, our mouse gastric cancer cells of glandular origin uniquely recapitulate human gastric adenocarcinomas in genetic composition.

The specific role of E-cadherin loss in the development of diffuse-type gastric adenocarcinomas was clearly documented by this cross-tissue tumorigenesis study. We demonstrate that loss of expression of E-cadherin occurs only in the gastric cancer model with the *Cdh1* heterozygote and is a similar phenomenon that occurs in the human disease. This finding has not previously been demonstrated in a genetically-engineered mouse model system. *CDH1* promoter hypermethylation is the most common cause of the second hit in human gastric cancer that develop in germline *CDH1* mutation carriers (Grady, Willis et al. 2000). However, Concolino,

et al. reported that 4 of 6 human diffuse-type gastric carcinoma (HDGC) patients had promoter hypermethylation but the other two patients did not (Concolino, Papa et al. 2004). Thus, molecular mechanisms other than promoter hypermethyation, such as transcription factor mediated events, may play a role in *CDH1* down-regulation in HDGC. According to current data, *CDH1* promoter hypermethylation is detectable in about 50% of HDGC cases and in 40-80% of sporadic diffuse gastric cancer cases.

Promoter methylation has been described in association with aging. While *CDH1* somatic mutation and promoter hypermethyation is also frequent in sporadic diffuse-type gastric cancers, early onset gastric cancers are known to have relatively few methylation events for common tumor suppressors such as *MLH1* (Carvalho, Milne et al. 2004). Our mouse models, which develop gastric cancer without carcinogen exposure, therefore, are relevant to human gastric cancer despite the low incidence of *CDH1* promoter hypermethylation. Loss of expression of E-cadhein in the $Cdh1^{F/+}$ background appears to be a required, selected molecular change that is needed for both the human and mouse tumor formation. Studies are ongoing in our laboratory to identify gastric tissue-specific epigenetic events or signaling pathway activation leading to E-cadherin loss that may be promoted by loss of Smad4 or p53.

While Smad4 is inactivated in 40% of human gastric cancers (Wang, Kim et al. 2007), functional roles of Smad4 in gastric cancer

progression have not been fully evaluated using *in vivo* models. Especially, the anti-metastatic role of Smad4 in gastric cancer, which has not been previously demonstrated *in vivo.* Our study is the first to demonstrate the Smad4 loss-induced β-catenin activation in gastric cancer, and is consistent with a prior report that Smad4 mediates canonical BMP signaling by repressing the transcription of β-catenin in SW480 colon cancer cells (Oliveira, Sousa et al. 2009). Therefore, inhibition of β-catenin may be a converging node for the anti-metastatic signaling pathways driven by E-cadherin and Smad4 in *Pdx-1-Cre;Smad4*$^{F/F}$*;Trp53*$^{F/F}$*;Cdh1*$^{F/+}$ mice.

CSCs are promising for the development of anticancer drugs because it could explain resistance to chemotheraphy and eventual tumor relapse. The existence of a CSC in gastric cancer has been investigated in several reports, but robust CSC markers have not been identified in human and mouse gastric cancers. Sca-1 was overexpressed in metastatic NCC-S1M cells that demonstrate cancer stem cell-like features such as increased tumorigenicity, metastasis, and chemoresistance. High Sca-1 expression is associated with enhanced tumorigenicity or metastasis in breast or prostate cancers but not in gastrointestinal cancers (Cohn, Kramerov et al. 1997; Treister, Sagi-Assif et al. 1998; Witz 2000; Li, Welm et al. 2003; Xin, Lawson et al. 2005; Grange, Lanzardo et al. 2008; Batts, Machado et al. 2011). Our study is the first to

identify Sca-1 as an enrichment marker for tumor-initiating and chemoresistant population of gastric cancers. Sca-1 gene expression signature identified in our mouse tumor cells clustered pretreatment biopsy samples of patients according to their survival durations after cisplatin/fluorouracil chemotherapy. To our knowledge, our study is the first to demonstrate that Sca-1 is an enrichment marker for chemoresistance.

Our study revealed the activation of the interleukin-1 receptor signaling in Sca-1 high gastric cancer cells. Activation of interleukin-1 receptor signaling pathway has been associated with aggressive tumor phenotypes such as growth, invasion, and metastasis in several types of mouse or human cancers(Gemma, Takenaka et al. 2001; Elaraj, Weinreich et al. 2006; Germano, Allavena et al. 2008). Especially, Bcl-xL over-expressed in Sca-1 high cells. Bcl-xL confers resistance to multiple chemotherapy agent (Minn, Rudin et al. 1995) and multiple kinases, including JNKs, mediate phosphorylation of Bcl-xL (Kharbanda, Saxena et al. 2000; Upreti, Galitovskaya et al. 2008). Our data is consistent with these data in the literature, and further studies need to be performed to evaluate whether and how cancer stem cell phenotypes of Sca-1 high cells are attributable to each of these components of interleukin-1 receptor signaling pathway.

This long-term *in vivo* experiment evaluated the effect of loss of one allele of E-cadherin, alone and in combination with loss of

Smad4, on the development and metastasis of diffuse type gastric carcinoma in mice. By creating genetically-engineered mouse models closely recapitulating the mutation profiles in humans, we demonstrated the critical role of E-cadherin loss in the development of diffuse type gastric adenocarcinomas by cross-tissue tumorigenesis study. Moreover, the metastatic phenotype of our mutant mice provides us a unique opportunity to dissect the roles of E-cadherin and Smad4 in gastric cancer progression, and in relation to EMT. We also demonstrated that the loss of E-cadherin and Smad4 expression cooperate to promote lung metastasis through accumulating nuclear β-catenin. Taken together, our unique and novel murine gastric cancer models would be important to clarify the mechanism underlying HDGC formation and metastasis. It is also an excellent model for preclinical studies given its similarities with HDGC and its metastatic propensity. In addition, gene expression profiles of these models would facilitate the identification of putative gastric cancer stem cell markers as well as important genes associated with gastric cancer development and progression.

국문초록

위선암의 발생 및 전이에서 E-cadherin, Smad4, 그리고 p53 의 역할

박 준 원

지도 교수: 김 대 용

서울대학교 대학원 수의학과 수의병리학 전공

E-cadherin (*Cdh1*), Smad4 그리고 p53의 기능 상실은 위암 발생에서 중요한 역할을 하는 것으로 알려져 있다. 우리는 위암, 대장암, 그리고 유방암에서의 위 세 유전자의 역할을 정의하고 비교하기 위해서 *Pdx-1-Cre, Villin-Cre,* 그리고 *MMTV-Cre* 유전자 삽입 마우스를 이용하여 위장관 및 유선 상피세포 특이적으로 이 세 유전자를 불활화시킨 마우스를 제작하였다. *Pdx-1-Cre;Smad4$^{F/F}$;Trp53$^{F/F}$;Cdh1$^{F/+}$* 마우스에서 *Pdx-1-Cre;Smad4$^{F/F}$;Trp53$^{F/F}$* 마우스보다 위선암이 훨씬 높은 빈도로 발생하는 것이 확인되었다 [P<0.001]. *Pdx-1-Cre;Smad4$^{F/F}$;Trp53$^{F/F}$;Cdh1$^{F/+}$* 마우스에서 발생한 위선암은 E-cadherin 의 발현이 관찰되지 않았다. 그러나 *Villin-Cre;Smad4$^{F/F}$;Trp53$^{F/F}$;Cdh1$^{F/+}$* 와 *MMTV-*

Cre;Smad4$^{F/F}$*;Trp53*$^{F/F}$*;Cdh1*$^{F/+}$ 마우스의 장과 유선에서 발생한 선암에서는 E-cadherin 발현이 관찰되었으며, 야생형의 *Cdh1* 유전자를 가지고 있는 마우스와 종양 발생에서 차이를 보이지 않았다. *Pdx-1-Cre;Smad4*$^{F/F}$*;Trp53*$^{F/F}$*;Cdh1*$^{F/+}$ 마우스에서 *Pdx-1-Cre;*$^{F/F}$*;Trp53* $^{F/F}$*;Cdh1*$^{F/F}$ 마우스보다 더 빨리 위선암이 발생하였는데, 이는 *Cdh1* 이형접합이 Smad4와 p53이 불활화된 상태에서 위암의 발생과 진행을 촉진한다는 것을 보여준다. *Pdx-1-Cre;Smad4*$^{F/F}$*;Trp53*$^{F/F}$*;Cdh1*$^{F/+}$ 마우스의 14.2%에서 폐로의 전이가 관찰되었으며, 다른 유전자형에서는 전혀 관찰되지 않았다. *Pdx-1-Cre;Smad4*$^{F/F}$*;Trp53*$^{F/F}$*;Cdh1*$^{F/+}$ 마우스에서 발생한 위선암의 침습적인 성장을 보이는 부위에서 핵 내 β-catenin 의 축적이 관찰되었다. 이와 같은 현상은 E-cadherin 혹은 Smad4가 정상인 마우스에서 덜 관찰되었으며, 이는 E-cadherin 혹은 Smad4에 의한 β-catenin 신호 체계의 억제가 *Pdx-1-Cre;Smad4*$^{F/F}$*;Trp53*$^{F/F}$*;Cdh1*$^{F/+}$ 마우스에서 특이적으로 관찰된 폐로의 전이에 관련될 수 있음을 보여준다. *Pdx-1-Cre;Smad4*$^{F/F}$*;Trp53*$^{F/F}$*;Cdh1*$^{F/+}$ 마우스에서 발생한 위선암으로 부터 확립된 세포주들의 β-catenin 의 발현을 감소시켰을 때, 유의성 있게 세포주들의 이동 능력이 감소하는 것을 확인하였다. 결국, 이와 같은 결과는 E-cadherin 과 Smad4의 손실은 p53의 손실과 함께 위선암의 발생과 전이 과정을 촉진하는데 협동한다는 것을 보여준다.

또한 우리는 *Villin-Cre;Smad4*$^{F/F}$*;Trp53*$^{F/F}$*;Cdh1*$^{F/+}$ 마우스에서 발생한 위선암으로부터 마우스 위암 세포주를 확립하였고, NCC-S1 이라 명명하였다. 이 세포주를 면역결핍마우스의 옆구리 피하에

주사하여 만들어진 종양 조직으로부터 폐로 전이되어 형성된 전이소에서 전이성이 향상된 세포주를 확립하였다. 이 세포주를 NCC-S1M 으로 명명하였다. 이 세포주를 위 내 주사하였을 때 일관성 있게 종양을 형성하였고 NCC-S1 에 비해 마우스에서 향상된 전이 능력을 보여주었으며, 상피 세포에서 간질 세포로의 변이가 관찰되었다. NCC-S1M 은 종양의 형성 능력 및 항암제에 대한 저항성을 포함하여 다양한 암줄기세포의 특징을 보여주었다. 흥미롭게도, NCC-S1 에 비해서 NCC-S1M 에서는 Sca-1 의 과발현이 관찰되었다. Sca-1 양성 종양 세포들은 Sca-1 음성 종양 세포들에 비해 마우스에서 종양을 형성하는 능력 및 항암제에 대한 저항성이 높음을 확인할 수 있었다. Sca-1 양성 종양 세포들은 Sca-1 음성 종양 세포들에 비해 interleukin 1 신호 전달 경로의 활성화가 관찰되었다. 또한 Sca-1 양성 종양 세포들에서 Sca-1 음성 세포들에 비해 증가한 유전자들을 이용하여 123 명의 전이된 위암 소견을 보이는 환자들을 cisplatin 과 fluorouracil 치료 후 전반적인 생존 시간에 따라 단위 지을 수 있음을 확인하였다. 결국, 우리는 이 전이성이 확보된 새로운 마우스 위암 세포주 모델을 이용하여 마우스 위암 줄기 세포로서 Sca-1 을 발굴하였다.

핵심어: E-cadherin, Smad4, p53, β-catenin, Sca-1, 암 줄기세포, 전이

학 번: 2011-31099

References

Alberts, S. R., A. Cervantes, et al. (2003). "Gastric cancer: epidemiology, pathology and treatment." Ann Oncol 14 Suppl 2: ii31-36.

Andrechek, E. R., W. R. Hardy, et al. (2000). "Amplification of the neu/erbB-2 oncogene in a mouse model of mammary tumorigenesis." Proc Natl Acad Sci U S A 97(7): 3444-3449.

Barker, N. and H. Clevers (2010). "Leucine-rich repeat-containing G-protein-coupled receptors as markers of adult stem cells." Gastroenterology 138(5): 1681-1696.

Batts, T. D., H. L. Machado, et al. (2011). "Stem cell antigen-1 (sca-1) regulates mammary tumor development and cell migration." PLoS One 6(11): e27841.

Becker, K. F., M. J. Atkinson, et al. (1994). "E-cadherin gene mutations provide clues to diffuse type gastric carcinomas." Cancer Res 54(14): 3845-3852.

Birchmeier, W. and J. Behrens (1994). "Cadherin expression in carcinomas: role in the formation of cell junctions and the prevention of invasiveness." Biochim Biophys Acta 1198(1): 11-26.

Boussadia, O., S. Kutsch, et al. (2002). "E-cadherin is a survival factor for the lactating mouse mammary gland." Mech Dev 115(1-2): 53-62.

Brosh, R. and V. Rotter (2009). "When mutants gain new powers: news from the mutant p53 field." Nat Rev Cancer 9(10): 701-713.

Carvalho, R., A. N. Milne, et al. (2004). "Early-onset gastric carcinomas display molecular characteristics distinct from gastric carcinomas occurring at a later age." J Pathol 204(1): 75-83.

Chen, L., S. Yang, et al. (2010). "Migrastatin analogues target fascin to block tumour metastasis." Nature 464(7291): 1062-1066.

Cohn, M. A., D. Kramerov, et al. (1997). "The differentiation antigen Ly-6E.1 is expressed in mouse metastatic tumor cell lines." FEBS Lett 403(2): 181-185.

Concolino, P., V. Papa, et al. (2004). "The unsolved enigma of CDH1 down-regulation in hereditary diffuse gastric cancer." J Surg Res 121(1): 50-55.

Correa, P. and Y. H. Shiao (1994). "Phenotypic and genotypic events in gastric carcinogenesis." Cancer Res 54(7 Suppl): 1941s-1943s.

Davis, R. J. (2000). "Signal transduction by the JNK group of MAP kinases." Cell 103(2): 239-252.

Derksen, P. W., X. Liu, et al. (2006). "Somatic inactivation of E-cadherin and p53 in mice leads to metastatic lobular mammary carcinoma through induction of anoikis resistance and angiogenesis." Cancer Cell 10(5): 437-449.

Dhawan, P., A. B. Singh, et al. (2005). "Claudin-1 regulates cellular transformation and metastatic behavior in colon cancer." J Clin Invest 115(7): 1765-1776.

Driessens, G., B. Beck, et al. (2012). "Defining the mode of tumour growth by clonal analysis." Nature 488(7412): 527-530.

El-Haibi, C. P., G. W. Bell, et al. (2012). "Critical role for lysyl oxidase in mesenchymal stem cell-driven breast cancer malignancy." Proc Natl Acad Sci U S A 109(43): 17460-17465.

El-Omar, E. M., M. Carrington, et al. (2000). "Interleukin-1 polymorphisms associated with increased risk of gastric cancer." Nature 404(6776): 398-402.

el Marjou, F., K. P. Janssen, et al. (2004). "Tissue-specific and

inducible Cre-mediated recombination in the gut epithelium." Genesis 39(3): 186-193.

Elaraj, D. M., D. M. Weinreich, et al. (2006). "The role of interleukin 1 in growth and metastasis of human cancer xenografts." Clin Cancer Res 12(4): 1088-1096.

Elliott, R. L. and G. C. Blobe (2005). "Role of transforming growth factor Beta in human cancer." J Clin Oncol 23(9): 2078-2093.

Elston, R. and G. J. Inman (2012). "Crosstalk between p53 and TGF-beta Signalling." J Signal Transduct 2012: 294097.

Fukamachi, H., S. Shimada, et al. (2011). "CD133 is a marker of gland-forming cells in gastric tumors and Sox17 is involved in its regulation." Cancer Sci 102(7): 1313-1321.

Gemma, A., K. Takenaka, et al. (2001). "Altered expression of several genes in highly metastatic subpopulations of a human pulmonary adenocarcinoma cell line." Eur J Cancer 37(12): 1554-1561.

Germano, G., P. Allavena, et al. (2008). "Cytokines as a key component of cancer-related inflammation." Cytokine 43(3): 374-379.

Grady, W. M., J. Willis, et al. (2000). "Methylation of the CDH1 promoter as the second genetic hit in hereditary diffuse gastric cancer." Nat Genet 26(1): 16-17.

Graff, J. R., J. G. Herman, et al. (1997). "Mapping patterns of CpG island methylation in normal and neoplastic cells implicates both upstream and downstream regions in de novo methylation." J Biol Chem 272(35): 22322-22329.

Grange, C., S. Lanzardo, et al. (2008). "Sca-1 identifies the tumor-initiating cells in mammary tumors of BALB-neuT transgenic mice." Neoplasia 10(12): 1433-1443.

Guilford, P., J. Hopkins, et al. (1998). "E-cadherin germline

mutations in familial gastric cancer." Nature 392(6674): 402-405.

Gumbiner, B. M. (2005). "Regulation of cadherin-mediated adhesion in morphogenesis." Nat Rev Mol Cell Biol 6(8): 622-634.

Gutierrez, A., S. E. Dahlberg, et al. (2010). "Absence of biallelic TCRgamma deletion predicts early treatment failure in pediatric T-cell acute lymphoblastic leukemia." J Clin Oncol 28(24): 3816-3823.

Hingorani, S. R., E. F. Petricoin, et al. (2003). "Preinvasive and invasive ductal pancreatic cancer and its early detection in the mouse." Cancer Cell 4(6): 437-450.

Hirohashi, S. (1998). "Inactivation of the E-cadherin-mediated cell adhesion system in human cancers." Am J Pathol 153(2): 333-339.

Ho, S. B., K. Takamura, et al. (2004). "The adherent gastric mucous layer is composed of alternating layers of MUC5AC and MUC6 mucin proteins." Dig Dis Sci 49(10): 1598-1606.

Hu, Y. and G. K. Smyth (2009). "ELDA: extreme limiting dilution analysis for comparing depleted and enriched populations in stem cell and other assays." J Immunol Methods 347(1-2): 70-78.

Humar, B., V. Blair, et al. (2009). "E-cadherin deficiency initiates gastric signet-ring cell carcinoma in mice and man." Cancer Res 69(5): 2050-2056.

Jaiswal, R., D. Breitsprecher, et al. (2013). "The formin Daam1 and fascin directly collaborate to promote filopodia formation." Curr Biol 23(14): 1373-1379.

Jemal, A., R. Siegel, et al. (2008). "Cancer statistics, 2008." CA Cancer J Clin 58(2): 71-96.

Jonkers, J., R. Meuwissen, et al. (2001). "Synergistic tumor

suppressor activity of BRCA2 and p53 in a conditional mouse model for breast cancer." Nat Genet 29(4): 418-425.

Judd, L. M., B. M. Alderman, et al. (2004). "Gastric cancer development in mice lacking the SHP2 binding site on the IL-6 family co-receptor gp130." Gastroenterology 126(1): 196-207.

Kahlert, U. D., D. Maciaczyk, et al. (2012). "Activation of canonical WNT/beta-catenin signaling enhances in vitro motility of glioblastoma cells by activation of ZEB1 and other activators of epithelial-to-mesenchymal transition." Cancer Lett 325(1): 42-53.

Kharbanda, S., S. Saxena, et al. (2000). "Translocation of SAPK/JNK to mitochondria and interaction with Bcl-x(L) in response to DNA damage." J Biol Chem 275(1): 322-327.

Kim, H. K., I. J. Choi, et al. (2012). "Three-gene predictor of clinical outcome for gastric cancer patients treated with chemotherapy." Pharmacogenomics J 12(2): 119-127.

Lane, D. P. (1992). "Cancer. p53, guardian of the genome." Nature 358(6381): 15-16.

Larsson, L. I., O. D. Madsen, et al. (1996). "Pancreatic-duodenal homeobox 1 -role in gastric endocrine patterning." Mech Dev 60(2): 175-184.

Lauren, P. (1965). "The Two Histological Main Types of Gastric Carcinoma: Diffuse and So-Called Intestinal-Type Carcinoma. An Attempt at a Histo-Clinical Classification." Acta Pathol Microbiol Scand 64: 31-49.

Lefebvre, O., M. P. Chenard, et al. (1996). "Gastric mucosa abnormalities and tumorigenesis in mice lacking the pS2 trefoil protein." Science 274(5285): 259-262.

Lendahl, U., L. B. Zimmerman, et al. (1990). "CNS stem cells express a new class of intermediate filament protein." Cell 60(4): 585-595.

Leung, K. M., R. M. Elashoff, et al. (1997). "Censoring issues in survival analysis." Annu Rev Public Health 18: 83-104.

Li, X., M. Commane, et al. (2001). "IL-1-induced NFkappa B and c-Jun N-terminal kinase (JNK) activation diverge at IL-1 receptor-associated kinase (IRAK)." Proc Natl Acad Sci U S A 98(8): 4461-4465.

Li, Y., L. Wang, et al. (2012). "IL-1beta promotes stemness and invasiveness of colon cancer cells through Zeb1 activation." Mol Cancer 11: 87.

Li, Y., B. Welm, et al. (2003). "Evidence that transgenes encoding components of the Wnt signaling pathway preferentially induce mammary cancers from progenitor cells." Proc Natl Acad Sci U S A 100(26): 15853-15858.

Liu, J. and A. Lin (2005). "Role of JNK activation in apoptosis: a double-edged sword." Cell Res 15(1): 36-42.

Liu, S., C. Ginestier, et al. (2011). "Breast cancer stem cells are regulated by mesenchymal stem cells through cytokine networks." Cancer Res 71(2): 614-624.

Machado, J. C., C. Oliveira, et al. (2001). "E-cadherin gene (CDH1) promoter methylation as the second hit in sporadic diffuse gastric carcinoma." Oncogene 20(12): 1525-1528.

Maesawa, C., G. Tamura, et al. (1995). "The sequential accumulation of genetic alterations characteristic of the colorectal adenoma-carcinoma sequence does not occur between gastric adenoma and adenocarcinoma." J Pathol 176(3): 249-258.

Matheu, A., M. Collado, et al. (2012). "Oncogenicity of the developmental transcription factor Sox9." Cancer Res 72(5): 1301-1315.

Matsuda, Y., Z. Naito, et al. (2011). "Nestin is a novel target for suppressing pancreatic cancer cell migration, invasion and

metastasis." Cancer Biol Ther 11(5): 512-523.

Minn, A. J., C. M. Rudin, et al. (1995). "Expression of bcl-xL can confer a multidrug resistance phenotype." Blood 86(5): 1903-1910.

Miyaki, M. and T. Kuroki (2003). "Role of Smad4 (DPC4) inactivation in human cancer." Biochem Biophys Res Commun 306(4): 799-804.

Nagafuchi, A., Y. Shirayoshi, et al. (1987). "Transformation of cell adhesion properties by exogenously introduced E-cadherin cDNA." Nature 329(6137): 341-343.

Oka, H., H. Shiozaki, et al. (1993). "Expression of E-cadherin cell adhesion molecules in human breast cancer tissues and its relationship to metastasis." Cancer Res 53(7): 1696-1701.

Oliveira, C., M. C. Bordin, et al. (2002). "Screening E-cadherin in gastric cancer families reveals germline mutations only in hereditary diffuse gastric cancer kindred." Hum Mutat 19(5): 510-517.

Oliveira, C., S. Sousa, et al. (2009). "Quantification of epigenetic and genetic 2nd hits in CDH1 during hereditary diffuse gastric cancer syndrome progression." Gastroenterology 136(7): 2137-2148.

Oshima, H., A. Matsunaga, et al. (2006). "Carcinogenesis in mouse stomach by simultaneous activation of the Wnt signaling and prostaglandin E2 pathway." Gastroenterology 131(4): 1086-1095.

Oskarsson, T., S. Acharyya, et al. (2011). "Breast cancer cells produce tenascin C as a metastatic niche component to colonize the lungs." Nat Med 17(7): 867-874.

Pharoah, P. D., P. Guilford, et al. (2001). "Incidence of gastric cancer and breast cancer in CDH1 (E-cadherin) mutation carriers from hereditary diffuse gastric cancer families." Gastroenterology 121(6): 1348-1353.

Qiao, X. T. and D. L. Gumucio (2011). "Current molecular markers for gastric progenitor cells and gastric cancer stem cells." J Gastroenterol 46(7): 855-865.

Qiao, X. T., J. W. Ziel, et al. (2007). "Prospective identification of a multilineage progenitor in murine stomach epithelium." Gastroenterology 133(6): 1989-1998.

Rashid, M. G., M. G. Sanda, et al. (2001). "Posttranslational truncation and inactivation of human E-cadherin distinguishes prostate cancer from matched normal prostate." Cancer Res 61(2): 489-492.

Rivlin, N., R. Brosh, et al. (2011). "Mutations in the p53 Tumor Suppressor Gene: Important Milestones at the Various Steps of Tumorigenesis." Genes Cancer 2(4): 466-474.

Rosivatz, E., I. Becker, et al. (2002). "Differential expression of the epithelial-mesenchymal transition regulators snail, SIP1, and twist in gastric cancer." Am J Pathol 161(5): 1881-1891.

Roussel, Y., A. Harris, et al. (2007). "Novel methods of quantitative real-time PCR data analysis in a murine Helicobacter pylori vaccine model." Vaccine 25(15): 2919-2929.

Sakurai, T., S. Maeda, et al. (2006). "Loss of hepatic NF-kappa B activity enhances chemical hepatocarcinogenesis through sustained c-Jun N-terminal kinase 1 activation." Proc Natl Acad Sci U S A 103(28): 10544-10551.

Schepers, A. G., H. J. Snippert, et al. (2012). "Lineage tracing reveals Lgr5+ stem cell activity in mouse intestinal adenomas." Science 337(6095): 730-735.

Schipper, J. H., U. H. Frixen, et al. (1991). "E-cadherin expression in squamous cell carcinomas of head and neck: inverse correlation with tumor dedifferentiation and lymph node metastasis." Cancer Res 51(23 Pt 1): 6328-6337.

Schmierer, B. and C. S. Hill (2007). "TGFbeta-SMAD signal

transduction: molecular specificity and functional flexibility." Nat Rev Mol Cell Biol 8(12): 970-982.

Seki, E., D. A. Brenner, et al. (2012). "A liver full of JNK: signaling in regulation of cell function and disease pathogenesis, and clinical approaches." Gastroenterology 143(2): 307-320.

Shibata, W., S. Maeda, et al. (2008). "c-Jun NH2-terminal kinase 1 is a critical regulator for the development of gastric cancer in mice." Cancer Res 68(13): 5031-5039.

Shimada, S., A. Mimata, et al. (2012). "Synergistic tumour suppressor activity of E-cadherin and p53 in a conditional mouse model for metastatic diffuse-type gastric cancer." Gut 61(3): 344-353.

Sigal, A. and V. Rotter (2000). "Oncogenic mutations of the p53 tumor suppressor: the demons of the guardian of the genome." Cancer Res 60(24): 6788-6793.

Singh, S. R. (2013). "Gastric cancer stem cells: a novel therapeutic target." Cancer Lett 338(1): 110-119.

Sirard, C., J. L. de la Pompa, et al. (1998). "The tumor suppressor gene Smad4/Dpc4 is required for gastrulation and later for anterior development of the mouse embryo." Genes Dev 12(1): 107-119.

Sun, J., H. He, et al. (2011). "Fascin protein is critical for transforming growth factor beta protein-induced invasion and filopodia formation in spindle-shaped tumor cells." J Biol Chem 286(45): 38865-38875.

Takaishi, S., T. Okumura, et al. (2009). "Identification of gastric cancer stem cells using the cell surface marker CD44." Stem Cells 27(5): 1006-1020.

Takaku, K., M. Oshima, et al. (1998). "Intestinal tumorigenesis in compound mutant mice of both Dpc4 (Smad4) and Apc genes." Cell 92(5): 645-656.

Tian, X., Z. Liu, et al. (2011). "E-cadherin/beta-catenin complex and the epithelial barrier." J Biomed Biotechnol 2011: 567305.

Treister, A., O. Sagi-Assif, et al. (1998). "Expression of Ly-6, a marker for highly malignant murine tumor cells, is regulated by growth conditions and stress." Int J Cancer 77(2): 306-313.

Umbas, R., W. B. Isaacs, et al. (1994). "Decreased E-cadherin expression is associated with poor prognosis in patients with prostate cancer." Cancer Res 54(14): 3929-3933.

Upadhyay, G., Y. Yin, et al. (2011). "Stem cell antigen-1 enhances tumorigenicity by disruption of growth differentiation factor-10 (GDF10)-dependent TGF-beta signaling." Proc Natl Acad Sci U S A 108(19): 7820-7825.

Upreti, M., E. N. Galitovskaya, et al. (2008). "Identification of the major phosphorylation site in Bcl-xL induced by microtubule inhibitors and analysis of its functional significance." J Biol Chem 283(51): 35517-35525.

Vincan, E. and N. Barker (2008). "The upstream components of the Wnt signalling pathway in the dynamic EMT and MET associated with colorectal cancer progression." Clin Exp Metastasis 25(6): 657-663.

Visvader, J. E. and G. J. Lindeman (2008). "Cancer stem cells in solid tumours: accumulating evidence and unresolved questions." Nat Rev Cancer 8(10): 755-768.

Visvader, J. E. and G. J. Lindeman (2012). "Cancer stem cells: current status and evolving complexities." Cell Stem Cell 10(6): 717-728.

Wang, L., Z. Liu, et al. (2012). "Interleukin-1beta and transforming growth factor-beta cooperate to induce neurosphere formation and increase tumorigenicity of adherent LN-229 glioma cells." Stem Cell Res Ther 3(1): 5.

Wang, L. H., S. H. Kim, et al. (2007). "Inactivation of SMAD4 tumor

suppressor gene during gastric carcinoma progression." Clin Cancer Res 13(1): 102-110.

Wang, T. C., C. A. Dangler, et al. (2000). "Synergistic interaction between hypergastrinemia and Helicobacter infection in a mouse model of gastric cancer." Gastroenterology 118(1): 36-47.

Witz, I. P. (2000). "Differential expression of genes by tumor cells of a low or a high malignancy phenotype: the case of murine and human Ly-6 proteins." J Cell Biochem Suppl 34: 61-66.

Xin, L., D. A. Lawson, et al. (2005). "The Sca-1 cell surface marker enriches for a prostate-regenerating cell subpopulation that can initiate prostate tumorigenesis." Proc Natl Acad Sci U S A 102(19): 6942-6947.

Xu, X., S. G. Brodie, et al. (2000). "Haploid loss of the tumor suppressor Smad4/Dpc4 initiates gastric polyposis and cancer in mice." Oncogene 19(15): 1868-1874.

Yang, G. and X. Yang (2010). "Smad4-mediated TGF-beta signaling in tumorigenesis." Int J Biol Sci 6(1): 1-8.

Yang, X., C. Li, et al. (2002). "Generation of Smad4/Dpc4 conditional knockout mice." Genesis 32(2): 80-81.